Chapter One
Introduction

1.1 Liquid Crystals

Many materials exhibit a series of phases that are neither truly ordered nor fully disordered [1]. Materials that flow moderately easily but have long range orientational order are called liquid crystals. Liquid crystal materials generally have several common characteristics. Among these are a rod-like molecular structure, rigidness of the long axis, and strong *dipoles* and / or easily polarizable substituents.

The distinguishing characteristic of the liquid crystalline state is the tendency of the molecules (*mesogens*) to point along a common axis, called the *director* ($\hat{n}$). This is in contrast to molecules in the liquid phase, which have no intrinsic order. In the solid state, molecules are highly ordered and have little translational freedom. The characteristic orientational order of the liquid crystal state is between the traditional solid and liquid phases and this is the origin of the term mesogenic state, used synonymously with liquid crystal state. The average alignment of the molecules for each phase is shown in Figure 1.1.

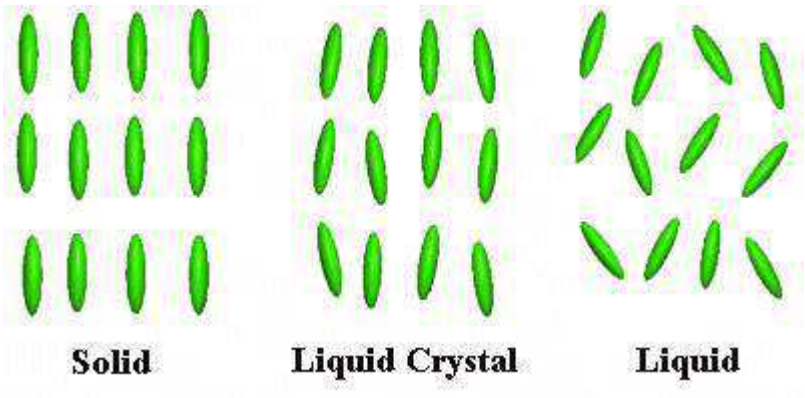

Figure 1.1 Alignment of the molecules for solid, liquid crystal and liquid phases.

To quantify just how much order is present in a material, an *order parameter* (S) is defined as follows[2]:

$$S = (1/2)\left(3\cos^2\theta - 1\right)$$

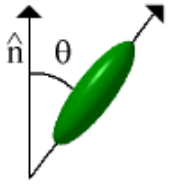

where θ is the angle between the director ($\hat{n}$) and the long axis of each molecule. The brackets denote an average over all of the molecules in the sample. In an isotropic liquid, the average of the cosine terms is zero, and therefore the order parameter is equal to zero. A perfect crystal, has an order parameter equal to one. Typical values for the order parameter of a liquid crystal range between 0.3 and 0.9, with the exact value depending on the temperature, as a result of kinetic molecular motion as shown in Figure 1.2.

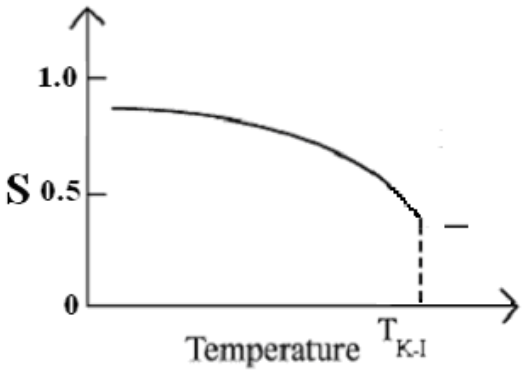

Figure 1.2 Typical temperature dependence of the liquid crystals order parameter with temperature. T_{k-I} is the nematic- isotropic transition temperature.

The tendency of the liquid crystal molecules to point along the director leads to a condition known as *anisotropy*. This term means that the properties of a material depend on the direction in which they are measured. The anisotropic nature of liquid crystals is responsible for the unique optical properties[3].

1.2 Characterization of Liquid Crystals

The following parameters describe the liquid crystalline structure:

- ***Positional Order***
- ***Orientational Order***
- ***Bond Orientational Order***

Each of these parameters describes the extent to which the liquid crystal sample is ordered. *Positional order* refers to the extent to which an average molecule or group of molecules shows translational symmetry (as crystalline material showed). *Orientational order* represents a measure of the tendency of the molecules to align along the director on a long-range basis. *Bond Orientational Order* describes a line joining the centers of nearest-neighbor molecules without requiring a regular spacing along that line.

Most liquid crystal compounds exhibit *polymorphism*, or a condition where more than one phase is observed in the liquid crystalline state. The term *mesophase* is used to describe the "subphases" of liquid crystal materials. Mesophases are formed by changing the amount of order in the sample, either by imposing order in only one or two dimensions, or by allowing the molecules to have a degree of translational motion.

1.3 Liquid Crystal Phases[4]

Liquid crystal phases are formed by a wide variety of molecules. They can be divided into two classes, thermotropic and lyotropic. Transitions to thermotropic phases are initiated by changes in temperature, while those to lyotropic phases can also be initiated by changes in concentration.

1.3.1 Thermotropic Phases

Thermotropic liquid crystals can generally be formed by prolate (calamitic) molecules or oblate (discotic) molecules. Liquid crystal phases formed by calamitic molecules fall into four different categories: nematic, chiral nematic, smectic and discotic.

1.3.1.1 Nematic Liquid Crystal Phase

The simplest liquid crystal phase is called the nematic phase (N). It is characterized by a high degree of long range orientational order but no translational order. Molecules in a nematic phase spontaneously order with their (for calamitic molecules) long axes roughly parallel. A schematic diagram of a nematic phase is shown in Figure 1.3.

Figure 1.3 Molecular arrangement of nematic phase.

1.3.1.2 Chiral Nematic Liquid Crystal Phase[5]

Chiral molecules can also form nematic phases called chiral nematic (or cholesteric) phases (N*). This phase showed nematic ordering but the preferred direction rotates throughout the sample. The axis of this rotation is normal to the director. The shape of this type of liquid crystal is shown in Figure 1.4.

Figure 1.4 Schematic of chiral nematic liquid crystal.

1.3.1.3 Smectic Liquid Crystal Phases

Smectic phases have further degrees of order compared to the nematic phase. Nine smectic structures have been described in literature[6]. They are identified as smectic A through smectic I. The simplest is the smectic-A (S_A) phase, in which the molecules order into layers, normal parallel to the director. Within the layers, liquid like structure remains and the system is optically uniaxial. In smectic C each layer is still a two-dimensional liquid but the material is optically biaxial, as shown in Figure 1.5.

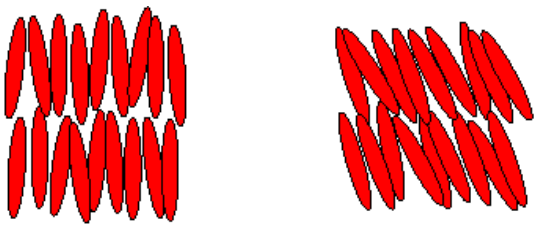

Smectic A **Smectic C**

Figure 1.5 Molecular arrangement of different types of smectic phases.

1.3.1.4 Discotic Liquid Crystal Phases[7]

Liquid crystal phases formed by discotic molecules fall into three different categories: discotic nematic, discotic chiral nematic, and columnar. The discotic nematic is similar in structure to the calamitic nematic, although in this case the short axes of the molecules tend to lie parallel. The same holds for the discotic chiral nematic phases.

Columnar phases are the discotic equivalent of the smectic phase. Here the molecules form columns as shown in Figure 1.6. In the simplest case the short axes of the molecules lie parallel to the axis of the column and the columns are randomly distributed in space. More complicated discotic phases exist, where the short molecular axes lie at an angle to the column and translational order exists between the columns, analogous to the more complicated smectic phases.

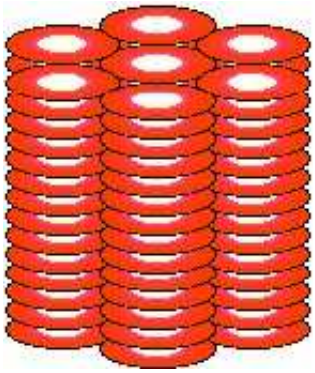

Figure 1.6 Schematic representation of columnar discotic liquid crystal phase.

1.3.2 Lyotropic Liquid Crystal Phases[8]

These are formed by amphiphilic molecules. These often consist of a polar head group attached to one or more non-polar chains and are often known as *surfactants* (surface active agents). A schematic of this phase is shown in Figure1.7.

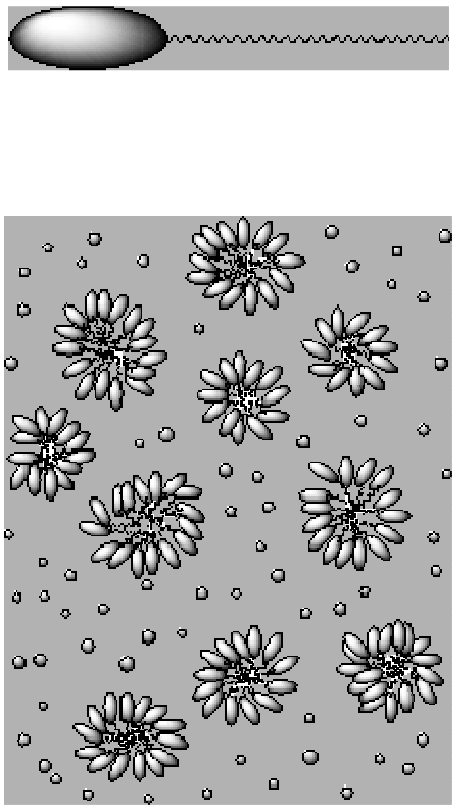

Figure 1.7 Schematic patterns of lyotropic mesophase.

1.4. Characteristic of Liquid-Crystal as Stationary Phases in Gas Chromatography (GC)

Thermotropic liquid crystals have drawn the attention of the chromatographers to be used as stationary phases in gas chromatography follows from their unique separating properties, which are due to the structure and ordering of their molecules[9]. At a certain temperature range (from the melting point to the point of transition to the isotropic liquid phase) thermotropic liquid crystal have some degree of orientational molecular ordering, and thus have properties that are intermediate between the solid and the isotropic liquid[10].

The liquid crystal compounds that are used as stationary phases belong to many chemical-groups such as Schiff bases, azo and azoxy compounds, esters, isothiocyanates, and biphenyl and terphenyl derivatives[11]. These are the rod-like liquid crystals whose molecules have a shape that resembles a flattened cigar.

Like other phases, liquid-crystal stationary phases should demonstrate high thermal stability; they should not decompose at normal column operating temperatures and should have low vapor pressures so that the quantity of the phase in the column is not reduced to a degree that affects chromatographic reproducibilities. Many liquid crystals meet these requirements, and their properties were studied in packed column for many years[12]. Liquid-crystal stationary phases have been developed to be used at temperatures above 300ºC[13]. It is desirable, especially in capillary chromatography, that liquid crystals used as stationary phases demonstrate a wide mesophase temperature range so as to enable column

temperature programming[14]. Nematic liquid crystals reveal the widest mesophase temperature ranges.

1.5. Physico-Chemical Studies of Liquid-Crystalline Stationary Phases (LCSP's)

The ordering of the liquid crystal structure is known to be of decisive importance in the separation of components of mixtures by distinguishing the shape of their molecules. However, investigations on the effect of other physico-chemical properties of liquid crystals on their behavior as stationary phases in a chromatographic column are still necessary[15]. The results of such investigations should facilitate a search for liquid crystals of good separation properties to meet the general requirements best set for stationary phases. It is also important to learn more about the relationships between general physico-chemical properties of liquid crystals and their separation ability. The selectivity of liquid crystals in relation to substances of different molecular shape can be determined by the dependence of the selectivity coefficient (α) of test substances on temperature: $\ln \alpha = f(1/T)$. On the basis of the dependence: $\ln \alpha = -\Delta(\Delta G_{a,b})/(RT)$, it is possible to determine quantitatively differences of partial molar free energies of the substances a and b chromatographed on liquid crystal. Using $\Delta G = \Delta H - T\Delta S$, and from the slope of straight lines $\ln \alpha = f(1/T)$ for each pair of isomers, $\Delta(\Delta H_{a,b}/R)$ was calculated[16].

The retention of chromatographed isomers substances considerably depends on the type of the mesophase of the liquid-crystalline stationary Phase[17]. It results from the fact that the type of mesophase affects the diffusion of isomers of the chromatographed substance to a different degree. Medina[18] studied the influence of the type of mesophase of the liquid-crystalline stationary phase on the diffusion of xylene isomers on

4,4 -bis(Heptyloxy)azoxybenzene (BHOAB) as stationary phase deposited on glass beads. The order of elution's of xylene isomers was typical of liquid-crystalline stationary phases—*meta* , *para* and *ortho* . However, the diffusion coefficients in the smectic, nematic and isotropic phases decreased in the order *p*-xylene, *o*-xylene and *m*-xylene. The diffusion coefficient of *p*-xylene compared to *m*- and *o*–xylene was disproportionately larger in the smectic phase than in the other phases. Medina concluded, from the comparison of the values of diffusion coefficients of xylene isomers with their polarity, the length to width ratio and the molar volume that the diffusion coefficient of *para*-isomer was larger than *m*– and *o*-isomers was associated with its smaller polarity and the larger molecule length to width ratio than that of the other isomers.

The described behavior of *para*- xylene isomers could account for its larger retention on liquid-crystalline stationary phases than that of the *m*-xylene isomer. The retention on conventional stationary phases is reversed and attributed to their boiling points. A clearly great difference in the activation energy of the diffusion of xylene isomers in smectic and nematic mesophases as well as in isotropic liquid resulted from the ordered structure of a smectic and a nematic mesophases, and from the disorder of the isotropic liquid. Molar diffusion coefficients of selected polyaromatic hydrocarbons in the side chain liquid-crystalline polymer determined by gas chromatography confirm the influence of the shape of molecules on its behavior in nematic and isotropic phases[19].

The non-planar *o*–terphenyl diffused more easily in the nematic phase of this liquid crystal than planar fluorene[20]. In the isotropic phase molar diffusion coefficients for fluorene and *o*-terphenyl did not differ much. Activation energies of the diffusion of naphthalene with (length-to-breadth) L/B = 1.24 and that of fluorene with L/B = 1.52 in the isotropic

phase did not differ much and were (32 and 30 kJ/mol), respectively, whereas in the ordered nematic phase they were clearly larger and different for naphthalene (40 kJ/mol) and for fluorene (68 kJ/mol)[21].

The separation effect of components of mixtures on LCSP's was associated with the different energy of the interactions of the components with liquid crystals[22]. Therefore, the determination of these interactions in different systems could be contributed to a better knowledge of the nature of liquid crystal-chromatographed substance interactions. The values of excess molar thermodynamic functions (enthalpy, entropy and Gibbs free energy) and of the activity coefficients in the liquid crystal - C_5- C_9 alkanes systems: (linear, branched and cyclic) were calculated by [23]. The two liquid crystals: *p*-pentylo-triphenyl- *p´* -ethoxyazoxybenzene and *p*-(*n*-hexyloxy)phenyl-*p´*-methoxybenzoate were chosen for the investigations. The activity coefficients of *n*–alkanes dissolved in both liquid crystals decreased in the order: nonane > octane > heptane > hexane > pentane. Excess molar enthalpies of the substances dissolved in liquid crystals were positive, which accounted for the endothermic effect of their mixing. Excess molar enthalpies of the mixing were found to be higher in the mesophase than in the isotropic liquid, which meant that the dissolution in the anisotropic liquid needed more energy, i.e. the dissolution of molecules in the ordered structure of the mesophase was made more difficult. The effect of steric factors on the separation of *m*- and *p*-xylene isomers on liquid crystals: *para*–azoxyanisole PAA and 4-methoxy-benzylidene-4-butylaniline MBBA was reported[24]. The ratio of dissolution activity factors of *m*-xylene to *p*-xylene was smaller than unity and in practice it did not change in the isotropic phase while it was larger than unity in the nematic phase and depended on the structure of the liquid crystal. The dissolution activity coefficients of *m*-, *o*-and *p*-

nitrotoluene in the liquid-crystalline phase (C_7H_{15}-O-C_6H_4-COO-C_6H_4-COO-C_6H_4-O-C_7H_{15}), PBHPB, were calculated on the basis of the lattice model for anisotropic systems as given by Flory[25] were consistent with the experimental data obtained from the chromatographic measurements[26].

The diffusion and dissolution of chromatographed substances in stationary phases were determined by the mass transfer resistance which affects the efficiency of chromatographic columns. The efficiencies of columns with liquid-crystalline stationary phases were generally lower than of those columns with conventional stationary phases[27]. Therefore, it could be advisable to mix liquid-crystalline stationary phases with conventional phases. This has been shown by examining mixtures of 4-propoxy-4´-ethoxyazoxy-benzene, PEAB, with polymethylhydrogen-siloxane, PMHS, in capillary columns[28]. Xylene isomers were chromatographed on these phases. With the suitable mixture ratio, LCSP's and the small mass transfer resistance of the conventional stationary phase resulted in the separation of the components of the mixture. The mixture of PEAB and PMHS in the ratio of 83:17 had showed good separation properties. It was noted that the film of the stationary phase mixture coated on the wall of a glass capillary column was more homogenous than the film of the liquid-crystalline stationary phase itself. Little attention was paid to the effect of polarity of LCSP's on their separation properties. It was justifiable as the effect of polarity of LCSP's on obtaining the separation of components of mixtures was smaller than the effect of the ordered structure of the stationary phase. The effect of polarity should not be neglected, though, because in some cases it could be positive and might improve the separation of components of mixtures. The investigation of the polarity of three liquid-

crystalline stationary phases, azoxydiphenetole, ADP, bis(metoxybenzylidineanil-chloraniline), $(MBCA)_2$, and bis(methoxybenzylidineanil-bi-toluidine), $(MBT)_2$, was reported by Betts[29]. Depending on the method used, the first two phases were found to be strongly polar than the third one, which was moderately or weakly polar. Like in conventional stationary phases, the thickness of the film of a liquid crystal should be thick enough not to let the support affect its interaction with chromatographed substances, however, it should be as thin as possible[30].

1.6. The Separation Mechanism on Liquid-Crystalline Stationary Phases

The chromatographic separation of components of mixtures using most of the conventional stationary phases is associated with the polarity of these phases and with the polarity and polarizability of the chromatographed substances as well as the subsequent intermolecular interactions[31]. The mechanism of the chromatographic separation on LCSP's is mostly connected with the differentiation of the structure of molecules of chromatographed substances. This resulted from the ordering of the liquid crystal structure and depended on the type of mesophase and thermodynamic effects of dissolution of solutes in LCSP[32]. In the case of nematic liquid crystals, the best separations were obtained at the lowest temperatures of their existence, usually slightly above the melting point, but also below it, in the supercooled mesophase. However, the mass transfer resistances in the highly ordered supercooled mesophase were very strong and the efficiencies of chromatographic columns with such mesophases were low. The efficiencies of columns with LCSP's were generally lower than those of the columns with

conventional stationary phases and, therefore, the mixture of a liquid crystal with the conventional stationary phase (e.g. the silicon one) could be advantageous[33]. This kind of mixture has been found to increase the efficiency of the column by improving the homogeneity of the coated stationary phase film upon the wall of a capillary column. The mixture of two liquid crystals could also prove advantageous[34]. Apart from non-ideal solutions of such mixed stationary phases, there were systems in which the liquid crystal dispersed in the conventional stationary phase[35]. In such systems both stationary phases interact with chromatographed substances independently, according to different mechanisms; the liquid crystal by the ordered structure and the conventional stationary phase by polarity. This system could show better properties than the liquid crystal alone due to two different mechanisms. With a certain composition of mixture being separated, disadvantageous effects of separation could not be excluded.

Monomeric liquid crystals were successfully used mostly for the separation of volatile organic compounds, (VOC), whereas polymeric ones for the separation of high-boiling compounds (e.g. polyaromatic hydrocarbons)[36]. Some monomeric LCSP's, of high molecular weights, have been found to contribute to the separation of high-boiling compounds at temperatures corresponding to the solid of a liquid crystal[37]. In such conditions, separation was obtained in a shorter time than in the mesophase range. Small differences in the structure of molecules of liquid crystals related to terminal or lateral position of the same functional group were also found to affect not only the range of their mesophase but also their separation properties[38].

The mesophase of the liquid crystal existing after its melting could be cooled when the temperature of a column decreases. The stability of the

cooled mesophase depended on the kind of liquid crystal and on the support on which it was deposited. The separation in the cooled mesophase took place according to the same mechanism as in the conventional mesophase at stronger mass transfer resistances in the cooled phase.

The effects that explaining the separation of components of mixtures, including isomers, on LCSP's at temperatures below their melting points, as well as within the mesophase temperature range were difficult. The explanation that given by Betts et al.[39] seemed very probable. The chromatographed solute moving down in the chromatographic column could produce locally a liquid eutectic mixture with a liquid crystal. If the liquid crystal has been previously heated above the melting point, it could then retain the ordered structure of the mesophase after being cooled below the melting point and solidified. Such ordering did not occur in a liquid crystal which has been not molten earlier. Therefore, the interaction of the liquid crystal melted earlier with the chromatographed substance in the eutectic mixture could be stronger than that of the liquid crystal which has not been molten[40]. It appeared that the separation of components of the same mixture could be different and took place according to different mechanisms related to the thermal history of a chromatographic column. Considering the separation properties of LCSP's, the interactions in the chromatographic system, connected with polarity, could not be completely omitted although they were not large compared with the separation mechanism resulting from the ordered structure of these stationary phases[41]. It is noticeable in the case of separating *m*- and *p*-xylene isomers on conventional stationary phases, if separated, were eluted in the order *para* and *meta* , whereas on LCSP's they were eluted in the order *meta* and *para*[42].

The two isomers were very frequently used to assess the separation abilities of LCSP's. However, according to Krupčik et al[43]. the use of saturated cyclic compounds for assessing the selectivity of LCSP's was better than the use of xylenes. It was justified by the fact that the polarity of cyclic compounds was smaller than that of xylenes and the influence of their polarity on the selectivity of the separation could be minimized. It could then be assumed that, like in the case of conventional stationary phases, the polarity of LCSP and the polarity of chromatographed substances were likely to affect the separation of mixture components.

The different separation of the same mixtures in different types of the mesophase of liquid crystals (smectic, nematic, isotropic) could be related to different diffusion coefficients of the same substances in individual types of mesophase[44].

1.7. Factors Effecting the Separation of Mixture Components on LCSP's

1.7.1. *Kind of Mesophase of the Liquid Crystal*

A nematic liquid crystal would be expected to show a selective affinity for linear molecules, since these should be able to fit better into its "lattice". On this basis, one might expect columns of nematic to retain selectivity *p*-disubstituted benzene, relative to the ortho and meta isomers.

In general it is assumed that nematic liquid crystals have better separation properties than those of smectics, and that smectics with a low degree of ordering of the mesophase (S_A, S_B) have better separation properties than those of a high degree of ordering[45-47].

A possible explanation of this seems to be that smectic stationary phases may not, like normal liquids, operate under equilibrium conditions. The viscosity of a smectic liquid crystal is extremely anisotropic, being very great for shear across the planes of two-dimensional liquid[48]. This is a consequence of the layered structure, the mechanical properties of a smectic phase being similar to those of graphite. It therefore, seems possible that diffusion through a smectic stationary phase may be slow enough to affect the residence time. In this case two factors could operate in the transition from smectic to nematic; the decrease in order would lead to an increase in retention time, while the viscosity effect should lead to a decrease.

1.7.2. Molecular Structure of the Liquid Crystal and of the Chromatographed Substances

A fact of intermolecular reactions or interactions between the liquid crystal and the chromatographed substances is important for the understanding of the phenomena taking place in the chromatographic column. The structure of the molecules and their polarity and polarizability affect, as well as, the solubility of the chromatographed substances in the liquid crystal plays an important influence on the separation.

The process of dissolution dominate in the column during chromatography on a liquid crystal. However, as liquid crystals are usually phases of medium polarity[(49)], the mechanism of the retention of the substances chromatographed on them is accompanied by adsorption. Nevertheless, the contribution of adsorption to the total retention is usually much smaller that of dissolution.

The properties of the liquid crystal stationary phases depend both on the structure of the main chain of the molecule and on the terminal substituents which strongly affect the polarity of the molecules[(50)]. However, an equally important or even greater effect on the chromatographic properties of liquid crystals is exerted by the lateral substituents. These substituents not only affect the intermolecular reactions between the liquid crystal and the chromatographed substance but also the liquid crystal – liquid crystal interactions. The lateral substituents also affect the selectivity of the liquid crystal owing to the changes they produce in the distance between its molecules[(51)]. This relates not only to monomers but also polymers[(52)].

The direct quantitative correlation between the retention of the chromatographed substances and their molecular structure has been studied in several studies[53]. It is generally assumed that the ratio of the length to the smallest transverse dimension of the molecule, (L/D) (shape factor), is a decisive quantity for the retention of chromatographed substance on liquid crystal stationary phases.

1.7.3. Effect of the Support

Although great attention has been paid to the practical applications of liquid crystal stationary phases, relatively little concern has been devoted to fundamental studies of interactions of the liquid crystals with the surface of the support[54].

The effect of the surface of the substrate on which the liquid crystals is deposited in the chromatographic column is rarely accounted for in analytical practice. This is also the case with other stationary phases. However, this effect may be important on separations, although sometimes this effect may be positive[55].

The surface of the support or the column wall may not only contribute substantially to the retention of the chromatographed substances but may also influence the orientation of the liquid crystal molecules in various ways. The distribution of the liquid crystal on the support and hence the properties of the whole system are affected no only by the chemical characters (silanized or non-silanized) and porous structure of the support, but also by the amount of the liquid crystal deposited on its surface[56]. The effect of the support surface also manifests itself by the changes in the phase transition temperatures of the deposited liquid crystal. This effect is related to the conditions under which the column

filling is heat treated. During heating, a redistribution of the liquid crystal on the support takes place and as a result the properties of the system are changed[57-58]. In some instances conditioning at high temperatures leads to a more advantageous ordering of the liquid crystals in the column. Therefore, if this treatment is not long enough or is conducted at an insufficiently high temperature, sometimes the selectivity of the column may change in the course of its use[59]. The occurrence of this phenomenon is related to the kind of liquid crystal used and the properties of the surface on which it has been deposited.

The selectivity of the system depend strongly on the kind of support used and on the amount of the liquid crystal deposited on it[60]. The selectivity also depends on the thickness of the liquid crystal layer on the column wall and the character of the wall surface[61]. The reproducibility and reliability of the retention data are better when the surface of the column wall is inactive and the thickness of the liquid crystal layer is relatively thick (140 nm)[62].

The liquid crystal molecules may be introduced on the support in two states as a film on the surface or in bulk form in the columns. The proportion of the two states influences the properties of the system and depends on the kind of the support and the kind and amount of the deposited liquid crystal.

The interaction of the support surface with the liquid crystal stationary phase may give specific effects. One is lowering the melting point of the liquid crystal by 7ºC owing to its contact with silanized surface [63]. The lowering of the melting point is due to the formation, under the influence of the support, of a layer phase with a crystalline structure different from that of the bulk liquid crystal beyond the support. This effect is not

related to the kind of substance chromatographed but depends on the kind and amount of the liquid crystal deposited on the support and is a feature of the liquid crystal–silanized support system. It appears when the amount of the liquid crystal on the support exceeds 3% and manifests itself by a new phase transition not observed thermo–optically. Hence this effect differs from the normal interactions of the liquid crystal with the support at small converges which manifest themselves by a shift of the phase transition connected with the liquid crystal melting point and not by a new phase transition.

The nature of the surface of the support considerably affects the relative retention of the chromatographed substance. On silanized chromosorb P, the relative retention are greater compared with the same, small converges of the supports with the liquid crystal stationary phase on the silanized support. The observed difference decreases with increasing converge of the support.

1.10. Literature Survey

The use of liquid crystals as stationary phase in gas liquid chromatography (GLC) for hydrocarbon analysis began in 1963. Kelker-[64] used the mesophase 4-4-azoxyphenetol [1] as a liquid stationary phase GLC for the separation of some aromatic compounds and xylene isomers. In his work benzene was eluted first then toluene, ethyl benzene and finally o-xylene. The phase showed a pronounced increase in efficiency of resolution at temperatures above the transition point.

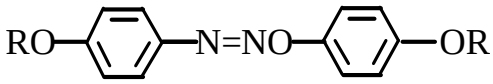

[1]

R= CH_3, C_2H_5, n-C_6H_{13}, n-C_7H_{15}.

Dewar and Schroeder[65] used the mesophase 4-azoxyanisole [2] to separate some positional isomers o-, m-, and p-xylenes which have very close boiling points.

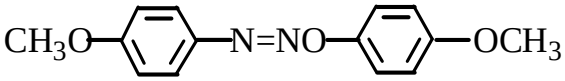

[2]

Barrall et al.[66] studied the effect of temperature on the behavior of some hydrocarbons using cholesteric liquid crystal as stationary phase, were noted that, sharp changes in the elution of the studied solutes at or near the liquid crystal transition temperature. However, aromatic

compounds exhibited shorter elution time than those for corresponding aliphatic compounds of equal carbon number.

Grushka and solsky[67] tried to expand the temperature range of the mesophase by using a mixed phase capable of forming a eutectic mixture and also pointed out[68] changes in the height equivalent of a theoretical plate ,H, as a function of changes in the temperature of the nematic crystal. The enantiomers of N-perfluoroacyl derivatives of 2- aminoethyl benzene, 2-amino-3-phenylpropane and 2-amino-4-phenyl butane were separated on optically active esters of carbonyl-bis-valine and carbonyl-bis-leucine[69].

On high melting liquid crystalline stationary phases, 1,2,3-phenylene tri [4-(4-decyloxyphenylazo)benzoate], where: *R* =$C_{10}H_{21}$ [3], Hall and Mallen[70] separated benefin and trifluralin and the isomers of benzoxaprofene[71].

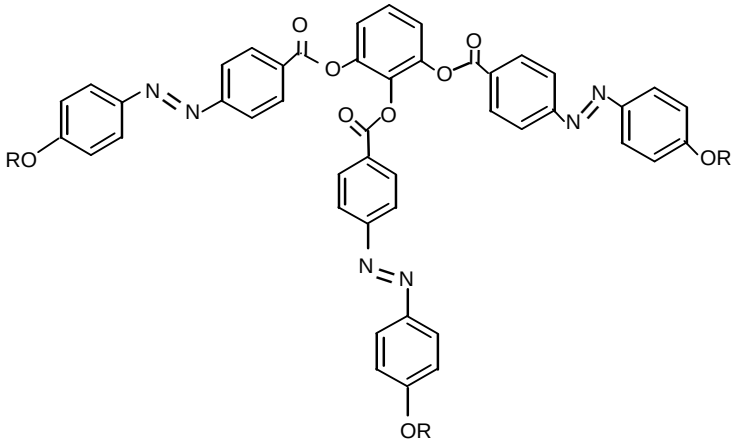

[3]

Pailer and Hlozek[72] separated azo heterocyclic compounds α–pinene, eucalyptol, fenchone, 4-terpfenchone, 4-terpineol and α-terpineol using the mesophase bismethoxy-benilidinebitoluidine [4].

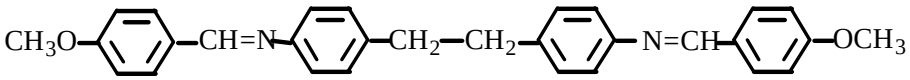

[4]

Kraus et al.[73] showed the optimization of stationary phase selectivity for GLC separation of C_8 cyclic and aromatic hydrocarbons using squalane and liquid crystal glass capillary columns.

Sojak et.al.[74] studied the separation of diastereomeric C_8-C_{20} alkanes using mesogenic stationary phases of **(**4-n-pentylactophenone-o-4-n-pentyloxybenzoyloxime) and [5] in glass capillary columns.

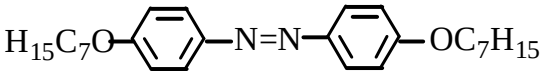

[5]

Coca et al.[75] discussed the thermodynamic properties of 22 solutes at infinite dilution in the mesophases 4,4-heptoxy azobenzene [5] in relation to solute-solvent(liquid crystal).

Eight cyclic monoterpene volatile oil constituents of short retention time were studied using three liquid crystals as gas chromatographic stationary phases in packed columns[76]. Two phases azoxy diphentole [6], bismethoxy-benilidinebitoluidine [7] exhibited a different solute elution sequence after melting and supercooling. The third bis-(methoxy-benilidineanilchloroaniline) [8], did not, but still showed fairly good resolution.

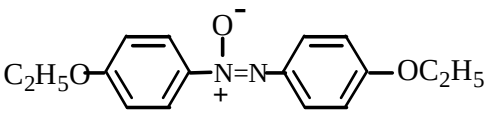

[6]

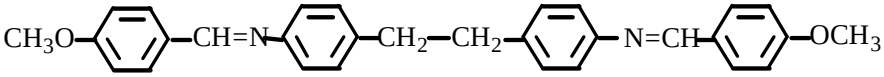

[7]

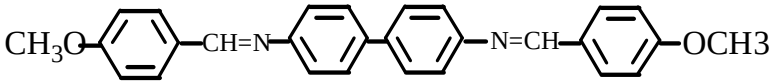

[8]

Monomeric liquid crystals containing transition metals in organic complexes were described by Hudson and Maitlis[77]. The synthesis of polymeric liquid crystals were complexes of zinc(II) and nickel(II) with 4-(dec-9 -en-1-oxy)dithio-benzoate[78] which were bound to the polysiloxane chain. The formula of such a liquid crystal is given below [9]

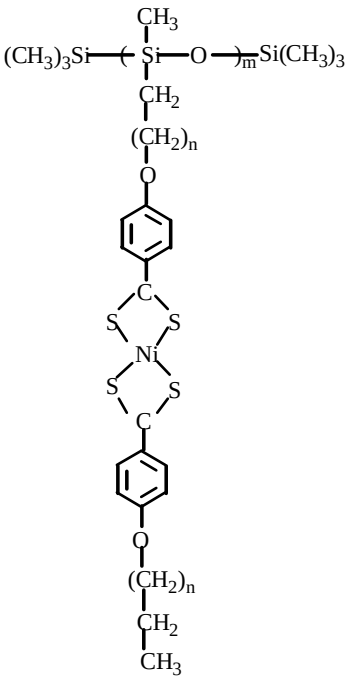

[9]

Very often polymers with liquid-crystalline properties have a polysiloxane backbone. Among the polymeric liquid crystals were the ones in which molecules possessing alkoxyl groups[79] 4,4´-biphenylene-bis(4-butyloxybenzoate) [10] and crown ethers[80] 4-(allyloxy)-4'-(4'-carboxybenzo-15-crown-5)-biphenyl [11] were bound to the polysiloxane chain.

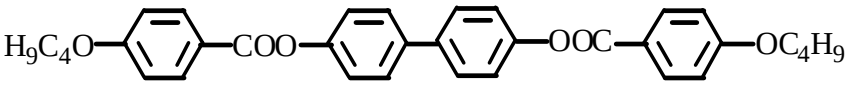

[10]

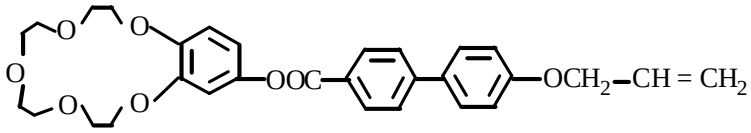

[11]

The liquid-crystalline stationary phase whose molecule contains both crown ether and a cholesterol fragment[81] [12] was also obtained.

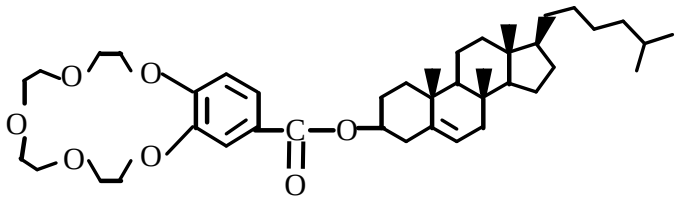

[12]

Liquid crystals with a polyglutamine skeleton were note-worthy among polymers with no polysiloxane skeleton. Decyl- and *n* -hexadecyl groups [13,14][82] were connected with this skeleton.

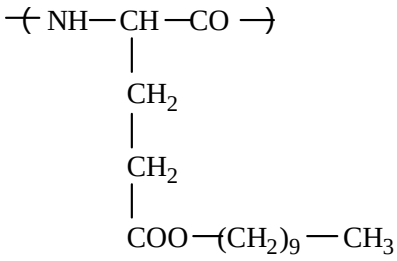

[13]

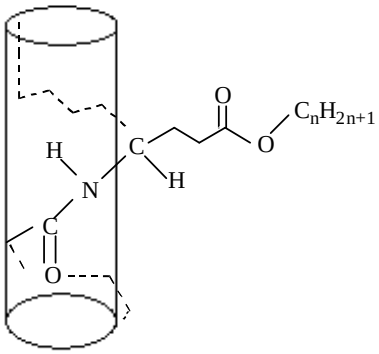

[14]

Synthesis, analytical performances, thermodynamic and surface properties of two new liquid crystals substituted with poly(ethylene oxide) chains were described by Judeinstein, and Berdagué[83]. The first one was *N*,*N*′-diphenyl-[4-{2,3,4-tri[2-(2-metoxyethoxy) ethoxy] benzylidene}imine]piperidine and the second was 2-hydroxy-3-methyl-4-{4-[2-(2-butoxyethoxy)ethoxy]}4′-{4-[2-(2-butoxyethoxy)ethoxy]styr-yl}azobenzene. Comparison of the analytical performances showed a better efficiency in the nematic state.

In another works[84], the LCSP's 4-(4-*trans*-pentyl cyclo hexanecarboxyloxy)-2`-methoxy-4`-(4-*trans*-pentylcyclohex-anecarboxy loxy)-*trans*-azobenzene [15] and 4-(4-*trans*-pentylcyclohexane carboxyloxy)-2`-butoxy-3`-methyl-(4-butoxybenzoyloxy)-*trans*-azoben-

zene [16] and their properties were found useful in the chromatographic separation of composite mixtures of aromatic compounds like polyaromatic hydrocarbons, chlorobenzenes, and methyl esters.

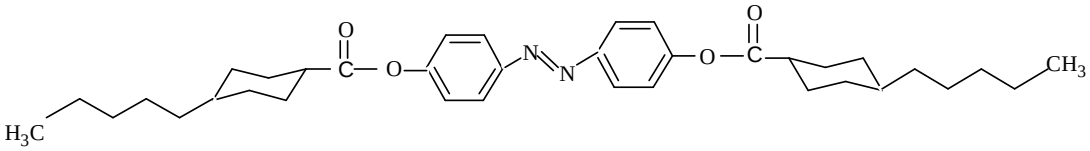

[15]

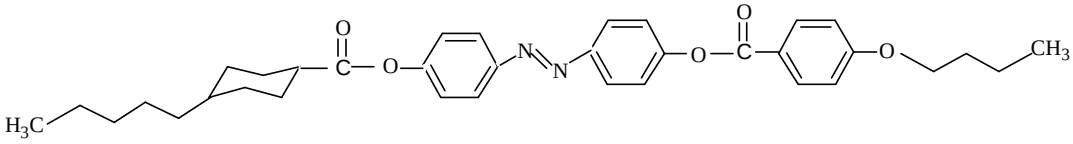

[16]

The chromatographic behavior of liquid crystalline compounds [17,18] as stationary phases for the separation of dimethylphenol isomers was also studied[(85)]. It was found that isomer separation was obtained with 20% loading for both liquid crystal materials [17] and [18].

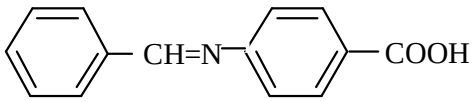

[17]

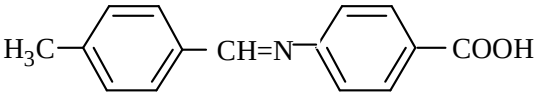

[18]

1.8. Aim of the work

Gas chromatography is of great importance in modern chemical analysis and physico-chemical investigation. So, the aims of this work are:

- Synthesis and characterization of liquid crystalline compounds with related structural properties.
- Study the effect of heterocyclic unit on the liquid crystal properties.
- Study the properties of gas-chromatographic columns packed with the synthesized liquid crystal compounds.
- Study the interaction and elution characteristics of positional isomers and poly aromatic hydrocarbons by determination the thermodynamic and physical properties.

Chapter Two
Experimental

2.1 Chemicals

The following chemicals were used directly from their mentioned suppliers, without further purification:

Table 2.1 Chemicals and their manufactures.

Material	Supplied from
p-aminobenzoic acid	BDH
Anisic acid	Fluka
Anisaldehyde	BDH
n-alkyl bromide	Fluka
Butyric acid	BDH
Calcium chloride	Hannover
Chloroform	Hopkin and Williams
Carbon disulfide	BDH
Dimethylformamide(DMF)	BDH
Ethanol	BDH
Hydrochloric acid	Merck
Hydrazine hydrate	BDH
p-Hydroxybenzoic acid	Fluka
Potassium hydroxide	BDH
n-Propanol	BDH
Pyridine	Merck
Phosphorous oxychloride($POCl_3$)	Fluka
Petroleum ether (40-60 ^{o}c)	BDH
Sodium hydroxide	Fluka
Sodium bicarbonate	BDH
Sulphuric acid	Fluka
Thionyl chloride	Merck

2.2 Instruments and Equipments

- ***Fourier Transform Infrared Spectrometer (FTIR)***

FTIR spectra in the range (4000-400) cm^{-1} were recorded using potassium bromide disc on ***FTIR instrument Model 8300 Shimadzu*** Spectrophotometer, Japan.

- ***Proton Nuclear Magnetic Resonance Spectrometer (^{1}HNMR)***

^{1}H spectra were recorded on a ***Brüker ACF 300*** spectrometer operating at 300MHz, in the university of Exeter, England.

- ***Melting Points***

Uncorrected melting points were recorded on hot stage ***Gallen kamp*** melting point apparatus (U.K.)

- ***Differential Scanning Calorimeter (DSC)***

All DSC measurements were made with a ***Perkin-Elmer DSC-6*** in unsealed aluminum pans in a dry nitrogen atmosphere with an empty aluminum pans as reference. Indium (156.6 ºC) of purity 99.999 standards was used for temperature calibration. These analyses were carried out the in university of Exeter, England.

- ***Hot-stage Polarizing Microscope***

The optical behavior observations were made using ***Olympus BX40*** microscope equipped with a Link – AmTH600 hot stage and PR600 controller. These analyses were carried out in university of Exeter, England.

- ***Gas Chromatograph (GC)***

The gas chromatograph used in this work was ***Pye-Unicam***, England, which has been equipped with flame ionization detector.

- ***Rotary Evaporator***

The rotary evaporator used in evaporating processes of organic solvents, was Buchi 461.

- ***Vacuum Pump***

Vacuum pump type Edwards, 50 Hz, (England), was used for packing the columns.

- ***Shaker***

Shaker type national, 110V, (Japan) was used in packing the columns.

- ***Flow meter***

The flow rate of the carrier gas have been measured using soap bubble flow-meter.

- ***Hydrodynamics Syringe***

Samples were injected using a calibrated 1 ml hydrodynamics syringe type Hamilton 7002 NCH.

- ***Column***

The dimensions of the glass column were 1.75 m in length, 3.0 mm internal diameter (i.d).

2.3 Preparation Procedures

2.3.1 Preparation of compound 2-thiobutanoyl-5-[4-(4´-methoxybenzylideneamino)phenyl]1,3,4-oxadiazole (1_e):

This compound was prepared as shown in the following scheme and as described below:-

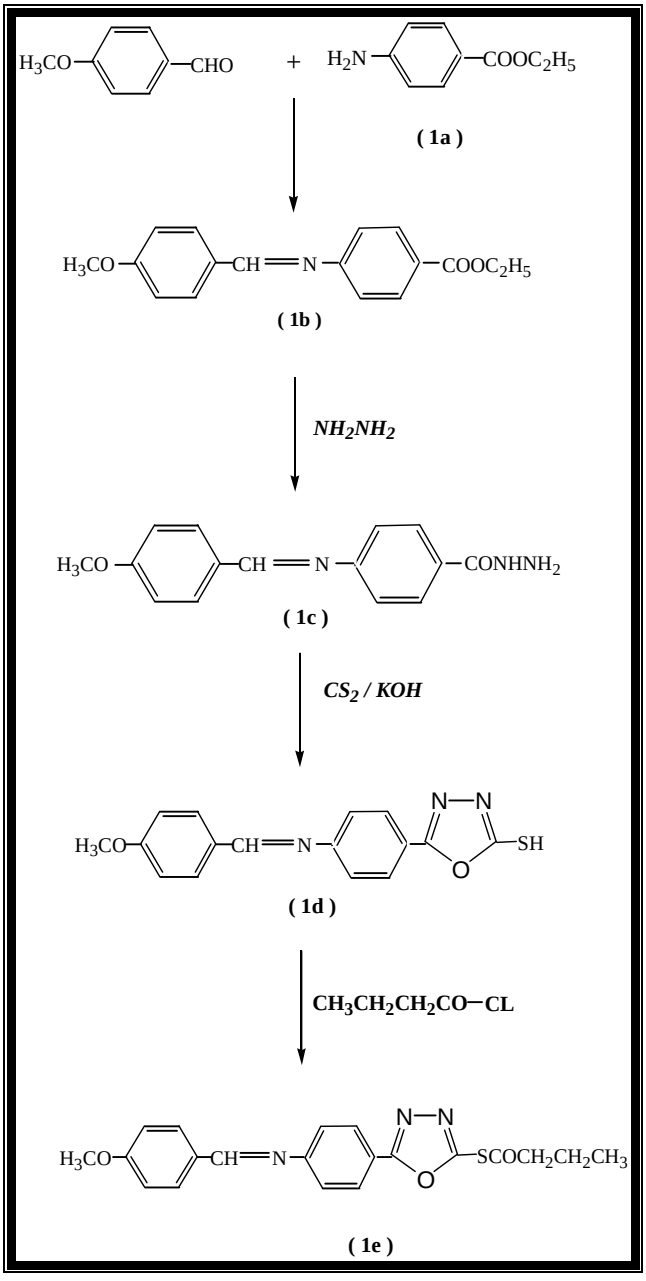

Scheme 2.1 Preparation of compound 2-thiobutanoyl-5-[4-(4´-methoxybenzylideneamino)phenyl]1,3,4-oxadiazole

2.3.1.1 Ethyl-4-amino benzoate(1_a):

This compound was prepared according to the method described in literature[86], as follows:

Dry hydrogen chloride was passed, (which was prepared by the reaction of conc. H_2SO_4 with fused ammonium chloride in a Kipp's apparatus), through 80 mL of absolute ethanol in a 250 mL conical flask equipped with a two-holed cork and wash-bottle tubes until saturated, the increase in weight was about 20g.The solution was transferred to a 250 mL round bottomed flask, 12g of *p*-aminobenzoic acid (0.08 mol)introduced, and the mixture was refluxed for 2 hrs. The hot solution was poured into excess of water and sodium carbonate was added to the clear solution until it is neutral to litmus. The precipitated ester was filtered off at the pump and dried. The yield of ethyl-*p*- amino benzoate, (m.p. = 88- 90ºC) was 70 %.

2.3.1.2 4-(4´-methoxybenzylideneamino)ethyl benzoate (1_b):

Compound 1_b was prepared by the condensation reaction between anisaldehyde(1.36g, 0.01 mol) and compound 1_a (1.65g, 0.01mol) in boiling absolute alcohol (20mL), two drops of glacial acetic acid were added. After reflux for 3hrs., the solid product was filtered and dried. Recrystallization from alcohol gave colored crystals 95% yield, (m.p.=66-68ºC).

2.3.1.3 4-(4´-methoxybenzylideneamino) phenyl acid hydrazide (1_c):

Hydrazine hydrate 15 ml were added to a (1.41g ,5mmol)of 1_b. The mixture was reflux for 4 hr., then 30 mL of ethanol were added and the reflux continued over night. The ethanol were distilled off and the mixture was cooled to room temperature. The obtained solid was

filtered, and washed with cold water. Recrystallization from ethanol yielded 90%, (m.p.= 223-226ºC).

2.3.1.4 5-[4-(4´-methoxybenzylideneamino)phenyl]-2-mercapto 1,3,4-oxadiazole (1_d):

Compound 1_c (1.34g ,5 mmol) was dissolve in 15 mL ethanol at 0 ºC and (0.3g, 5 mmol) of KOH was added. The reaction mixture was stirred for 15 min. then (0.375 mL, 5 mmol) of CS_2 was added. The reaction mixture was refluxed for 7 hr. The ethanol was distilled off using rotary evaporator, then 25mL of cold water was added to the mixture and 15mL 10% HCL. Crystals were precipitated , filtered , recrystallized from ethanol yield 75%, (m.p.= 230-234ºC).

2.3.1.5 2-thiobutanoyl-5-[4-(4´-methoxybenzylideneamino)phenyl] 1,3,4-oxadiazole (1_e):

Compound 1_d **(**1.55g, 5 mmol) was dissolve in 20mL dry benzene and 10mL triethyl amine were added. Then (0.7mL, 5 mmol) butyryl chloride in 10mL dry benzene was added dropwise at room temperature. The mixture was stirred for 10 hr., then it was poured into 100 mL of 10% HCL. The precipitate was filtered , washed with 10 % $NaHCO_3$ solution and then with water for several times, and dried to yield 75% product, (m.p.= 140-147ºC).

2.3.2 Preparation of compound 4-[4´-(4˝-methoxybenzylideneamion)benzoyloxy]propyl benzoate (2_d)

This compound was prepared as shown in the following scheme and as described below[87]:-

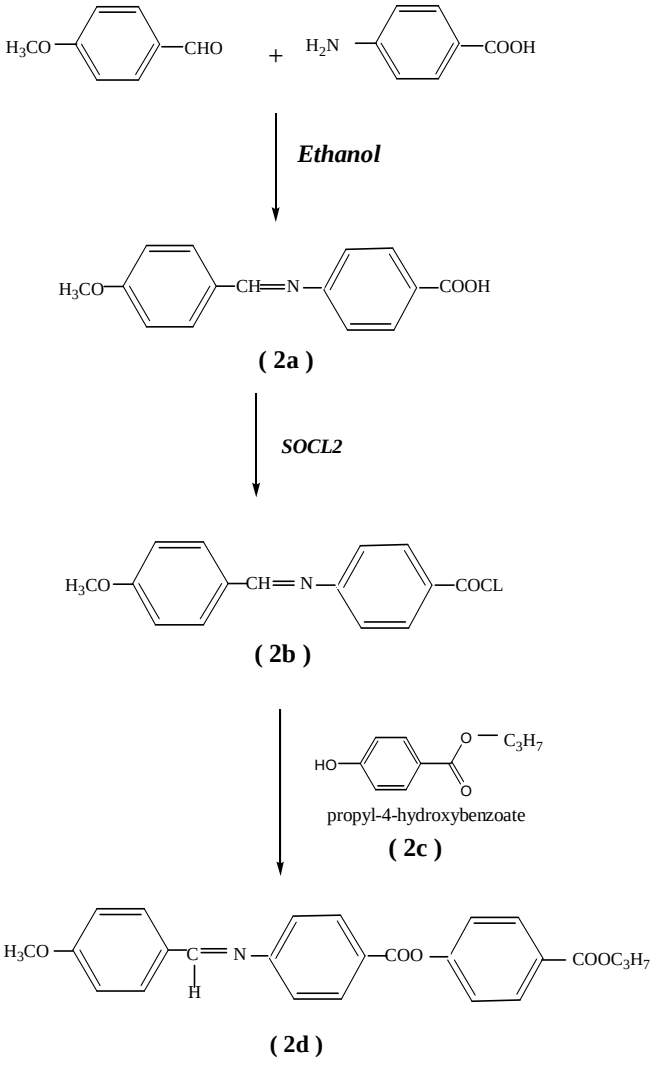

Scheme 2.2 Preparation of compound 4-[4´-(4˝-methoxybenzylideneamino)benzoyloxy]propyl benzoate 2_d

2.3.2.1 4-(4´-methoxybenzylideneamino)benzoic acid (2_a):

Compound 2_a was prepared as in section (2.3.1.2) using 4-aminobenzoic acid instead of ethyl-4-aminobenzoate, the product have (m.p.= 255-258ºC).

2.3.2.2 4-(4´-methoxybenzylideneamino) benzoyl chloride (2_b):

The acid chloride was prepared by refluxing a mixture of 1.25g of 2_a (0.01mol) with excess of thionyl chloride 5mL in the presence of one drop of DMF. After 3hr. the excess thionyl chloride was removed under reduced pressure and the product was filtered and dried to give 99% yield, (m.p.= 175-178ºC).

2.3.2.3 Propyl-4-hydroxybenzoate (2_c)[88]:

4-hydroxy benzoic acid (1.38g, 0.01mol) mixed with 1.8mL propanol , 5mL of dry benzene and 0.54mL conc. H_2SO_4 were refluxed for 10 hr. Then poured into 25mL of water and extracted with ether. The organic layer then treated with saturated sodium bicarbonate solution. The resultant solid washed with water, dried under magnesium sulphate which gave 95% yield, (m.p.= 94-96ºC).

2.3.2.4 4-[4´-(4˝-methoxybenzylideneamino)benzoyloxy]propyl benzoate(2_d):

To a stirred solution of 2_c (0.9g, 0.005 mol) in 20mL dry benzene and 10mL triethyl amine, (1.44g, 0.005 mol) of 2_b in 10mL dry benzene was added drop wise at room temperature. The mixture was stirred for 10 hr., then poured into 100 mL of 10% HCL. The precipitate was filtered , washed with solution of 10 % $NaHCO_3$, and water several times, then dried to yield 65%, (m.p.= 152-153ºC).

2.3.3 Preparation of Compound 2,5-bis-[4-amino phenyl]-1,3,4-oxadiazole 3_d

The route adopted for the synthesis of compound 3_d is given in scheme 2.3 and as described below:

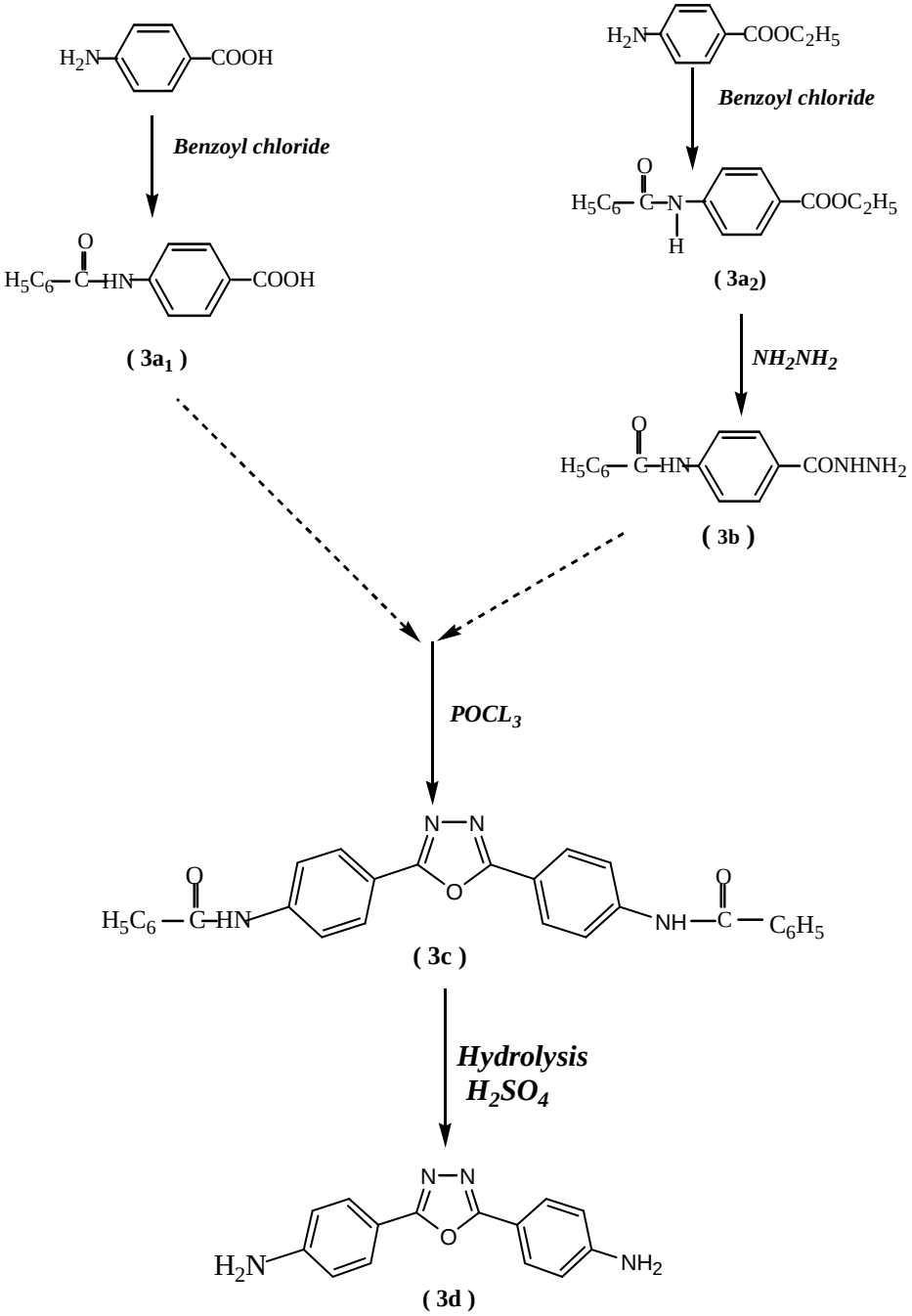

Scheme 2.3 Preparation of compound 2,5-bis-[4-amino phenyl]-1,3,4-oxadiazole 3_d

2.3.3.1 4-carboxybenzanilide (3_{a1}):

4-aminobenzoic acid (1.37g, 0.01 mol) was dissolved in 5mL of 10% NaOH, 1.2 mL cold benzoylchloride (0.01mol) was added to the mixture slowly with constant stirring. The reaction mixture was poured onto cold water, the solid product was filtered off and dried. Recrystallization from ethanol yielded 95%, (m.p.= 289 ºC).

2.3.3.2 4-N-benzoyl ethyl benzoate (3_{a2}):

Compound 1_a (1.65g, 0.01 mol) was dissolved in 5 mL pyridine and (1.2 mL) benzoylchloride. A (0.01mol) was added to the mixture and stirred for 1hr. in ice bath. The reaction mixture was poured in cold water, the solid was separated, filtered and dried. Recrystallization from ethanol yield 95%, (m.p. = 138-140 ºC).

2.3.3.3 4-N-benzoyl phenyl acid hydrazide (3_b):

The same procedure as in part 2.3.1.3 were carried out, using compound 3_{a1} instead of 1_b to yield 3_b.

2.3.3.4 2,5-bis-[benzanilide]-1,3,4-oxadiazole (3_c):

Compound 3_b (1.27g, 0.005mol) and 1.205g of 3_{a1} (0.05mol) with 5mL $POCl_3$ were refluxed for 24 hr.. The cold mixture was poured on crushed ice and made basic by adding $NaHCO_3$ solution. The resulting solid was filtered, dried and recrystallized from chloroform to give the oxadiazole with yield of 70-80%,(m.p. = 200-203ºC).

2.3.3.5 2,5-bis-[4-amino phenyl]-1,3,4-oxadiazole (3_d):

Compound 3_c (1g, 0.04mol) was refluxed with 15 mL of 70%sulphuric acid for 30 min. The mixture was allowed to cool. benzoic acid produced during the reaction was washed with hot water.

The remaining solid benzoic was filtered off and discarded. Render the filtrate alkaline with 10-20% sodium hydroxide solution, cooled, and extracted with ether to yield 65% of 3_d, (m.p.= 196-201ºC).

2.3.3.6 4-alkoxy benzaldehyde[89]:

A mixture of 2.22g 4-hydroxybenzaldehyde (0.01 mol) and 5.52g anhydrous K_2CO_3 (0.04 mol) were dissolved in 8 mL cyclohexanone, to which a (0.016 mol) of appropriate *n*-alkyl bromide was added. The mixture was refluxed with vigorous stirring for overnight. The reaction mixture was filtered and the solvent was distilled off. The product was extracted by adding 25 mL of aqueous 10% KOH and 50 mL ethyl acetate. The organic layer was dried over anhydrous $MgSO_4$ after evaporation the ethyl acetate we obtained the desired product was obtained with 67% yield.

2.3.3.7 2,5-bis-[4-(4´-alkoxybenzylideneamino)phenyl]-1,3,4-oxadiazole :

Compound 3_d (1.26g,0.005 mol) was dissolved in 15 mL ethanol, and 4-alkoxy benzaldehyde (0.01 mol) was added and acidified with two drops of glacial acetic acid. The mixture was reflux for 6 hr. then was allowed to cool at room temperature. The solid product was filtered and recrystallized from alcohol and glacial acetic acid to gave(75-80%)yield. Table 2.1 show the melting point and % yield of the prepared compounds.

Table 2.2 Melting point and %yield of compounds $3_{e1,f1,g1,h1,i1}$.

R-group	Comp. No.	Melting point	% Yield
CH_3	3_{e1}	165-167	80
C_2H_5	3_{f1}	157-159	76
C_3H_7	3_{g1}	153-155	78
C_4H_9	3_{h1}	145-148	80
C_5H_{11}	3_{i1}	135-138	75

2.3.3.8 4-n-alkoxy benzoic acid:

These compounds were prepared as described in literature[90] and as follow:

p-Hydroxybenzoic acid (5 g, 0.01 mol) was dissolved in 20 mL ethanol, 5.1 g KOH (0.09 mol) was added with stirring. The mixture was cooled to room temperature, then (0.165 mol) of appropriate alkyl bromide was added drop wise. The solution was refluxed over neight. Then 1.12 g of KOH (0.02 mol) dissolved in a little amount of water ~5 mL was added to the reaction mixture and heated for 2 hrs.. The solvent was evaporated and equal volume of water was added. The solution was heated till it became clear. Acidification with conc. HCL yielded white precipitate of *p*-n-alkoxybenzoic acid.

2.3.3.9 4-alkoxy benzoyl chloride

The same procedure as in part 2.3.2.2 were carried out, using *p*-n-alkoxybenzoic acid instead of compound 2_a.

2.3.3.10 2,5-bis-[4-(4´-alkoxybenzanilide)phenyl]-1,3,4-oxadiazole (3_f):

Compound 3_d (1.26g, 0.005 mol) was dissolved in (15 mL) dry pyridine, and 4-alkoxy benzoyl chloride (0.01 mol) was added. The mixture was stirred for 4 hrs. in ice bath. The reaction mixture was poured in cold water, the solid which separated was filtered off and dried. Recrystallization from ethanol yielded (85-90%). Table 2.3 show the melting point and % yield of prepared compounds by this method:

Table 2.3 Melting point and %yield of compounds $3_{e2,f2,g2,h2,i2}$.

R-group	Comp. No.	Melting point	% Yield
CH_3	3_{e2}	139-141	90
C_2H_5	3_{f2}	135-138	86
C_3H_7	3_{g2}	121-123	85
C_4H_9	3_{h2}	123-125	88
C_5H_{11}	3_{i2}	119-121	85

2.4 Stationary phase preparation

The stationary phase was prepared by coating each of the liquid crystal compounds on chromosorb W/Aw DMCS 60-80 mesh, solid support. A (2 g) of the liquid crystal compound and (8 g) of the solid support were used. The liquid crystal compound was first dissolved in (50 ml chloroform), the solid support was then added slowly to the solution with stirring to form slurry. The stirring was continued for 24 hours to ensure complete homogeneity and uniform coating of the liquid crystal on the solid support particles. The solvent was then evaporated using rotary evaporator. The resulting stationary phase was then dried at 100ºC for two hrs. the coating percentage was 20% for

each (liquid crystal) stationary phase. The columns were packed with these stationary phases and conditioned as follows. The column was maintained at (10-15^{o}C) below the liquid crystal melting point with a stream of nitrogen gas passing through the column. The column was kept for 10 hrs at these conditions. The above conditioning procedure was repeated for about 1.5-2 hrs. prior each analysis to ensure good reproducibility as indicated from the base line stability. In addition the column was weighted before and after packing to ensure complete and consistent packing.

2.5 The Packing Process and the Working Condition Tests

The glass column were packed by 20% (loading percent) of the two different liquid crystal stationary phases. the methodology of packing process is as described below.

A glass wool was inserted at one end of the column, were it connected directly to a vacuum pump. A plastic funnel was fixed on the top of the other end. After drying the freshly prepared stationary phases, they were added into the column through the funnel to ensure a complete and homogeneous packing. A vibration was used in addition to the vacuum pump. This would reduce the porosity between particles of stationary phases and eliminate all dead spaces in the column. At the completion of packing process, a glass wool was then inserted at the other end of the column.

Soap-bubble flow meter was used to measure the flow rate of the carrier gas, by connecting it to the outlet form the detector.

Before making any analysis in the newly packed column, a heat conditioning process for at least two days has been carried out. This

column conditioning was vital to discard the remaining solvent, humidity and any other volatiles[91a].

Each stationary phase was examined separately by increasing column temperature 20ºC between each run to cover the whole transition temperature ranges of the specific liquid crystal. A 1 μL of each sample was introduced to gas chromatograph by direct injection, the injector temperature was 275ºC with flow rate 25 mL/min.

CHAPTER ONE

INTRODUCTION

CHAPTER TWO

EXPERIMENTAL

CHAPTER THREE

RESULTS AND DISCUSSION

REFERENCES

Contents

List of Tables		III
List of Figures		**V**
Abstract		**X**
Chapter One		
1.1	**Liquid Crystals**	**1**
1.2	**Characterizing Liquid Crystals**	**3**
1.3	**Liquid Crystal Phases**	**4**
1.3.1	**Thermotropic Phases**	**4**
1.3.1.1	**Nematic Liquid Crystal Phase**	**4**
1.3.1.2	**Chiral Nematic Liquid Crystal Phase**	**5**
1.3.1.3	**Smectic Liquid Crystal Phases**	**5**
1.3.1.4	**Discotic Liquid Crystal Phases**	**6**
1.3.2	**Lyotropic Liquid Crystal Phases**	**7**
1.4	**Characteristic of Liquid-Crystal Stationary Phases**	**8**
1.5	**Physico-Chemical Studies of Liquid-Crystalline Stationary Phases**	**9**
1.6	**The Separation Mechanism on Liquid-Crystalline Stationary Phase**	**13**
1.7	**Factors Effecting the Separation of Components mixtures on Liquid Crystal Stationary Phases**	**17**
1.8	**Literature Survey**	**22**
1.9	**Aim of the Work**	**29**

	Chapter Two	
2.1	**Chemicals**	**30**
2.2	**Instruments and equipments**	**31**
2.3	**Preparation procedures**	**33**
2.4	**Stationary phase preparation**	**42**
2.5	**The packing Process and the Working Condition**	**43**
	Chapter Three	
3.1	**Synthesis and Characterization of compound 2-thio - butanoyl-5-[4-(4´-methoxy benzylidene amino) - phenyl]1,3,4-oxadiazole (1_e)**	**45**
3.2	**Synthesis and Characterization of 4-[4´-(4˝-methoxy benzylideneamino)benzoyloxy]propyl benzoate (2_d)**	**54**
3.3	**Synthesis and Characterization of Compound 2,5-bis-[4-amino phenyl]-1,3,4-oxadiazole (3_d)**	**58**
3.4	**Synthesis and Characterization of Compounds 2,5-bis-[4-(4´-alkoxybenzylideneamino)phenyl]-1,3,4-oxadiazole (3_{e1} -3_{i1})**	**64**
3.5	**Synthesis and Characterization of Compounds 2,5-bis-[4-(4´-alkoxybenzanilide)phenyl]-1,3,4-oxadiazole (3_{e2}-3_{i2})**	**68**
3.6	**Liquid Crystalline Properties of the Synthesize Compounds**	**73**
3.7	**Column Chromatography**	**82**
	Reference	**110**

List of Tables

2.1	**Chemicals and their manufactures.**	**30**
2.2	**Melting point and %yield of compounds $3_{e1,f1,g1,h1,i1}$.**	**41**
2.3	**Melting point and %yield of compounds $3_{e2,f2,g2,h2,i2}$.**	**42**
3.1	**FTIR spectral data (cm^{-1}) using KBr disc for the synthesized compounds 3_{e1}–3_{i1}**	**65**
3.2	**FTIR spectral data (cm^{-1}) using KBr disc for the synthesized compounds 3_{e2}–3_{i2}**	**69**
3.3	**The liquid crystal stationary phases**	**81**
3.4	**The time of unretened species t_m of Ethanol**	**82**
3.5	**Adjusted retention times (t'_R / minute) for mixture A on 20% 2-thio -butanoyl-5-[4-(4´-methoxybenzylideneamino)phenyl] 1,3,4-oxadiazol -e (1_e)**	**86**
3.6	**Adjusted retention times (t'_R / minute) for mixture B on 20% 2-thiobutanoyl-5-[4-(4´-methoxybenzylideneamino)phenyl]1,3,4-oxadiazole (1_e)**	**87**
3.7	**Resolution R_s for mixture A on 1_e .**	**89**
3.8	**Resolution R_s for mixture B on 1_e .**	**89**
3.9	**Selectivity factor (α) for mixture A on 1_e**	**90**
3.10	**Selectivity factor (α) for mixture B on 1_e**	**90**
3.11	**The effective plate number (N_{eff}) for mixture A on 1_e**	**91**
3.12	**The effective plate number (N_{eff}) for mixture B on 1_e**	**91**
3.13	**Adjusted retention times (t'_R / minute) for mixture A on 20% 4-[4´-(4˝methoxybenzylideneamino)benzoyloxy]propyl benzoate (2_d)**	**93**

3.14	**Adjusted retention times (t'_R / minute) for mixture B on 20% 4-[4´-(4˝methoxybenzylideneamino)benzoyloxy]propyl benzoate (2_d)**	**94**
3.15	**Selectivity factor α for mixture A on 2_d .**	**94**
3.16	**Selectivity factor α for mixture B on 2_d .**	**95**
3.17	**Resolution R_s for mixture A on 2_d .**	**95**
3.18	**Resolution R_s for mixture B on 2_d .**	**95**
3.19	**The effective plate number (N_{eff}) for mixture A on 2_d**	**96**
3.20	**The effective plate number (N_{eff}) for mixture B on 2_d**	**96**
3.21	**Adjusted specific retention volume (V'_R) for mixture A on 20% 2-thiobutanoyl-5-[4-(4´-methoxybenzylideneamino)phenyl]1,3,4-oxadiazole (1_e)**	**98**
3.22	**Adjusted specific retention volume (V'_R) for mixture B on 20% 2-thiobutanoyl-5-[4-(4´-methoxybenzylideneamino)phenyl]1,3,4-oxadiazole (1_e)**	**98**
3.23	**Adjusted specific retention volume (V'_R) for mixture A on 20% 4-[4´-(4˝methoxybenzylideneamino)benzoyloxy]propyl benzoate (2_d)**	**98**
3.24	**Adjusted specific retention volume (V'_R) for mixture B on 20% 4-[4´-(4˝methoxybenzylideneamino)benzoyloxy]propyl benzoate (2_d)**	**99**
3.25	**The solute activity coefficient (γ) for mixture A on 20% 2-thiobutanoyl-5-[4-(4´-methoxybenzylideneamino)phenyl]1,3,4-oxadiazole (1_e)**	**102**
3.26	**The solute activity coefficient (γ) for mixture B on 20% 2-thiobutanoyl-5-[4-(4´-methoxybenzylideneamino)phenyl]1,3,4-oxadiazole (1_e)**	**103**
2.27	**The solute activity coefficient (γ) for mixture A on 20% 4-[4´-(4˝methoxybenzylideneamino)benzoyloxy]propyl benzoate (2_d)**	**103**

3.28	The solute activity coefficient (γ) for mixture B on 20% 4-[4´-(4˝methoxybenzylideneamino)benzoyloxy]propyl benzoate (2_d)	103
3.29	The Gibbs free energy (ΔG), Enthalpy (ΔH) and entropy (ΔS) of mixture A on 20% 2-thiobutanoyl -5-[4-(4´- Methoxybenzylidene amino)phenyl]1,3,4-oxadiazole (1_e)	108
3.30	The Gibbs free energy (ΔG), Enthalpy (ΔH) and entropy (ΔS) of mixture B on 20% 2-thiobutanoyl-5-[4-(4´- Methoxybenzylidene -amino)phenyl]1,3,4-oxadiazole (1_e)	109
3.31	The Gibbs free energy (ΔG), Enthalpy (ΔH) and entropy (ΔS) of mixture A on 20% 4-[4´-(4˝methoxybenzylideneamino) benzoyloxy]propyl benzoate (2_d)	110
3.32	The Gibbs free energy (ΔG), Enthalpy (ΔH) and entropy (ΔS) of mixture B on 20% 4-[4´-(4˝methoxybenzylideneamino) benzoyloxy]propyl benzoate (2_d)	111

List of Figures

1.1	Alignment of the molecules for solid, liquid crystal and liquid phases.	1
1.2	Typical temperature dependence of the liquid crystals order parameter with temperature. T_{k-I} is the nematic- isotropic transition temperature.	2
1.3	Molecular arrangement of nematic phase.	4
1.4	Schematic of chiral nematic liquid crystal	5
1.5	Molecular arrangement of different types of smectic phases.	5
1.6	Schematic representation of columnar discotic liquid crystal phase	6
1.7	Schematic patterns of lyotropic mesophase	7

3.1	**FTIR spectrum of compound ethyl-4-amino benzoate (1_a)**	**46**
3.2	**FTIR spectrum of compound 4-(4′-methoxybenzylideneamino)ethyl benzoate (1_b)**	**47**
3.3	**FTIR spectrum of compound 4-(4′-methoxybenzylideneamino) phenyl acid hydrazide (1_c)**	**48**
3.4	**FTIR spectrum of compound 5-[4-(4′-methoxybenzylidene-amino)phenyl]-2-mercapto 1,3,4-oxadiazole (1_d)**	**50**
3.5	**^{1}HNMP spectrum of compound 5-[4-(4′-methoxy benzylidene-amino) phenyl]-2-mercapto 1,3,4-oxadiazole (1_d)**	**51**
3.6	**FTIR spectrum of compound 2-thiobutanoyl-5-[4-(4′-methoxy-benzylideneamino)phenyl]1,3,4-oxadiazole (1_e)**	**52**
3.7	**^{1}HNMP spectrum of compound 2-thiobutanoyl-5-[4-(4′-methoxy-benzylideneamino)phenyl]1,3,4-oxadiazole (1_e)**	**53**
3.8	**FTIR spectrum of compound 4-(4′-methoxybenzylideneamino)-benzoic acid (2_a)**	**55**
3.9	**FTIR spectrum of compound Propyl-4-hydroxybenzoate (2_c)**	**56**
3.10	**FTIR spectrum of compound 4-[4′-(4″-methoxybenzylidene-amino)benzoyloxy]propyl benzoate (2_d)**	**57**
3.11	**^{1}HNMR spectrum of compound 4-[4′-(4″-methoxybenzylidene-amino)benzoyloxy]propyl benzoate (2_d)**	**58**
3.12	**FTIR spectrum of compound 4-carboxybenzanilide (3_{a1})**	**59**
3.13	**FTIR spectrum of compound 4-N-benzoyl ethyl benzoate (3_{a2})**	**60**
3.14	**FTIR spectrum of compound 4-N-benzoyl phenyl acid hydrazide (3_b)**	**62**

3.15	**FTIR spectrum of compound 2,5-bis-[benzanilide]-1,3,4-oxadiazole 3_c**	**63**
3.16	**FTIR spectrum of compound 2,5-bis-[4-amino phenyl]-1,3,4-oxadiazole (3_d)**	**64**
3.17	**FTIR spectrum of compound 2,5-bis-[4-(4´-butoxybenzylidene-amino)phenyl]-1,3,4-oxadiazole (3_{h1})**	**65**
3.18	**^{1}HNMR spectrum of compound 2,5-bis-[4-(4´-methoxybenzylideneamino)phenyl]-1,3,4-oxadiazole (3_{e1})**	**66**
3.19	**^{1}HNMR spectrum of compound 2,5-bis-[4-(4´-propoxybenzylideneamino)phenyl]-1,3,4-oxadiazole (3_{g1})**	**67**
3.20	**FTIR spectrum of compound 2,5-bis-[4-(4´-propoxybenzanilide)phenyl]-1,3,4-oxadiazole 3_{g2}**	**69**
3.21	**^{1}HNMR spectrum of compound 2,5-bis-[4-(4´-methoxybenzanilide) -phenyl]-1,3,4-oxadiazole (3_{e2})**	**70**
3.22	**^{1}HNMR spectrum of compound 2,5-bis-[4-(4´-propoxybenzanilide) -phenyl]-1,3,4-oxadiazole (3_{g2})**	**71**
3.23	**Nematic texture of model compound 2-thiobutanoyl-5-[4-(4´-methoxybenzylideneamino)phenyl]1,3,4-oxadiazole (1_e)**	**73**
3.24	**DSC Thermogram of compound 2-thiobutanoyl-5-[4-(4´-methoxy -benzylideneamino)phenyl]1,3,4-oxadiazole (1_e)**	**73**
3.25	**a- Nematic texture of model compound 4-[4´-(4˝-methoxy -benzylideneamino)benzoyloxy]propyl benzoate (2_d)** **b- Smectic A texture of model compound 4-[4´-(4˝-methoxy -benzylideneamino)benzoyloxy]propyl benzoate (2_d)**	**74**

3.26	**DSC Thermogram of compound 4-[4´-(4˝-methoxybenzylidene -amino)benzoyloxy]propyl benzoate (2_d)**	**75**
3.27	**Nematic texture of model compound 2,5-bis-[4-(4´-propoxy -benzylideneamino)phenyl]-1,3,4-oxadiazole (3_{g1})**	**78**
3.28	**DSC Thermogram of compound 2,5-bis-[4-(4´-propoxybenzylidene -amino)phenyl]-1,3,4-oxadiazole (3_{g1})**	**78**
3.29	**Nematic texture of model compound 2,5-bis-[4-(4´-propoxy -benzanilide)phenyl]-1,3,4-oxadiazole (3_{g2})**	**80**
3.30	**DSC Thermogram of compound 2,5-bis-[4-(4´-propoxy -benzanilide)phenyl]-1,3,4-oxadiazole (3_{g2})**	**80**
3.31	**Effect of mobile phase flow rate on plate height for positional isomers (cresols).**	**83**
3.32	**Chromatogram of positional isomers (cresols) of 2-thiobutanoyl-5-[4-(4´methoxybenzylideneamino)phenyl]1,3,4-oxadiazole 1_e**	**84**
3.33	**Chromatogram of PAHs mixture B of 20% 2-thiobutanoyl-5-[4-(4´methoxybenzylideneamino)phenyl]1,3,4-oxadiazole (1_e)**	**85**
3.34	**Chromatogram of PAHs mixture B on 20% PEG**	**86**
3.35	**Chromatogram of positional isomers (cresols) mixture A of 20% 4-[4´-(4˝methoxybenzylideneamino)benzoyloxy]propylbenzoate(2_d)**	**92**
3.36	**Chromatogram of PAHs mixture B of 20% 4-[4´-(4˝methoxybenzylideneamino)benzoyloxy]propylbenzoate(2_d)**	**93**
3.37	**Natural logarithm retention volume (ln V'_R) versus reciprocal absolute temperature for mixture A on 20% 2-thiobutanoyl-5-[4-(4´methoxybenzylideneamino)phenyl]1,3,4-oxadiazole (1_e).**	**99**
3.38	**Natural logarithm retention volume (ln V'_R) versus reciprocal absolute temperature for mixture B on 20% 2-thiobutanoyl-5-[4-(4´methoxybenzylideneamino)phenyl]1,3,4-oxadiazole (1_e)**	**100**

3.39	**Natural logarithm retention volume (ln V'_R) versus reciprocal absolute temperature for mixture A on 20% coating 4-[4´-(4˝methoxybenzylideneamino)benzoyloxy]propyl benzoate(2_d).**	**100**
3.40	**Natural logarithm retention volume (ln V'_R) versus reciprocal absolute temperature for mixture B on 20% coating 4-[4´-(4˝methoxybenzylideneamino)benzoyloxy]propyl benzoate(2_d).**	**101**
3.41	**The logarithm of solute activity factor (log γ) versus reciprocal absolute temperature for mixture A on 20% 2-thiobutanoyl-5-[4-(4´methoxybenzylideneamino)phenyl]1,3,4-oxadiazole 1_e.**	**104**
3.42	**The logarithm of solute activity factor (log γ) versus reciprocal absolute temperature for mixture B on 20% 2-thiobutanoyl-5-[4-(4´methoxybenzylideneamino)phenyl]1,3,4-oxadiazole 1_e.**	**105**
3.43	**The logarithm of solute activity factor (log γ) versus reciprocal absolute temperature for mixture A on 20% 4-[4´-(4˝methoxy - benzylideneamino)benzoyloxy]propyl benzoate(2_d).**	**105**
3.44	**The logarithm of solute activity factor (log γ) versus reciprocal absolute temperature for mixture B on 20% 4-[4´-(4˝methoxy-benzylideneamino)benzoyloxy]propyl benzoate(2_d).**	**106**

Abstract

This thesis consists of the synthesis of new liquid crystalline compounds 2-thiobutanoyl-5-[4-(4´-methoxybenzylideneamino)phenyl]1,3,4-oxadiazole 1_e, 4-[4´-methoxyben- zylideneamion)benzoyloxy]propylbenzoate 2_d and two new homologous series derived from 2,5-bis-[4-amino phenyl]-1,3,4-oxadiazole 3_d, these are 2,5-bis-[4-(4´-alkoxybenzylideneamino)phenyl]-1,3,4-oxadiazole 3_{e1}-3_{i1} and 2,5-bis-[4-(4´-alkoxybenzanilide)phenyl]-1,3,4-oxadiazole 3_{e2}-3_{i2}.

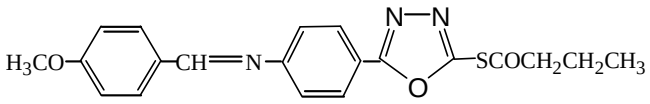

1_e

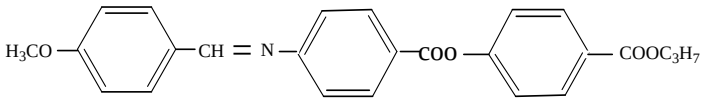

2_d

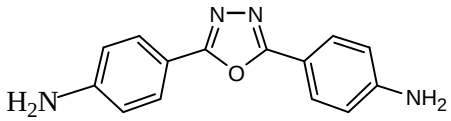

3_d

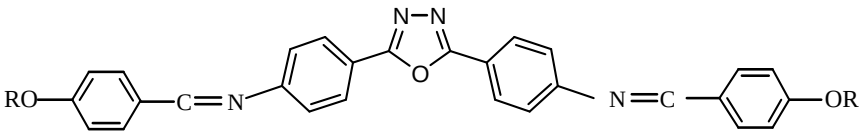

($3_{e1,f1,g1,h1,i1}$)

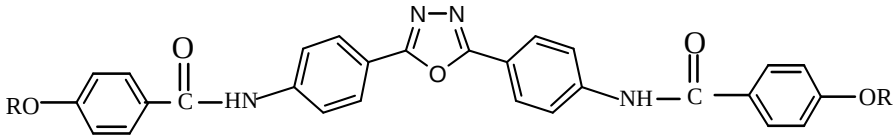

($3_{e2,f2,g2,h2,i2}$)

The characterization of the synthesized compounds using FTIR and ^{1}HNMR spectroscopy and the liquid crystalline properties of the prepared compounds which were verified using differential scanning calorimeter (DSC) and hot-stage polarizing microscope were discussed. The relation between the liquid crystalline behavior with chemical constitution was discussed on the basis of introduction of the heterocyclic unit, i.e., 1,3,4-oxadiazole. It was found that the replacement of aromatic rings by heterocyclic moiety play an important role in effecting the planarity, polarizibility and linearity which in turn effecting the thermal liquid crystalline stability. Compounds 1_e and 2_d were used as stationary phases in gas chromatography for separation of positional isomer hydrocarbons (o-, m-, *p*-cresol) and poly aromatic hydrocarbons (naphthalene, flourene, phenanthrene and anthracene).

Stationary phases for gas chromatography were prepared by loading the above compounds on solid support (chromosorb W/AW 60-80 mesh) at 20%. These stationary phases were packed on glass gas chromatographic columns. A gas- liquid chromatographic study of the interaction and elution characteristics of positional isomer hydrocarbons and poly aromatic hydrocarbons using liquid crystalline phases and at different column temperatures of 140ºC-300ºC for 2-thiobutanoyl-5-[4-(4´-methoxybenzylideneamino)phenyl]1,3,4-oxadiazole 1_e and 140ºC -260ºC for 4-[4´-methoxybenzylideneamion)benzoyloxy]propyl benzoate 2_d.

The best chromatographic conditions for the separation of hydrocarbons were characterized by measuring column efficiency N_{eff}, resolution R, and selectivity factors α in order to assess the performance and separation ability of these columns. It was found that best chromatographic performance can be achieved with operating temperature at which the thermal stability of the nematic mesophase starts to form. Specific retention volume V'_R calculated from the experimental retention time. Abnormal Chromatographic behavior, has been observed, an increase in V'_R and an important separation of aromatic hydrocarbons above the nematic temperature. From the plots of ln V'_R versus 1/T (K^{-1}), it is concluded that this behavior may be attributed to the penetration of solutes (aromatic hydrocarbons) through the ordered structure of the mesophase and the rod-like molecules of liquid crystals stationary phases. The study also included measurements of activity coefficient at infinite dilution and thermodynamic functions, Gibbs free energy ΔG, enthalpy ΔH and entropy ΔS of the separated hydrocarbons at the optimum chromatographic condition. The result showed that the dissolution of solutes (cresol isomers and poly aromatic hydrocarbons) on the stationary phases were spontaneous.

References

1- G. Friedel, *Ann. Physic*., **9**, 273 (1977).

2- A. Griffin and J. Johnson, "*Liquid crystals and Ordered Fluids*", Vol:1, plenum Publ. New York, (1976).

3- G.W.Gray, "*Thermotropic Liquid Crystals*", Wiley, New York, (1987).

4- G Brown and J. Wolken, "*Liquid Crystals and Biological Structures*" Academic Press 12, London, (1979).

5- S. Chandrasekhar,B. Sadashiva, K.Suresh, *Pramana*, **9,** 471 (1977).

6- J. Bernal, " *The Physical Basis of Life*", Rou Hedge and Kegan Paul, London, (1951).

7- H. Sackmann, D. Demus, *Mol. Cryst. Liq. Cryst.*, **21,** 239 (1975).

8- S. Fring, "Lyotrobic Liquid Crystals", *Adva. Chem. Ser*. Washigton, (1976).

9- H. Sackmann and D. Demus, *Mol. Cryst. Liq. Cryst.*, **21**, 239 (1975).

10- H. Sackmann, "Advances in Liquid Crystal Resolution Application", Pergamon Press, (1980).

11- S. Chandrashekhar, B. Sadashiva and K. Suresh, *Pramana*, **9**, 471 (1977).

12- D. Willey and G. Brown, *J. Phys. Chem.*, **76**, 99 (1972).

13- Z. Witkiewicz, J. Szule, R. Dabrowcki, *J. Chromatogr.*,**294,** 127 (1984).

14- M. Apfel, G. Janini and C. Smith, *Anal. Chem.*, **57**, 651 (1985).

15- H. Horie, A. Takagi, H. Hasebe, T. Ozawa and K. Ohta, *J. Mater.Chem*., **11**, 1063 (2001).

16- A. Habboush, S. Farroha, A. Kreishan, *J. Chromatogr*. *A*, **664**, 71 (1994).

17- E. Sokolova, A. Vlasov, R. Kozak, *Russ. Chem. Bull.*, **45,** 521 (1996).

18- I. Medina, *Chromatographia*, **35**, 539 (1993).

19- F. Hahne, G. Kraus, H. Zaschke, *J. Chromatogr*., **509**, 85 (1990).

20- T.J. Betts, *J. Chromatogr.*, **936**, 33 (2001).

21- M. Abalos, X. Prieto and J. Bayona, *J. Chromatogr*. *A*, **963**, 249 (2002).

22- T.J. Betts, *J. Chromatogr*., **605**, 276 (1992).

23- F. Ammar-Khodja, S. Guermouche, M. Guermouche, J. Bayle, *Chromatographia*, **57**, 249 (2003).

24- S. Boudah, S. Sebih, M. Guermouche, M. Rogalski, J. Bayle, *Chromatographia*, **57,** S307 (2003).

25- M. Sied, D. Lopez, J. Tamarit, M. Barrio, *Liq. Cryst.*, **29**, 57 (2002).

26- Y. Zhou, M. Jaroniec, G. Hann and R. Glipin, *Anal. Chem.,* **66**, 1454 (1994).

27- P. Berdague, F. Perez, J. Courtieu, J. Bayle, S. Guermouche, *J. High Resolut. Chromatogr.*, **18**, 304 (1995).

28- T.J. Betts, *J. Chromatogr*., **469**, 43 (1992).

29- D. Skoog, F. Holler and T. Nieman, "Principles of Instrumental Analysis", Saunders College Puplishing, Fifth Edition, (1998).

30- T.J. Betts, *J. Chromatogr*., **558**, 231 (1990).

31- T.J. Betts, *J. Chromatogr.A*, **743**, 341 (1996).

32- G. Price, I. Shillcock, *Can. J. Chem.*,**73**, 1883 (1995).

33- J. Krupcik, M. Valachovicova, G. Kraus, *J. Chromatogr. A*, **665**, 111 (1994).

34- G. Janini, N. Filfil, *J. Chromatogr*., **469,** 43 (1989).

35- Z. Witkiewicz, J. Oszczudlowski, *J. Chromatogr. A*, **1062**, 155 (2005).

36- P. Berdague, F. Perez, J. Courtieu, J. Bayle, O. Abdelhadi and S. Guermouche, *Chromatographia*, **40**, 581 (1995).

37- O. Ferroukhi, S. Guermouche, S. Sebih, M. Guermouche, P. Berdague, J. Bayle, *J. Chromatogr. A*, **971**, 87 (2002).

38- T. Andronikashvili, Z. Witkiewicz, N. Nadiradze, L. Kiknadze, *Zhur. Fiz. Chimii Akad. Nauk Gruzii*, **22**, 70 (1996).

39- T.J. Betts, C. Moir, A. Tassone, *J. Chromatogr*., **547**, 335 (1992).

40- T.J. Betts, *J. Chromatogr*., **626**, 294 (1992).

41- F. Gritti, G. Felix, , M. Achard, F. Hardouin, *J. Chromatogr. A*, **897,** 131 (2000).

42- P. Jing, Fu, R.-J. Dai, J.-L. Gu, Z. Huang, Y. Chen, *Chromatographia*, **43**, 546 (1996).

43- J. Krupčik, M. Valachovicova, G. Kraus, *J. Chromatogr. A*, **665**, 111 (1994).

44- K. Markides, H. Chang, C. Schregenberger, B. Tarbet, J. Bradshaw and M. Lee, *J. High Resolut. Chromatogr. Chromatogy. Commun*., **8,** 516 (1985).

45- B. Jones, J. Bradshaw, M. Nishioka and M. Lee, *J. Org. Chem*., **49**, 4947 (1984).

46- K. Markides, M. Nishioka, B. Tarbet, J. Bradshaw and M. Lee, *Anal. Chem*., **57**, 311 (1985).

47- Michael, J. Dewar and J. Schroeder, *Paul Haake and Joaquin Mantecon*, **86**, 5233 (1964).

48- N. Smirnov and O. Shcrbakova, *Izv. Vyssh. Uchebn. Zaved. Khim. Teknol*., **29**, 7 (1986).

49- E. Matisova, G. Kraus, A. Kraus, *J. Chromatogr.*,**439**, 381 (1988).

50- A. Zioleck, Z. Witkiewicz and R. Dabrowaki, *J. Chromatogr.*,**299**, 159 (1984).

51- A. Isenberg, G. Kraus and H. Zaschke, *J. Chromatogr*., **292**, 67 (1984).

52- A. Jadhav, K. Naikwadi, S. Rokushika, H. Hatona and M. Ohshema, *J. High Resolut. Chromatogr*. *Chromatogy. Commun.*, **6,** 16 (1983).

53- Z. Suprvnowicz, W. Buda, M. Mardarowicz and A. Patry, *J. Chromatogr.*, **333**, 11 (1985).

54- B. Altoiz and A. Popovski, Kolloidn, Zh., **49**, 419 (1987).

55- N. Berezkin, Gazo. Zhidko. Trierdofaznava Chromatografive, Khimia, Moscow, (1986).

56- W. Marciniak and Z. Witkiewicz, *Bial. Wojsk. Akad. Tech*., **35**, 37 (1986).

57- J. Szule and Z. Witkiewicz, *J. Chromatogr.*, **262**, 141 (1983).

58- U. Richle, T. Fhmann, M. Swerev and K. Ballschmiter, Fresenius, *Z. Anal. Chem.*, **331**, 821 (1988).

59- W. Marciniak and Z. Witkiewicz, *Bial. Wojsk. Akad. Tech*., **35**, 37 (1986).

60- L. Sojak, P. Farkas and I. Ostrovsky, *Ropa. Vhlie*, **25**, 102 (1983).

61- T. Tsvektov, Acta. Physica. Chim. URSS., **16**, 132 (1942).

62- E. Matise, D. Hudec, J. Garaj, G. Kraus, M. Schierhorn and A. Isenberg, *Chromatographia*, **20**, 601 (1985).

63- J. Rayss, Z. . Witkiewicz, A Waksmunadzki and R. Dabrowski, *J. Chromatogr.*, **188**, 107 (1988).

64- H. Kelker, Z. Fresenius, *Anal. Chem.*, **198**, 254 (1963).

65- M. Dewer, J. Schroeder, *J. Am. Chem. Soc.*, **86**, 5235 (1964).

66- E. Barrall, R. Porter and J. Johnson, *Chromatographia*, **21**, 392 (1966).

67- E. Grushka, J. Solsky, *Anal. Chem*., **45,** 48 (1973).

68- E. Grushka, J. Solsky, *J. Chromatogr*., **112**, 145 (1975).

69- C. Lochmüller, R. Souter, *J. Chromatogr*., **87**, 243 (1973).

70- M. Hall, D. Mallen, *J. Chromatogr*., **14**, 451 (1976).

71- M. Hall, D. Mallen, *J. Chromatogr*., **118**, 268 (1976).

72- M. Pailer, V. Hložek, *J. Chromatogr.*, **128**, 163 (1976).

73- G. Kraus, D. Repka, J. Mocak, *J. Chromatogr. A*, **355,** 99 (1986).

74- L. Sojak, G. Kraus, *J. Chromatogr. A*, **436**, 47 (1988).

75- J. Coca, I. Melina, S. Langer, *Chromatographia*, **25**, 825 (1988).

76- T.J. Beetts, *J. Chromatogr*. **605,** 276 (1992).

77- S. Hudson, P. Maitlis, *Chem. Rev*., **93**, 861 (1993).

78- P. Judeinstein, *J. Chromatogr. A*, **859**, 59 (1999).

79- A. Kraus, G. Kraus, I. Ostrowsky, L. Sojak, *Chem. Anal*., **42**, 497 (1997).

80- P. Jing, R. Dai, Z. Huang, *Chromatographia*, **43**, 546 (1996).

81- Q. Xiaotian, Z. Zaide, T. Ying, *Talanta*, **46**, 45 (1998).

82- A. Meddour, J. Courtieu, M. Guermonche, *Chromatographia*, **43**, 387 (1996).

83- P. Judeinstein, M. Berdagué, E. Rogalska , J. Bayle, and M. Guermouche, *J. Mol. Liquids*, **94**, 221 (2001).

84- S. Sebih, S. Boudah, J. Bayle, Proceedings of 24th International Chromatography Symposium, Leipzing, 2002.

85- M. Abdul Munem, A. Al-Haideri and M. Al-Mehdawy, *Tur. J. Chem*., **27**, 259 (2003).

86- A. Vocal, "*A Text Book of Practical Organic Chemistry*", 3rd edit. Longman, London, P 1000 (1974).

87-

88- A. Vocal, "*A Text Book of Practical Organic Chemistry*", 3rd edit. Longman, London, P 775 (1974).

89- C. Weygand, R. Gabler, and N. Bircan, *J. Prakt. Chemie*., **158**, 266 (1941).

90- J. Johnson and R. Port "*Liquid Crystal and Order Fluids*", **Vol.1**, Plenum Press, New York (1970).

91a- J. Porcaro and P. Shubiak, *J. Chromatogr. Sci.*, **9**, 690 (1974).

91b- M. Parra, J. Belmar, H. Zunza, C. Zúñiga, G. Fuentes and R. Martinez, *J. Prakt. Chem*., **337**, 239 (1995).

92- J. Bartulin, R. Martines, H. Műller, Z. Fan and W. Haase, *Mol. Cryst. Liq. Cryst*., **220**, 67 (1992).

93- R. Cai and E. Samulski, *Liq. Cryst*., **9**, 617 (1991).

94- I. Angilini, L. Angilini and F. Sparaco, *British Pat*., **61**, 801 (1969).

95- L. Nygaard, R. Hanzen and J. Nielsen, *J. Molec. Struct*., **12**, 59 (1972).

96- M. Parra, J. Belmar, H. Zunza, C. Zúñiga, G. Fuentes and R. Martinez, *J. Prakt. Chem*., **52b**, 1533 (1997).

97- A. Herbert, *Trans. Faraday Soc*. **63**, 555 (1967).

98- C. Liu, C. Hu and C. Yang, *J. Chromatography A*, **773**, 199 (1997).

99- S. Maki, M. Ali and H. Abed, *J. of Alnahrain*, **3(1)**, 71 (1999).

100- C. Chou, Y. Pai, C. Lin and T. Lin, *J. Chromatography A*, **1043**, 255 (2004).

101- D. Skoog and J. Leary, "Principles of Instrumental analysis, Saunders College Publishing, New York (1992).

102- B. Hillery, J. Girard, M. Schantz, S. Wise, A. Malik and M. Lee, *J. Microcol. Sep.*,**7**, 221 (1995).

103- J. Done, J. Knox and J. Loheac, "Application of High Speed Chromatography", John Wily, London (1974).

104- H. McNair and J. Miller, "Basic Gas Chromatography", John Wily, London (1980).

105- T. J. Betts, *J. Chromatography*. *A,* **936**, 331 (2001).

106- L. Ettre, *J. Chromatography*, **220**, 29 (1981).

107- H. Chang, K. Markides, J. Bradshaw and M. Lee, *J. Chromatogr. Sci.*,**26**, 280 (1988).

108- G. Schomburg, "Advances in Chromatography", Edward Arnold, Pub., London (1968).

109- A. Littlewood, C. Phillips and D. Price, *J. Chem. Soc*., 1480 (1995).

110- L. Ettre, *Pure and Appl. Chem*., **65**, 819 (1993).

111- A. James and A. Martine, *J. Biochem*., **50**, 679 (1952).

112- V. Davankov, *Chromatographia*, **48**, 71 (1998).

113- C. Hi, and C. Liu, *Anal. Chem. Acta*, **332**, 23 (1996).

114- C. Hi, C. Liu, and C. Tang, *J. Chromatogr.A,***773**, 199 (1997).

115- D. Martire and L. Pollara, *Adv. Chromatog*., **1**, 335 (1966).

116- D. Martire, "*Gas Chromatography*", Academic Press, New York (1977).

117- S. Langer and J. Purnell, *J. Phys. Chem*., **67**, 263 (1963).

118- A. Habboush, S. Farroha and A. Kreishan, *J.of High Resol. Chromatography*, **14**, 262 (1991).

References

Republic of Iraqi
Ministry of Higher Education
And Scientific Research
Al-Nahrain University
College of Science
Department of Chemistry

Synthesis and Characterization of Liquid Crystalline Materials as Stationary Phases In Gas –Liquid Chromatography

A thesis
Submitted to the College of Science
Al-Nahrain University
In partial fulfillment of Requirements
For the Degree of Doctor of Philosophy in Chemistry

BY
NASREEN RAHEEM JBER
B.SC. (AL-NAHRAIN UNIVERSITY 1997)
M.SC.(AL-NAHRAIN UNIVERSITY ٢٠٠٠)

November 2005 ***Shawal 1426***

Supervisor certification

We certify that this thesis was prepared under our Supervision in the Department of Chemistry, College of Science, Al-Nahrain university as a partial requirements for the degree of doctor of philosophy in chemistry.

Professor **Assistance Professor**

Dr.Ammar H. Al-Dujaili **Dr. Shahbaz A. Maki**

In view of the available recommendation, I forward this thesis for debate by the Examining Committee.

Assistance Professor
Dr. Shahbaz A. Maki
Head of the
Department of Chemistry
College of Science
Al-Nahrain University

Examining Committee's Certification

We the examining committees, certify that we read this thesis and examined the student ***Nasreen Raheem Jber***, in its contents and that, according to our opinion, is accepted as a thesis for the degree of Doctor of philosophy, in chemistry.

Signature:

Name: Prof. Dr. Yousif Z. Yousif
(Chairman)

Signature:
Name: Prof. Dr. AL-Haidery
(Member)

Signature:
Name: Prof. Dr. Muhanad J. Mohmoud
(Member)

Signature:
Name: Dr. Fadhel M.
(Member)

Signature:
Name: Dr. Sawsan H. Shawkat
(Member)

Signature:
Name: Dr.Ammar H. Al-Dujaili
(Member\advisor)

Signature:
Name: Dr. Shahbaz A. Maki
(Member\advisor)

Approved for the College of Graduate Studies

Assistant Professor
Dr. Laith Abd Al-Aziz
Dean of College of
Science Al-Nahrain
University

Acknowledgement

In my opinion, doing research is like running an off-road track. One can know in which direction wants to go, however, one can not foresee what will be coming along the way. The varying nature of challenges one meets stimulate ones mind and the passage of each obstacle gives a feeling of satisfaction and adds to the excitement of what is to come. Now, close to the finishing line of this run, I would like to address my sincere gratitude to the persons who have accompanied me along the course and those who have been there by the side to support me.

My supervisor Dr. Shahbaz A. Maki and Prof. Dr. Amar H. Al-Dujaili for their supervision, continuous encouragement, advice, discussion and suggestions throughout my study.

Also I would like to direct my deep thanks to my husband for his help and encouragement, and to my husband's family for their invaluable support.

I would like to express my special thanks to Prof. Dr. Duncan Bruce, professor of inorganic chemistry and head of chemistry department in Exeter University, England, for providing me with the ^{1}HNMR spectra, texture observation and DSC thermagrams.

My sincere thanks and appreciation to Dr. Z. Witkiewicz and Dr. J. Oszczudowski for providing me with new references.

I am most grateful for assistance given to me by the staff of chemistry department of Al- Nahrain University, especially Dr. Sawsan H. Shawkat.

Nasreen ♥♥ 2005

الخلاصة

تتضمن الأطروحة تحضير المركبات البلورات السائلة (٢- ثايوبيوتانويل-٥- [٤-(٤´-ميثوكسي بنزيليدين أمينو)فنيل]١،٣،٤-اوكسادايازول (1e)، ٤- [٤´- ميثوكسي بنزيليدين أمينو]بروبوكسي بنزويت (٢_d)، مع تحضير سلسلتين جديدتين مشتقة من المركب ٢،٥-بس-[٤- أمينوفنيل]١،٣،٤-اوكسادايازول (٣_d) وهما ٢،٥-بس-[٤-(٤´-الكوكسي بنزيليدين أمينو)فنيل]١،٣،٤ -اوكسادايازول (٣_{i1}-3 $_{e1}$) و ٢،٥-بس-[٤-(٤´-الكوكسي بنزانلايد)فنيل]١،٣،٤ –اوكسادايازول (٣_{i2}-3 $_{e2}$).

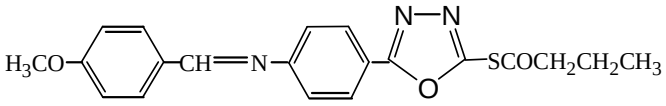

1_e

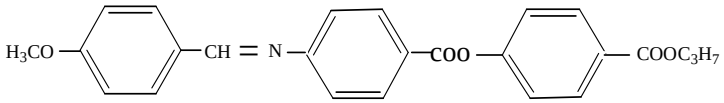

2_d

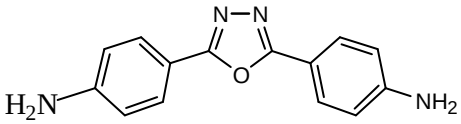

3_d

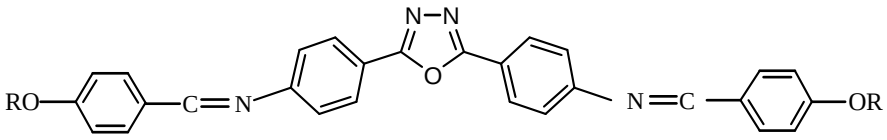

($3_{e1,f1,g1,h1,i1}$)

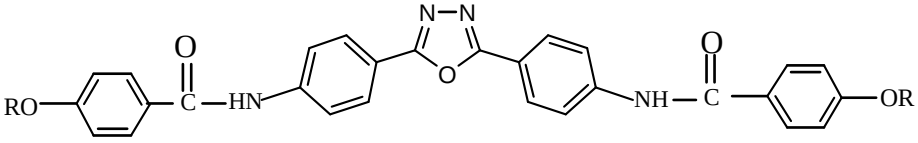

($3_{e2,f2,g2,h2,i2}$)

تم تشخيص المركبات المحضرة بالطرائق الطيفية والمتمثلة بطيف الأشعة تحت الحمراء وطيف الرنين النووي المغناطيسي. كذالك تم دراسة الخواص البلورية السائلة المحضرة باستخدام مسعر المسح التفاضلي ومجهر الضوء المستقطب المزود بمنصة تسخين. تمت دراسة علاقة التركيب الجزيئي بالحالة الميزومورفية والاستقرار الحراري، كذلك تأثير وجود حلقة غير متجانسة والمتمثلة بحلقة ١،٣،٤-اوكسادايازول وتم الاستنتاج بأن استبدال حلقة البنزين بحلقة غير متجانسة يؤدي إلى تغير كبير في الخطية، استقطاب واستوائية الجزيئة. وهذا بدوره يؤثر في الاستقرارية الحرارية للاطوار البلورية السائلة.

تم استخدام المركبات ($_e$ ١ و$_d$ ٢) كأطوار ثابتة في كروماتوغرافيا الغاز لفصل هايدروكاربونات اروماتية .

تم تعبئة أعمدة كروماتوغرافية وذلك بتحميل المواد البلورية السائلة المحضرة على الساند الصلب نوع كروموسورب المغسول حامضياً نوع بنسبة ٢٠%.

تمت دراسة التأثيرات والاستخلاص لكروماتوغرافيا الغاز – السائل للهايدروكاربونات على مدى من درجات الحرارة للطور البلوري السائل الثابت ولكل عمود حيث استخدمت المديات ١٤٠-٣٠٠ مئوية للعمود (٢- ثايوبيوتانويل-٥- [٤-(٤´-ميثوكسي بنزيليدين أمينو)فنيل]١،٣،٤- اوكسادايازول ($_e$ ١) و ١٤٠-٢٦٠ مئوية للعمود - [٤´- ميثوكسي بنزيليدين أمينو]بروبوكسي بنزويت ($_d$٢). تم اختيار ظروف الفصل للأعمدة للهايدروكاربونات وذلك من حساب كفاءة العمود وكفاءة التحليل ومعامل الانتقائية. ولوحظ ان قيم هذه الدوال تكون على احسنها على مدى الطور البلوري السائل النيماتي. ولكل عمود تم حساب الحجم النوعي للحجز وعند رسم اللوغاريتم الطبيعي لهذه الدالة مع معكوس درجة الحرارة. لوحظ ظهور تصرف غير اعتيادي لهذه الأعمدة يظهر بين انتقال الطور البلوري السائل. كما وتم في هذه الدراسة حساب معامل الفعالية عند التخفيف إلى ما لا نهاية والذي أُستخدم لحساب الدوال الثرموداينميكية كطاقة كبس الحرة(Δ G) والانثالبي (Δ H) والانتروبي (Δ S). وكانت قيم طاقة كبس الحرة سالبة مما يؤكد ان عملية ذوبان المذاب (الهايدروكاربونات الاروماتية) تجري بشكل تلقائي .

جمهورية العراق
وزارة التعليم العالي والبحث العلمي
جامعة النهرين
كلية العلوم
قسم الكيمياء

تحضير ودراسة خواص مواد بلورية سائلة كأطوار ثابتة في كروماتوغرافيا الغاز – السائل

رسالة
مقدمة الى كلية العلوم- جامعة النهرين
وهي جزء من متطلبات نيل درجة الدكتوراه فلسفة في الكيمياء

من قبل
نسرين رحيم جبر
بكالوريوس ١٩٩٧ (جامعة النهرين)
ماجستير ٢٠٠٠ (جامعة النهرين)

تشرين الثاني ٢٠٠٥ شوال ١٤٢٦

بِسم الله الرحمن الرحيم

نَـرفَـعُ دَرَجَـاتٍ مَـن نَـشَـاءُ

وَفَـوقَ كُـلِ ذي عِـلمٍ عَـلـيمُ

صَدَقَ اللهُ آلَعَظِيم

سورة يوسف (٧٦)

Chapter Three
Results and Discussion

3.1 Synthesis and Characterization of Compound 2-thiobutanoyl-5-[4-(4´-methoxybenzylideneamino)phenyl]1,3,4-oxadiazole (1_e):

The compound was prepared as previously shown in scheme 2.1.

Ethyl-4-amino benzoate **1_a** was prepared by condensation reaction of 4-amino benzoic acid with HCL saturated ethanol:

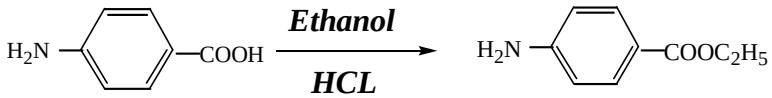

(1a)

The melting point of the compound was 88-90 ºC, the reported melting point 92 ºC[86]. It was also identified by FTIR spectroscopy.

Figure 3.1 shows the FTIR spectrum of **1_a** using KBr disc which showed the following characteristic absorption bands: 3413 cm^{-1} and 3334 cm^{-1} that could be attributed to NH_2 asymmetrical and symmetrical stretching, respectively, and bands at 2975 cm^{-1} and 2891 cm^{-1} due to aliphatic C-H stretching. The carbonyl of the ester appeared at 1683 cm^{-1} while the stretching of C-H aromatic appeared at 840 cm^{-1}.

The compound 4-(4'-methoxybenzylideneamino)ethyl benzoate **1_b** was prepared by the condensation reaction between anisaldehyde and **1_a** in boiling alcohol:

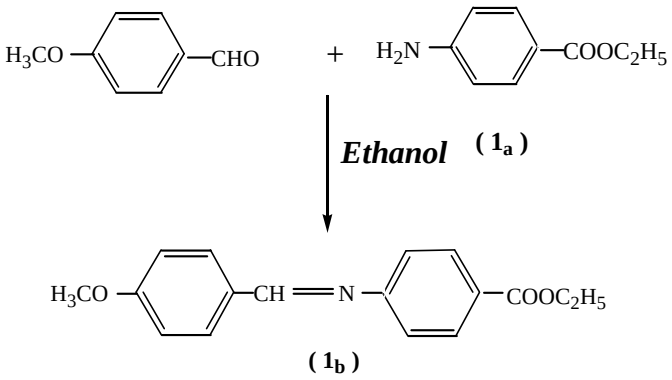

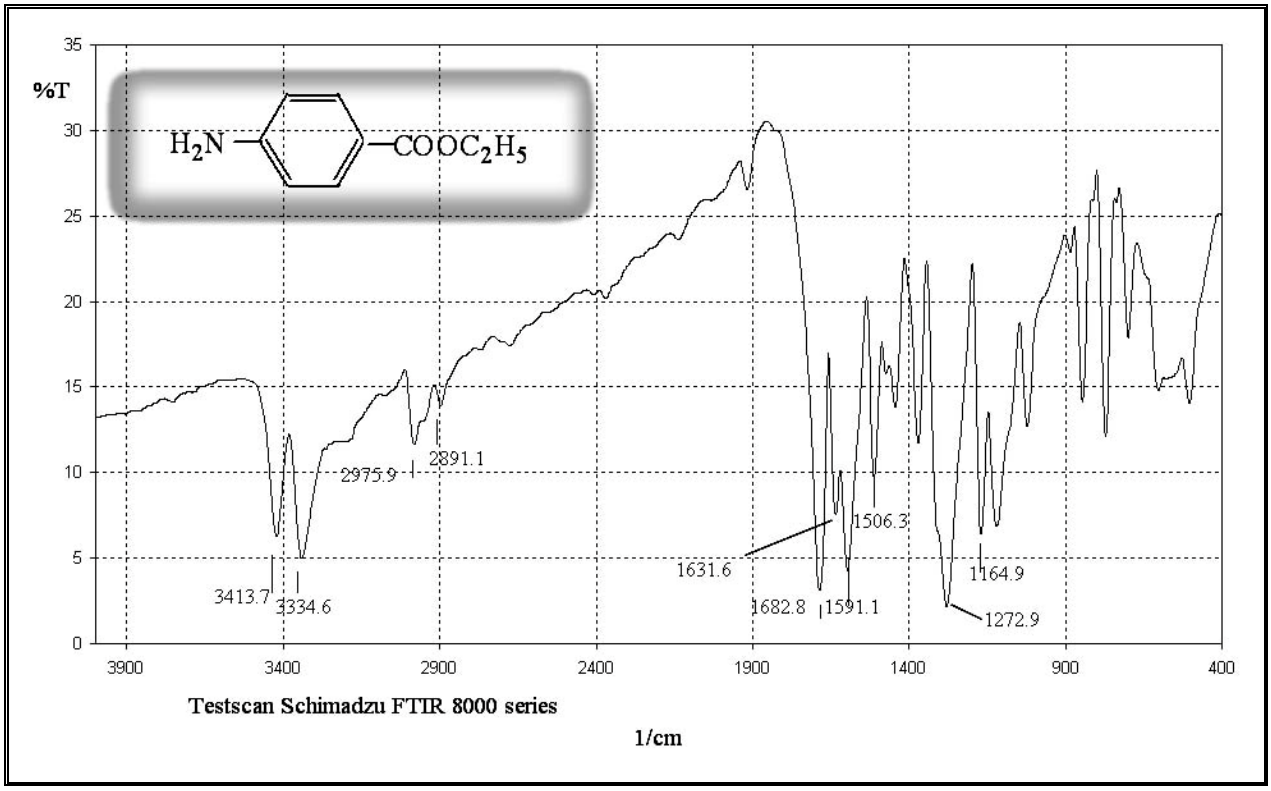

Figure 3.1 FTIR spectrum of compound ethyl-4-amino benzoate (1_a)

Figure 3.2 shows the FTIR spectrum of 1_b using KBr disc which showed the disappearance of the NH_2 bands and the appearance of band at 1587.6 cm^{-1} for C=N stretching.

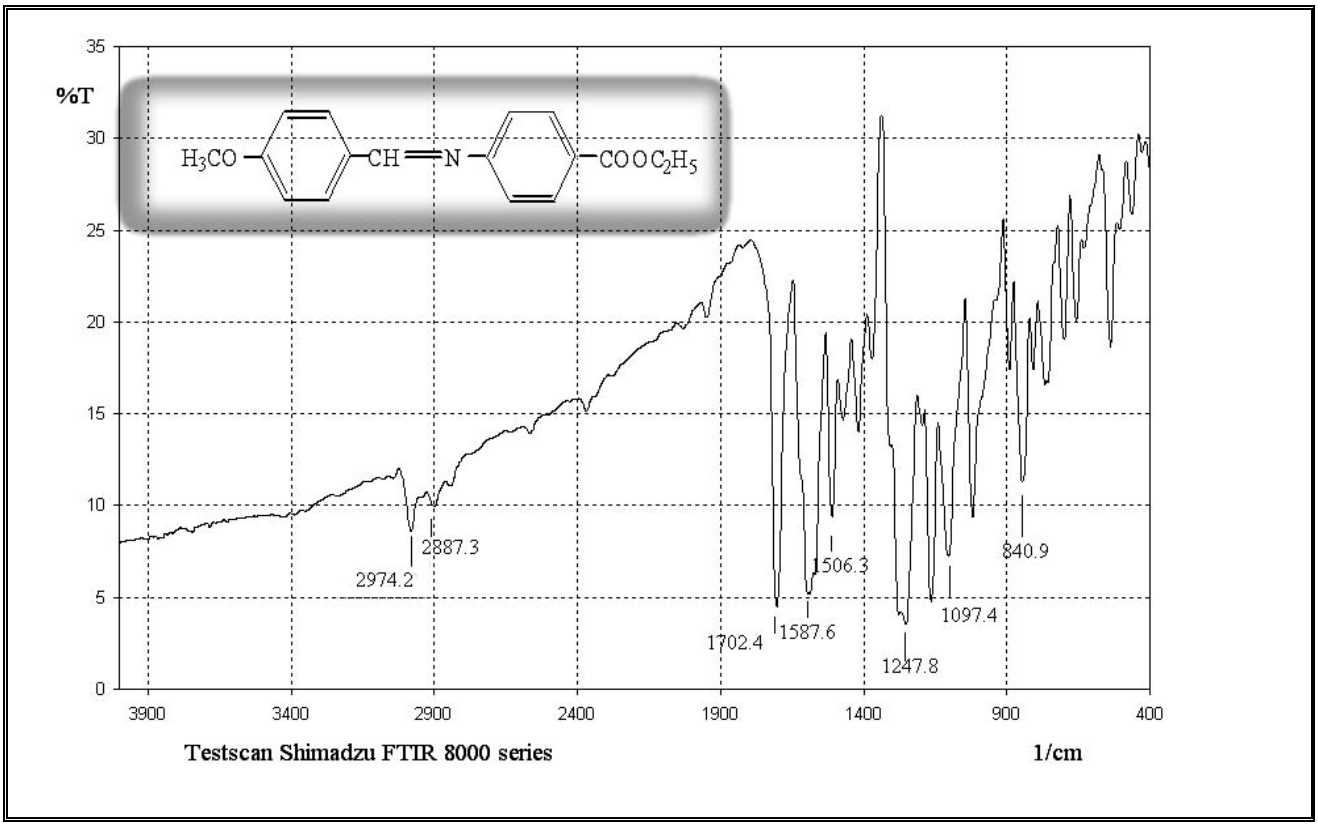

Figure 3.2 FTIR spectrum of compound 4-(4'-methoxybenzylideneamino)ethyl benzoate (1_b)

The 4-(4'-methoxybenzylideneamino) phenyl acid hydrazide $\mathbf{1_c}$ was prepared by the condensation of $\mathbf{1_b}$ with excess hydrazine hydrate in the presence of ethanol as solvent.

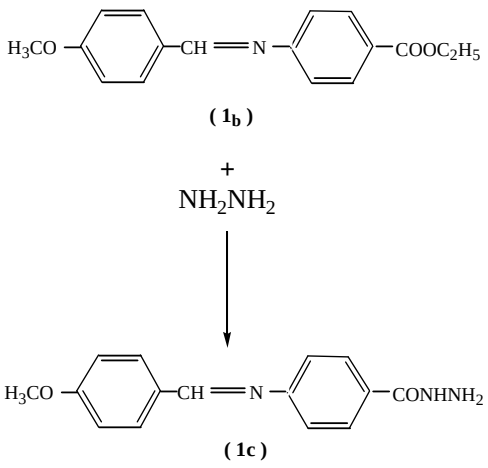

The product was verified by FTIR spectral data. The spectrum is shown in Figure 3.3. The appearance of bands at 3450 cm^{-1}, 3272 cm^{-1} and 3165 cm^{-1} that are due to NH_2 and N–H stretching. A new stretching band appeared at 1685 cm^{-1} which could be attributed to C = O stretching of amide group (amide I) and a band at 1598 cm^{-1} due to N–H bending (amide II).

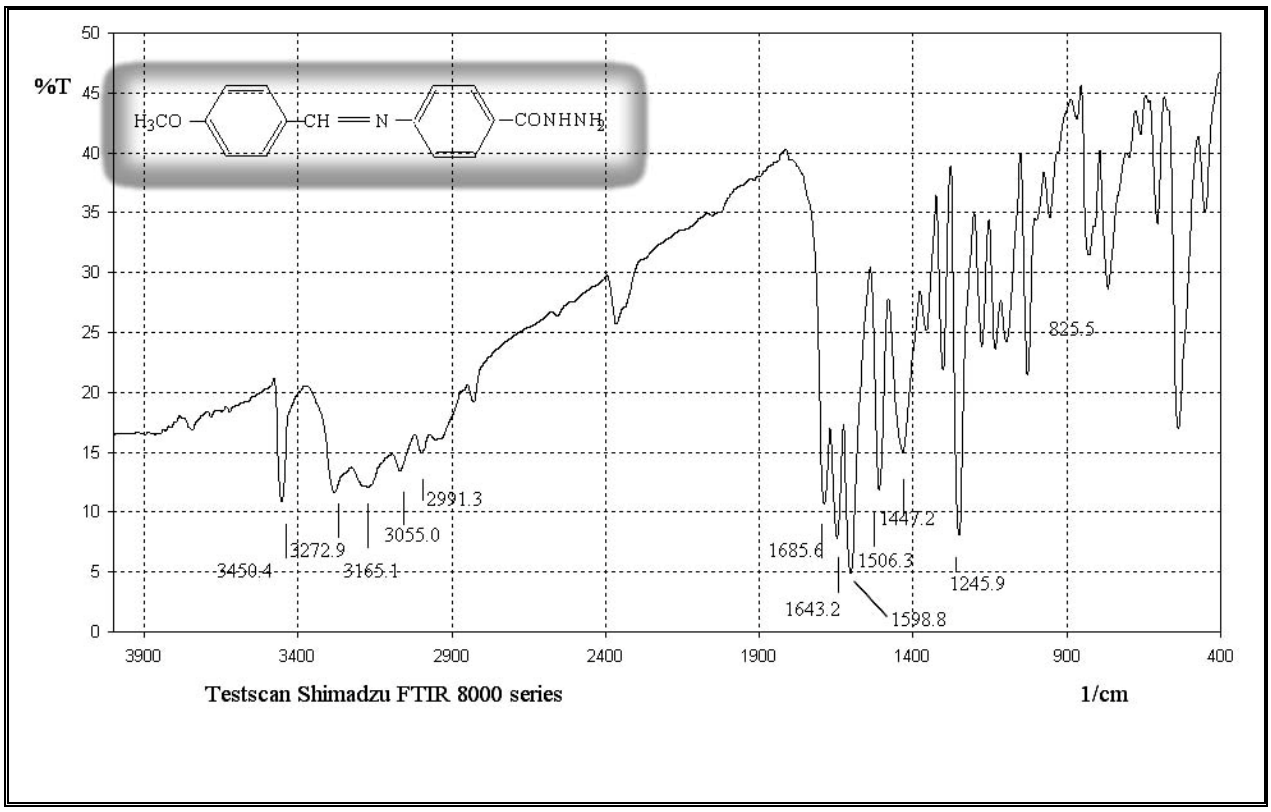

Figure 3.3 FTIR spectrum of compound 4-(4'-methoxybenzylideneamino) phenyl acid hydrazide (1_c)

Compound 5-[4-(4´-methoxybenzylideneamino)phenyl]-2-mercapto 1,3,4-oxadiazole $\mathbf{1_d}$ was prepared by the reaction of compound $\mathbf{1_c}$ with carbon disulfide in the presence of potassium hydroxide.

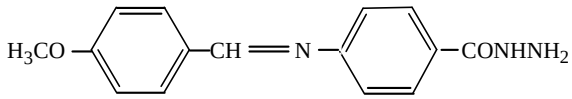

(1c)

+

CS_2 / KOH

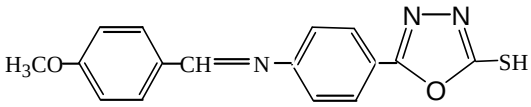

(1d)

The structure of this compound was elucidated by FTIR and ^{1}HNMR spectroscopy. The FTIR spectrum of this compound is shown in Figure 3.4. The spectrum revealed a sulphohydryl absorption band S–H at 2740 cm^{-1} and an absorption N–H stretching band at 3201 cm^{-1} and a new band at 1350 cm^{-1} due to C=S was observe due to the Thiol - Thion equilibrium[(91b)]:

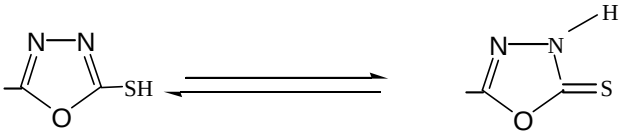

(Thiol) I ***(Thion) II***

The ^{1}HNMR spectrum of compound **1_d,** is shown in Figure 3.5. The following characteristic chemical shifts (DMSO, ppm) were appeared: two pairs of doublet at δ 7.26- 8.1 that could be attributed to the four protons of the alkoxy phenyl ring while the other two doublet at δ 6.6- 7.25 suggesting the attribution of the four protons of the benzene nucleus attached to the heterocyclic ring. ^{1}HNMR spectrum also showed a singlet at δ 9.9 that could be assigned to the thio proton, while the

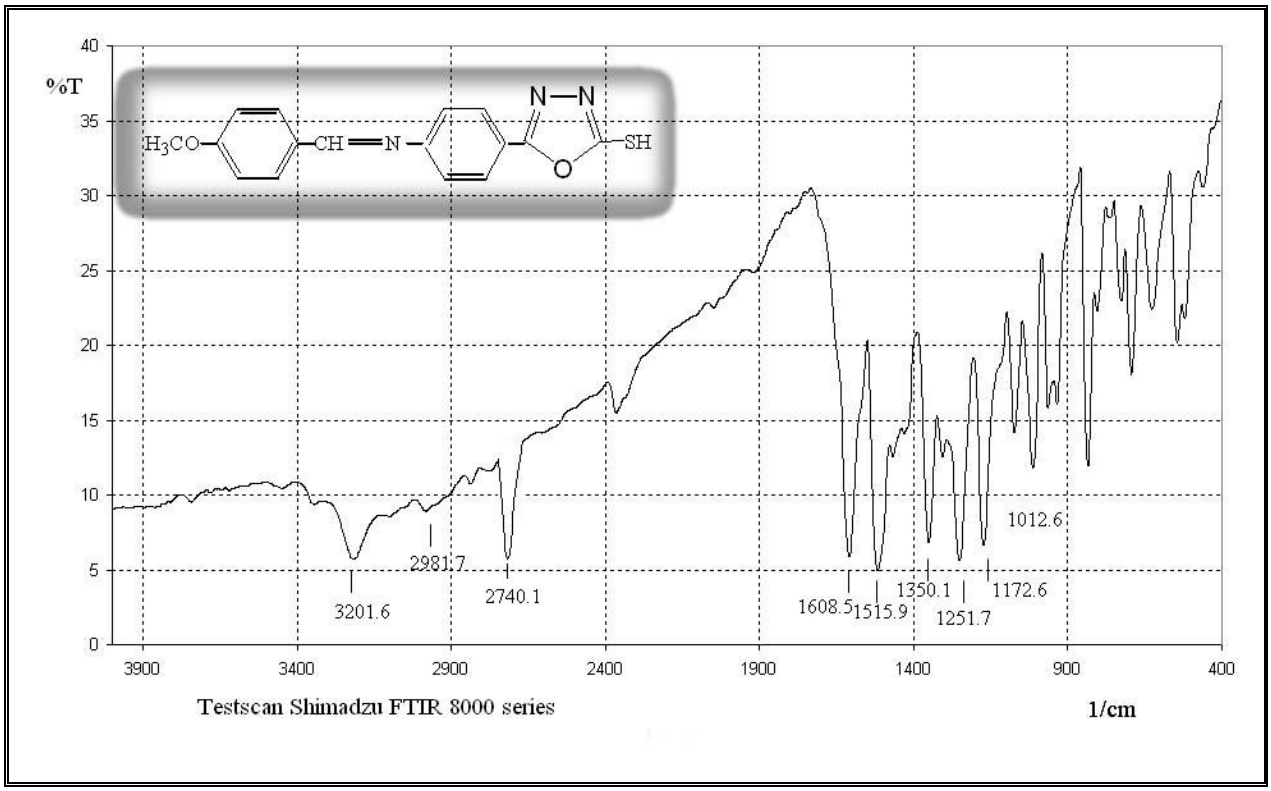

Figure 3.4 FTIR spectrum of compound 5-[4-(4´-methoxybenzylideneamino)phenyl]-2-mercapto 1,3,4-oxadiazole (1_d)

vinylic proton appear at δ 8.6. A three proton singlet at δ 3.8 ppm might be assigned to the $–OCH_3$ group. Therefore, the ^{1}HNMR spectrum of this compound together with the FTIR spectrum were good evidence for the structure suggested for compound 1_d.

The reaction of **1_d** with butyryl chloride yielded 2-thiobutanoyl-5-[4-(4'-methoxybenzylideneamino)phenyl]1,3,4-oxadiazole **1_e**, as shown below;

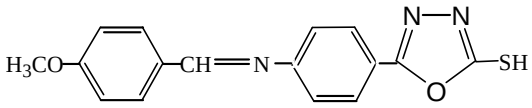

(1_d)

+

$CH_3CH_2CH_2CO-CL$

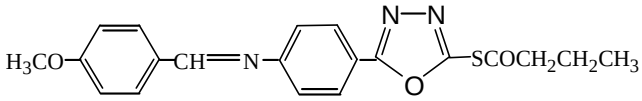

(1_e)

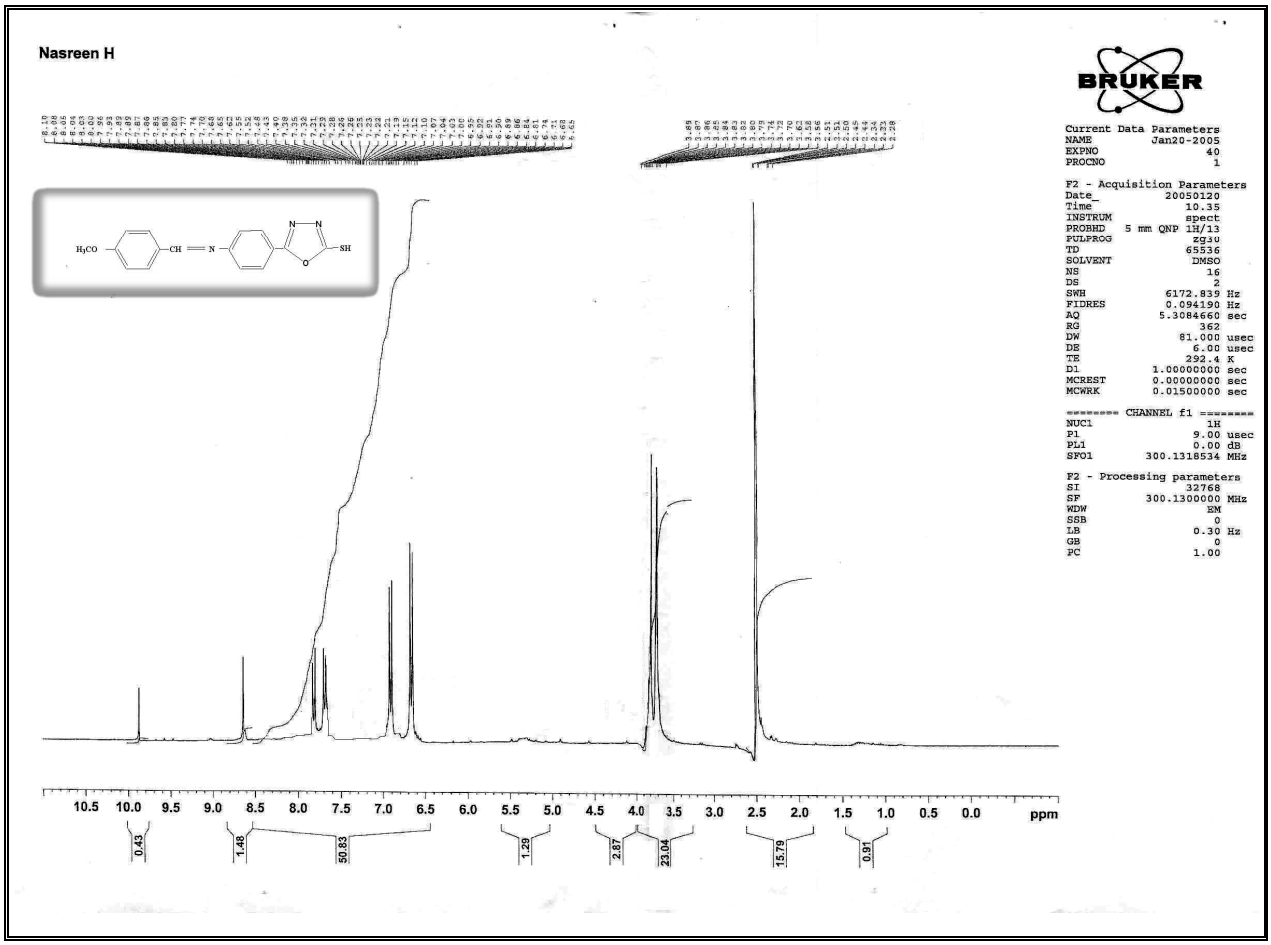

Figure 3.5 ^{1}HNMP spectrum of compound 5-[4-(4$^{'}$-methoxybenzylideneamino)phenyl]-2-mercapto 1,3,4-oxadiazole (1_d)

The product was characterized by FTIR and ^{1}HNMR spectroscopy. The FTIR spectrum of $\mathbf{1_e}$ is shown in Figure 3.6 which showed the disappearance of the absorption bands due to S–H stretching of $\mathbf{1_d}$. Besides this, a band at 1720 cm^{-1}due to C=O stretching was appeared.

The ^{1}HNMR spectrum of $\mathbf{1_e}$ is shown in Figure 3.7. The following characteristic chemical shifts (Acetone, ppm) were appeared: a doublet of doublets leaning on each other at δ 7.6- 8.06 that could be attributed to the four protons of the alkoxy phenyl ring while the other two doublet at δ 6.57- 7.07 suggesting the attribution of the four protons of the benzene nucleus attached to the heterocyclic ring.

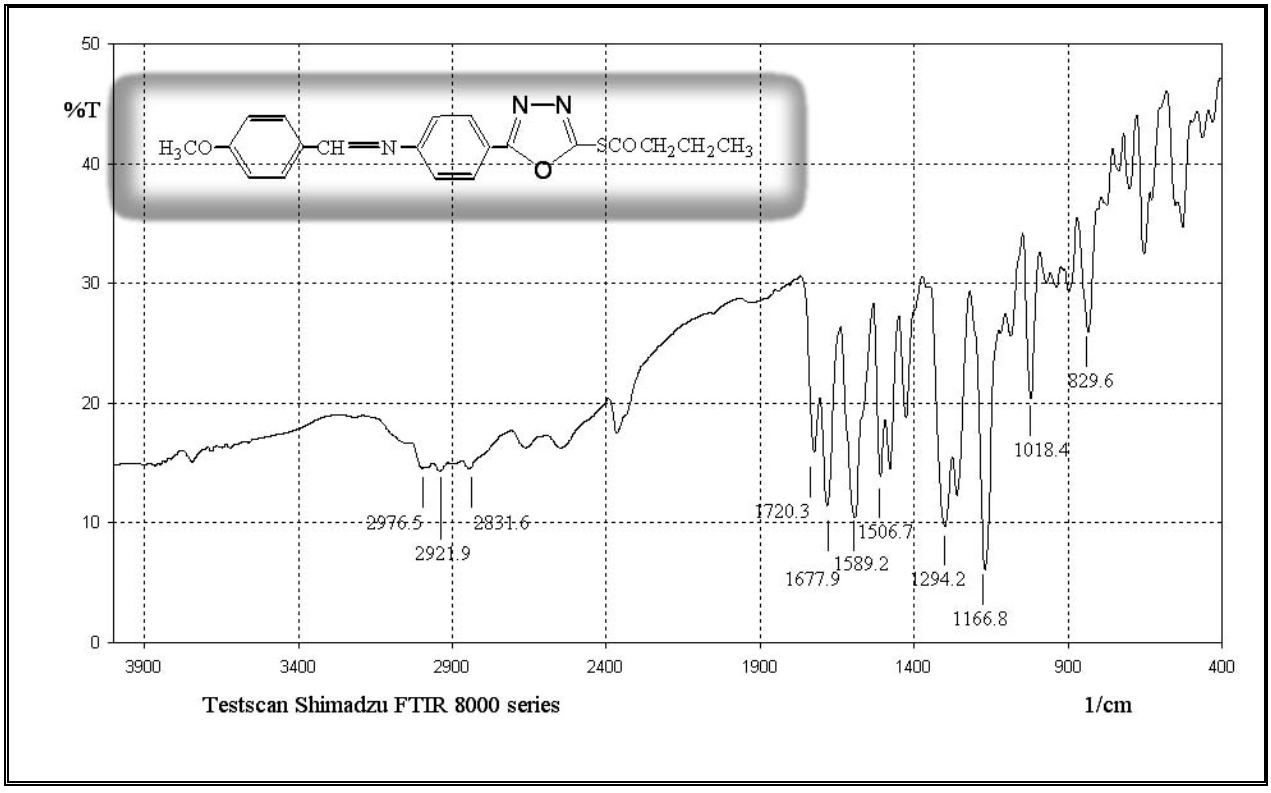

Figure 3.6 FTIR spectrum of compound 2-thiobutanoyl-5-[4-(4´-methoxybenzylidene amino)phenyl]1,3,4-oxadiazole (1_e)

The spectrum also showed a singlet at δ 8.34 that could be assigned to the vinylic proton . A three proton singlet at δ 3.8 ppm could be assigned to the $–OCH_3$ group.

The ^{1}HNMR spectrum also showed two protons triplet at δ 1.9- 2.1 could be assigned to CH_2 protons which was due to the splitting caused by the adjacent CH_2 protons. A two protons multiplet at δ 1.39- 1.41 due to CH_2 were also observed in this spectrum, while the CH_3 group appeared as a three protons triplet at δ 0.9- 1.1. The ^{1}HNMR spectrum is in agreement with the proposed structure.

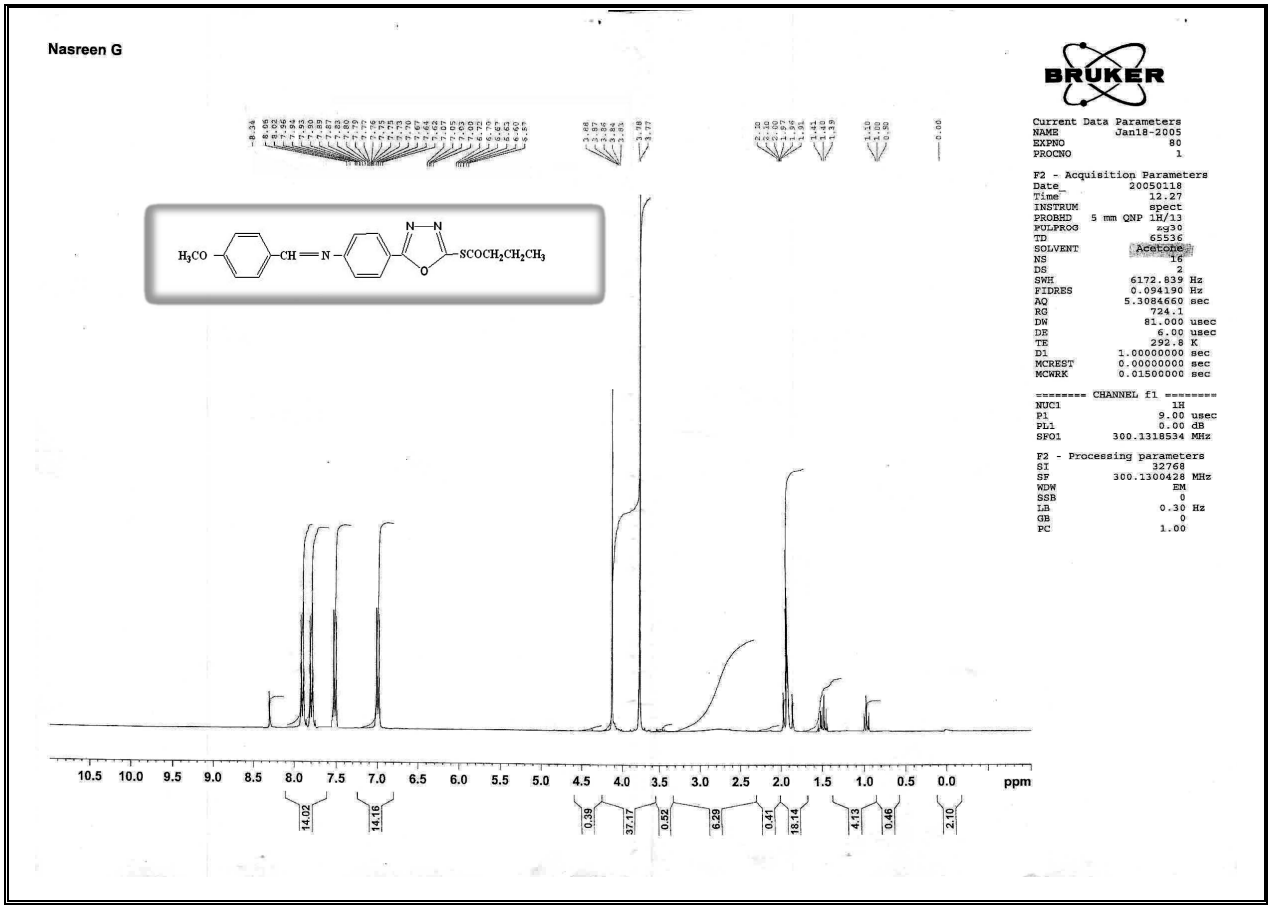

Figure 3.7 ^{1}HNMP spectrum of compound 2-thiobutanoyl-5-[4-(4´-methoxybenzylidene amino)phenyl]1,3,4-oxadiazole (1_e)

3.2 Synthesis and characterization of Compound 4-[4'-(4''-methoxy-benzylideneamino)benzoyloxy]propyl benzoate 2_d:-

This compound was prepared as shown in scheme 2.2.

The preparation of **2_a,** involve the reaction of 4-amino benzoic acid with anisaldehyde in boiling ethanol:

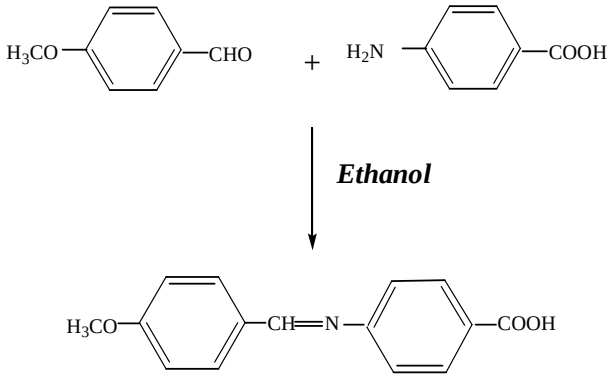

(2a)

This compound was verified using FTIR, as shown in Figure 3.8. It shows an absorption band for the OH stretching at 3345, two bands at 1679 and 1633 could be attributed to the stretching of C=O and C=N.

Reaction of **2_a** with excess of thionyl chloride in dry pyridine gave 4-(4'-methoxybenzylideneamino) benzoyl chloride **2_b**. Reaction of **2_b** with propyl-4-hydroxybenzoate **2_c**, yielded **2_d** .

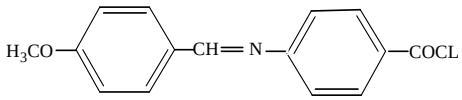

(2_b)

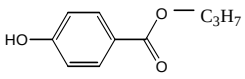

propyl-4-hydroxybenzoate

(2_c)

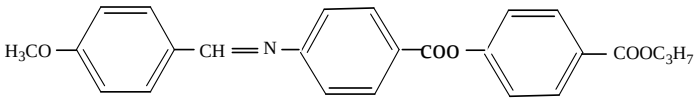

(2_d)

Compound **2_c** was characterized by its melting point 94-96 ºC (lit. 95-98 ºC[88]). It was also verified by FTIR shown in Figure 3.9. The following characteristic absorption bands (KBr disc cm^{-1}): 3249 for O-H stretching, 2975 due to C-H stretching were clearly identified . Bands at 1672, 1276 and 846 that were due to C=O stretching, C-O-C stretching and out of plane bending of *p*–disubstituted benzene ring, respectively.

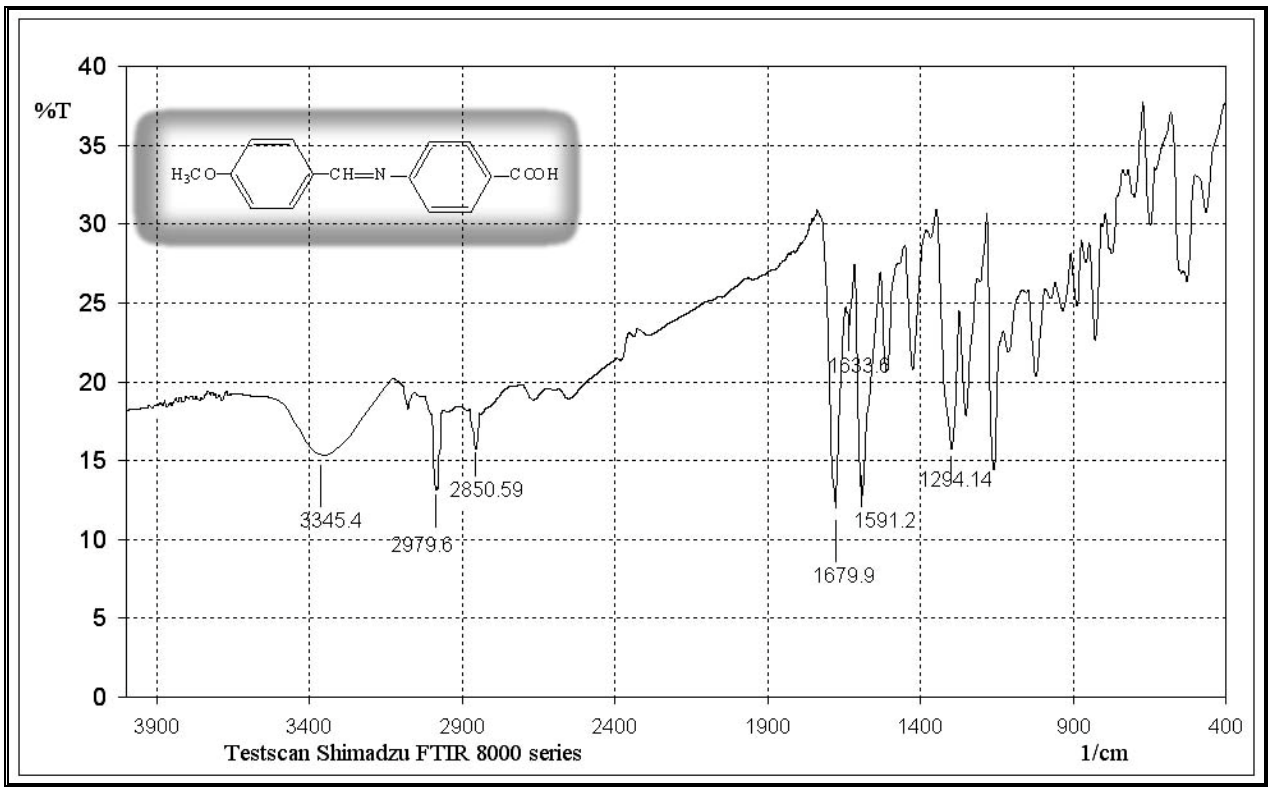

Figure 3.8 FTIR spectrum of compound 4-(4´-methoxybenzylideneamino)benzoic acid (2_a)

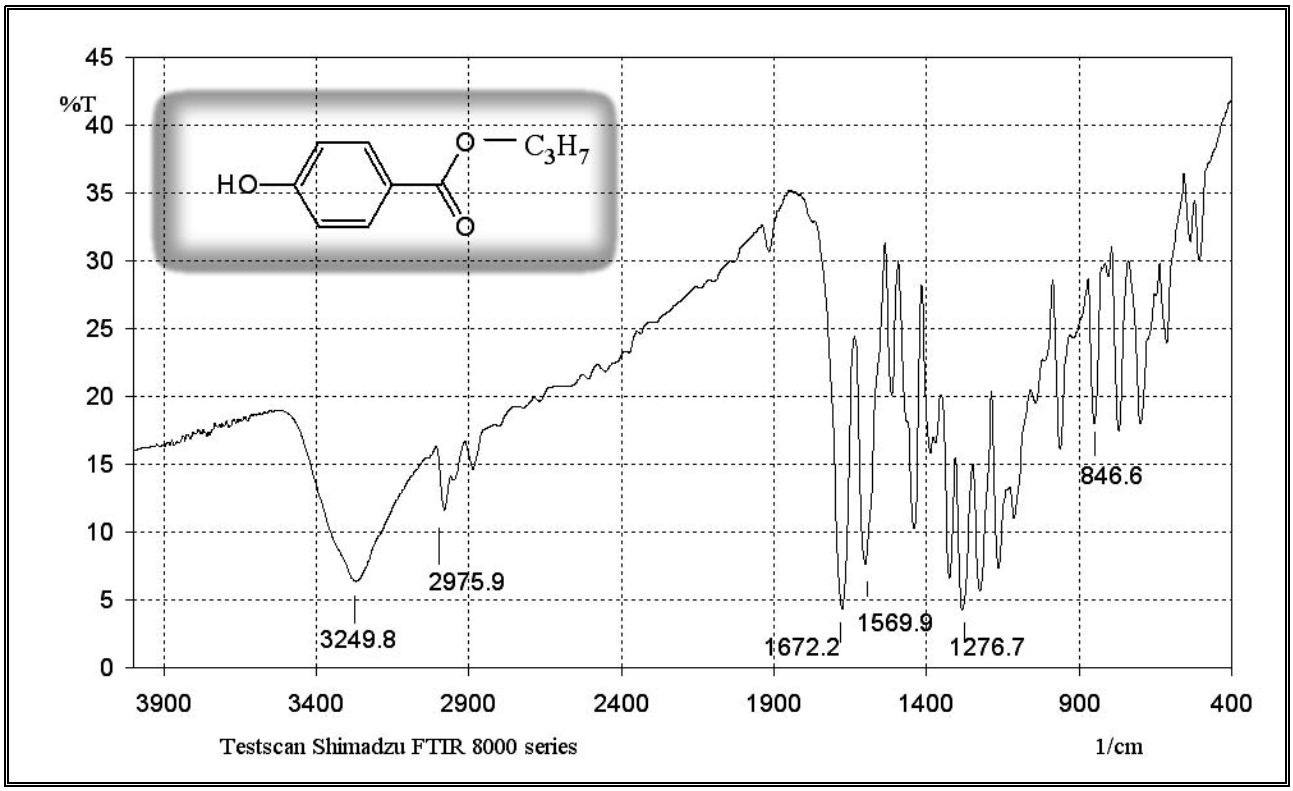

Figure 3.9 FTIR spectrum of compound Propyl-4-hydroxybenzoate (2_c)

The FTIR and ^{1}HNMR spectra of compound $\mathbf{2_d}$ are shown in Figure 3.10 and 3.11 respectively. FTIR spectrum showed the disappearance of O-H stretching at 3249 cm^{-1}.

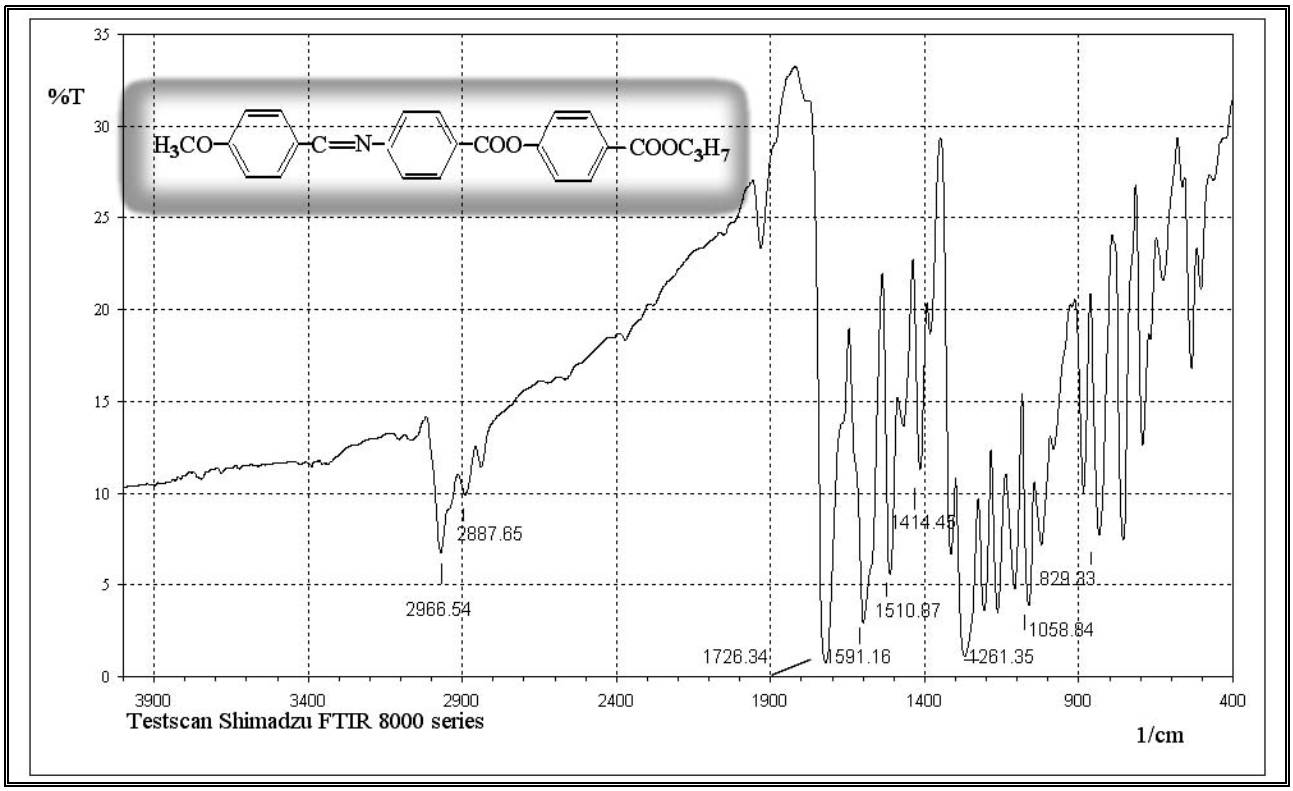

Figure 3.10 FTIR spectrum of compound 4-[4´-(4˝-methoxybenzylideneamino)benzoyloxy] propyl benzoate (2_d)

The ^{1}HNMR spectrum of the compound is shown in Figure 3.11. The following features ($CDCL_3$, ppm) were appeared: three pairs of doublet of doublet at δ 6.6-6.9, δ 7.7-7.8 and δ 7.9-8.3 which could be attributed to the three *p*-substituted benzene rings having different substituents at positions 1 and 4. The ^{1}HNMR spectrum also showed a triplet at δ 4.13-4.25 that could be assigned to O$^1CH_2$ protons due to the splitting caused by the adjacent $^2CH_2$ protons. A two protons multiplet at δ 1.67-1.79 due to –$^2CH_2$ were also observed in the spectrum. The $^3CH_3$ group appeared as a three protons triplet at δ 0.93-0.99 . A three protons singlet at δ 3.8 that could be assigned to the $–OCH_3$ group, and sharp singlet at δ 8.33 that could be assigned to the vinylic proton, while the sharp singlet at 9.8 could be attributed to phenolic proton of some unreacted materials The ^{1}HNMR spectrum of this compound together with the FTIR spectrum were good indication for the suggested structure of 2_d.

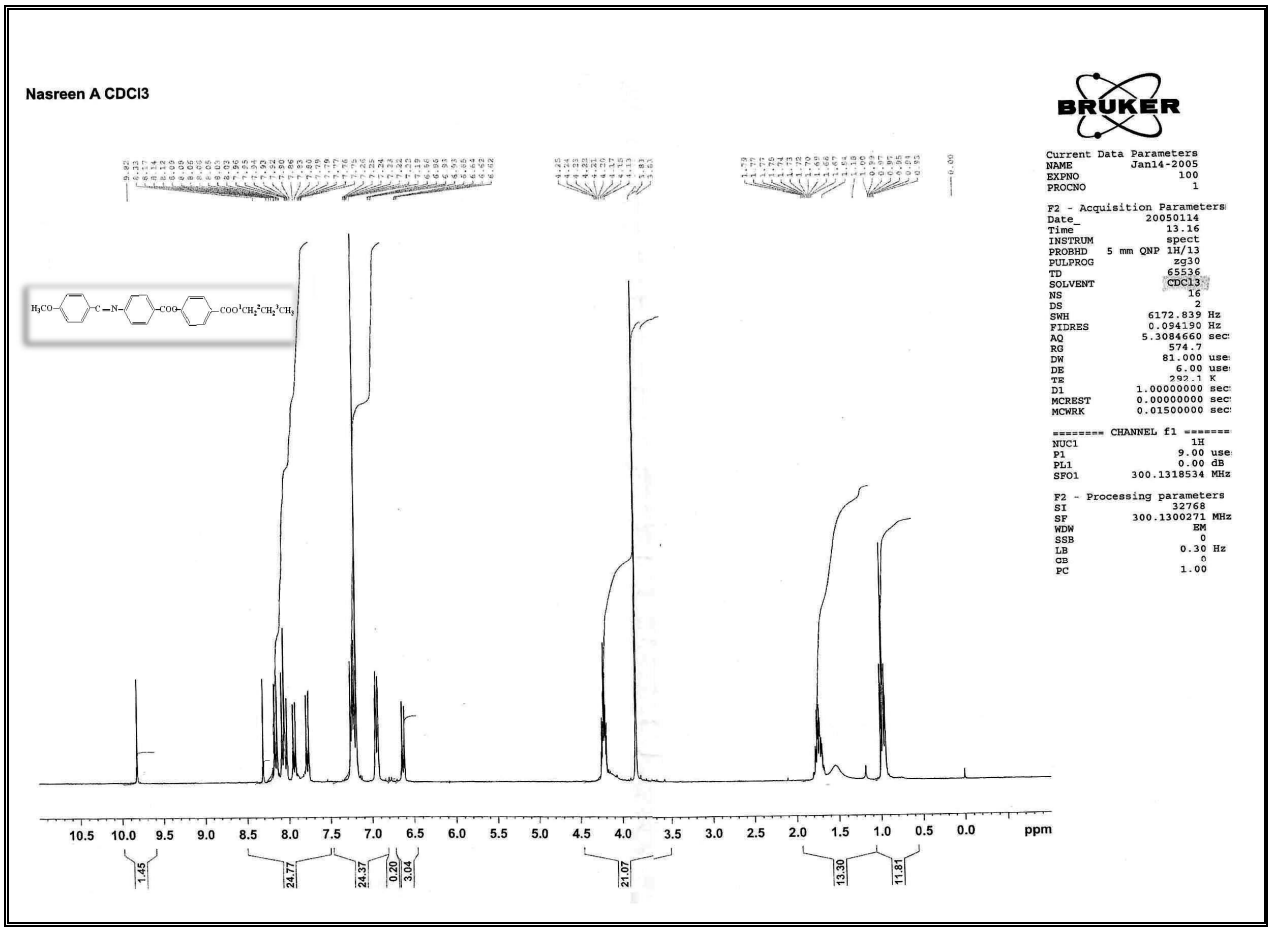

Figure 3.11 ^{1}HNMR spectrum of compound 4-[4´-(4˝-methoxybenzylideneamino)benzoy-loxy]propylbenzoate (2_d)

3.3 Synthesis and Characterization of Compound 2,5-bis-[4-amino phenyl]-1,3,4-oxadiazole (3_d)

The route adopted for the synthesis of compound **3_d** is given in scheme 2.3.

Compound 4-carboxybenzanilide **3_{a1}** was obtained from the reaction of benzoyl chloride with 4-aminobenzoic acid in 10% NaOH solution in ice bath:

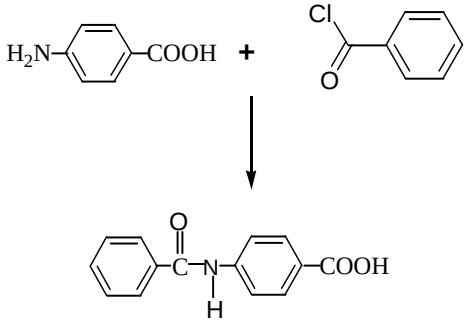

3_{a1}

The synthesized compound was characterized by FTIR (KBr, cm^{-1}) are shown in Figure 3.12. It showed the appearance of bands at 3460, and 3326 that were due to N–H and O–H stretching. A stretching bands appeared at 1678, 1650.8 and 1517 which could be attributed to C = O stretching of acid, amide group (amide I) and N–H bending (amide II) respectively.

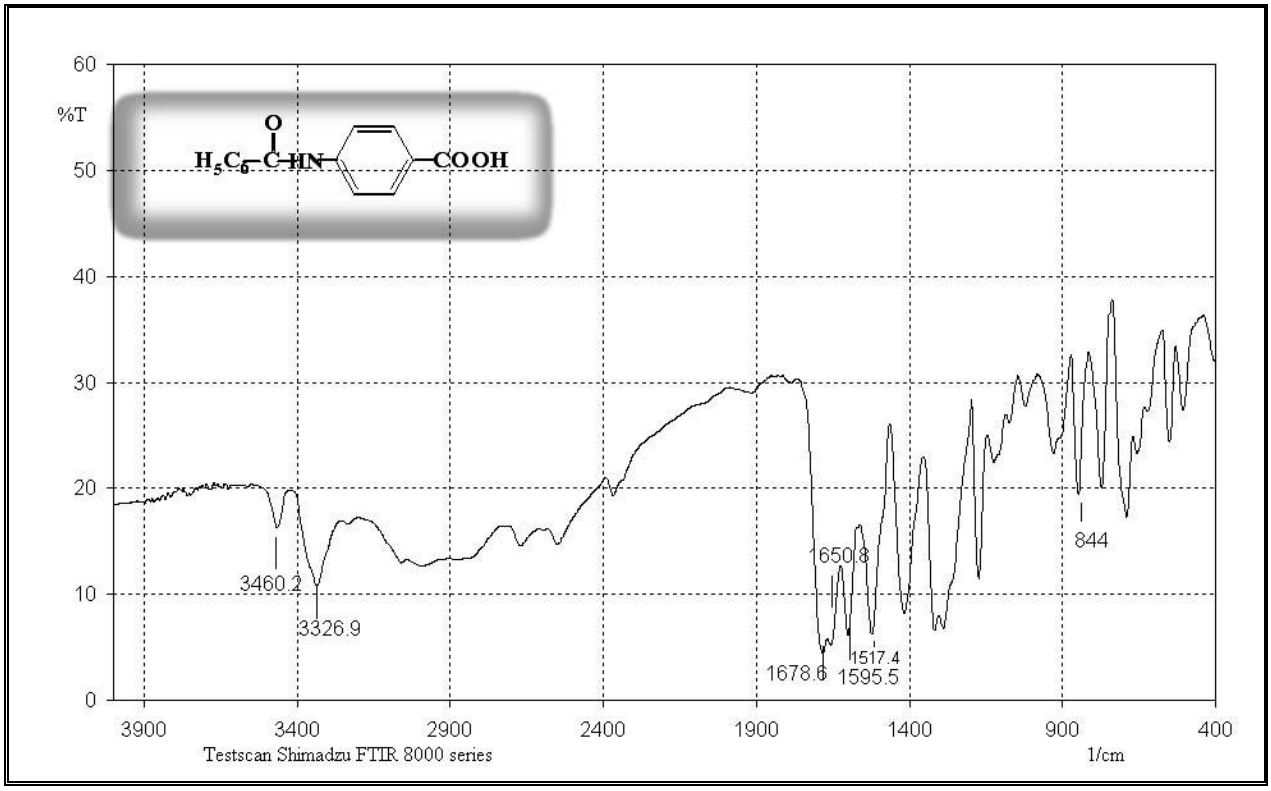

Figure 3.12 FTIR spectrum of compound 4-carboxybenzanilide (3_{a1})

Compound 4-N-benzoyl ethyl benzoate **3_{a2}** was obtained by the reaction of ethyl 4-aminobenzoate with benzoyl chloride in dry pyridine:

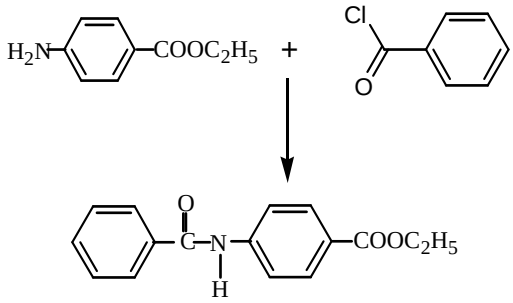

(3_{a2})

The synthesized compound was characterized by FTIR. The characteristic (KBr, cm^{-1}) as shown in Figure 3.13. A stretching bands appeared at 3265, 1676, 1605 and 1512 which could be attributed to N–H stretching, C = O stretching of ester, amide group (amide I) and N–H bending (amide II) respectively.

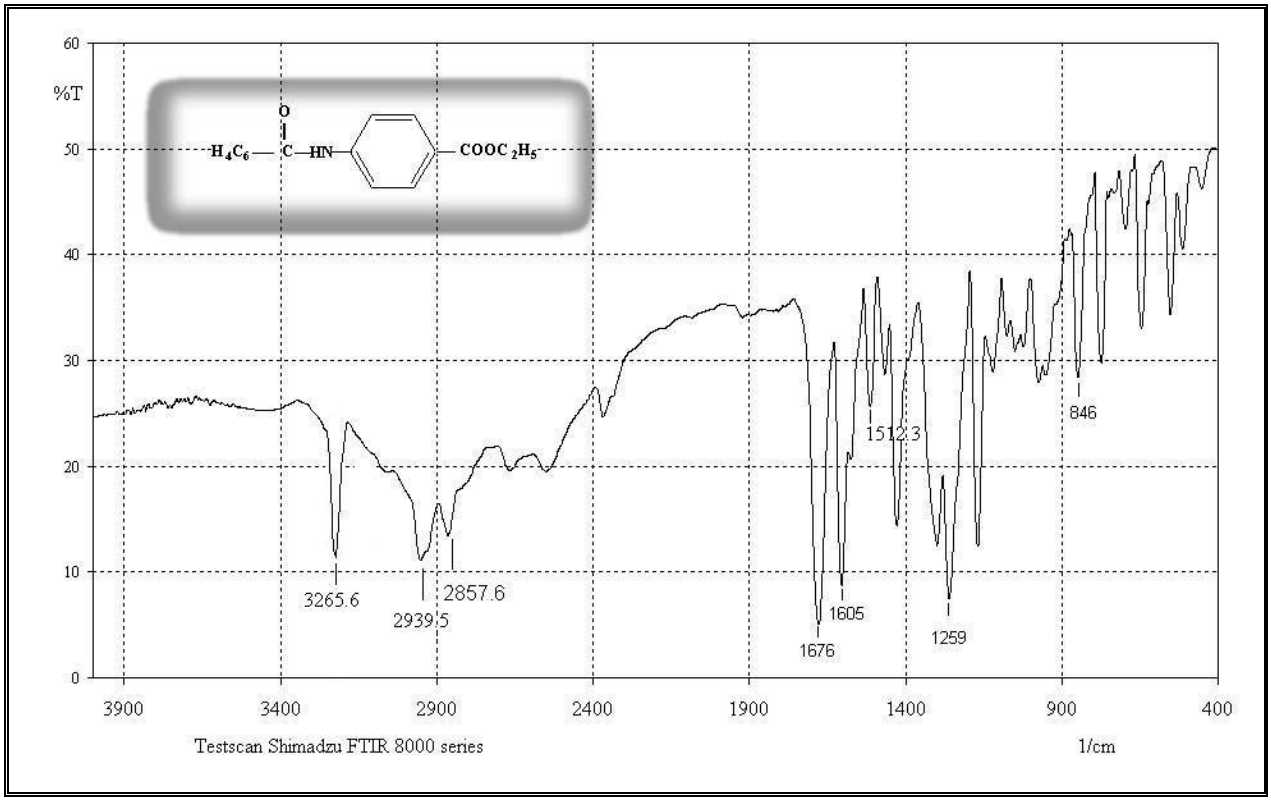

Figure 3.13 FTIR spectrum of compound 4-N-benzoyl ethyl benzoate (3_{a2})

4-N-benzoyl phenyl acid hydrazide **3_b** has been prepared by the reaction of compound **3_{a2}** with excess hydrazine hydrate in the presence of ethanol as solvent:

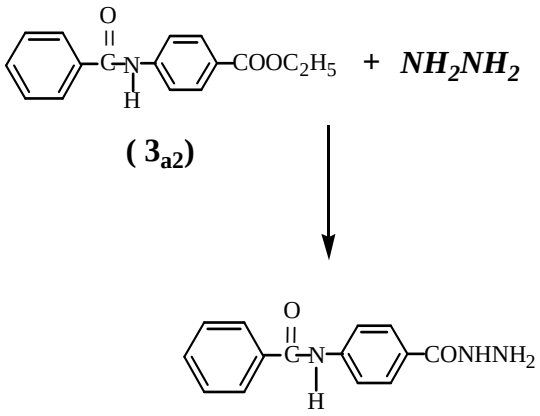

The constitution of this product was supported by FTIR spectral data. The FTIR spectrum (KBr, cm^{-1}) for the compound is shown in figure 3.14. A shift in the carbonyl stretching band from 1676 to 1652 (amide) was clear. Other bands at 3315, 3274 and 1512 could be attributed to N–H, NH_2 stretching and N–H bending (amide II), respectively.

Compound 2,5-bis-[benzanilide]-1,3,4-oxadiazole **3_c** was synthesized by refluxing compound **3_{a1}** and **3_b** in phosphorous oxychloride :

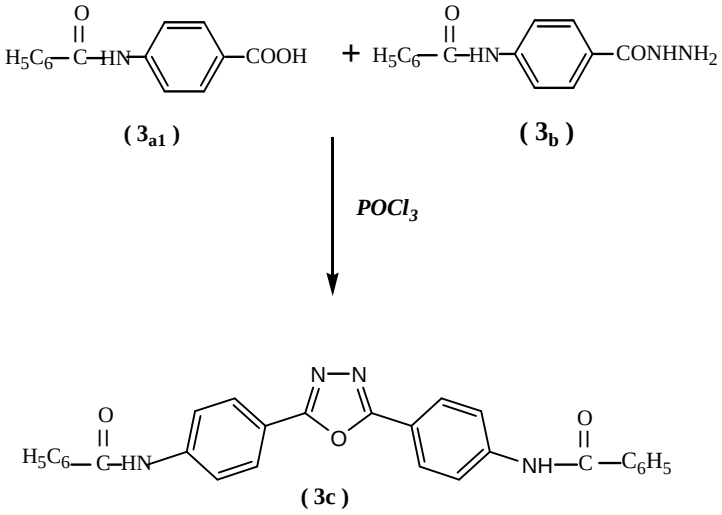

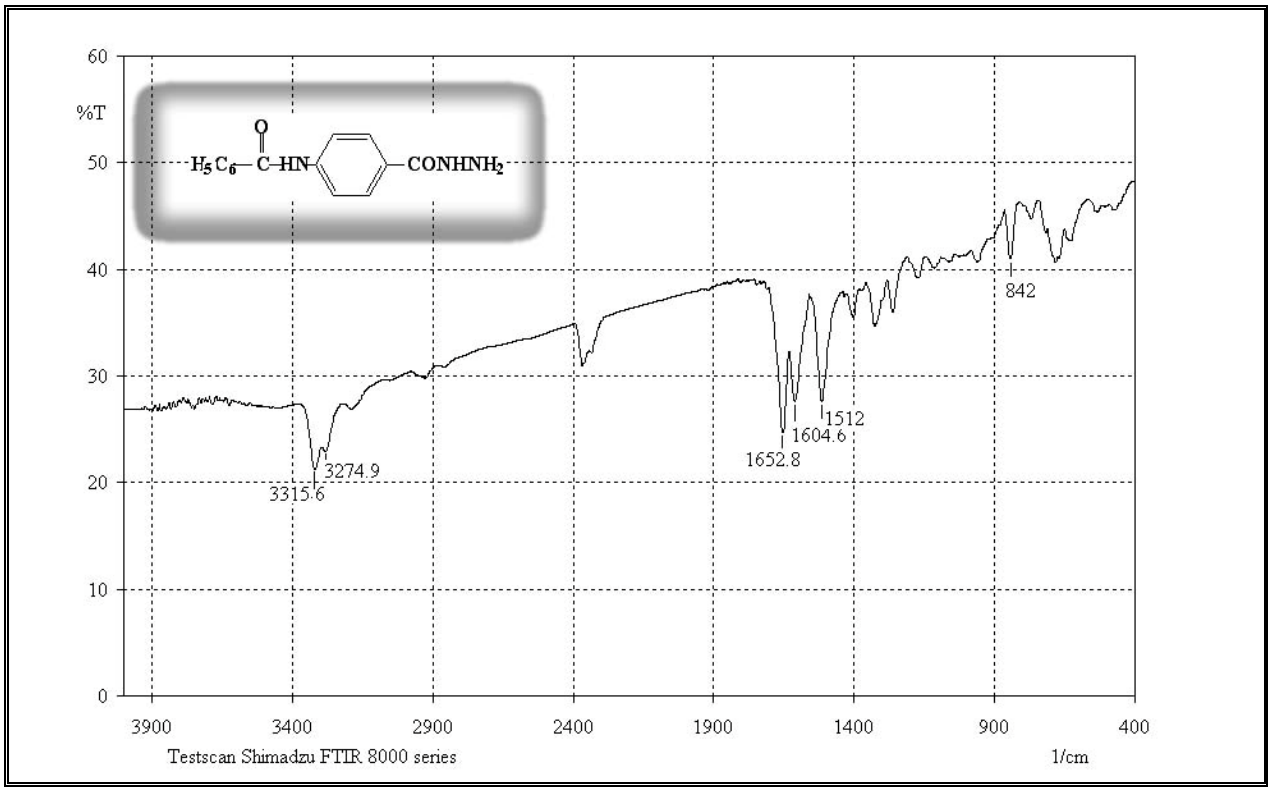

Figure 3.14 FTIR spectrum of compound 4-N-benzoyl phenyl acid hydrazide (3_b)

The characteristic bands (KBr, cm^{-1}) of $\mathbf{3_c}$ is shown in Figure 3.15 which showed a stretching bands appeared at 1658, 1598 and 1519 which could be attributed to C = O stretching of ester, amide group (amide I) and N–H bending (amide II) respectively.

Hydrolysis of $\mathbf{3_c}$ with 70% H_2SO_4 yielded compound 2,5-bis-[4-amino phenyl]-1,3,4-oxadiazole $\mathbf{3_d}$:

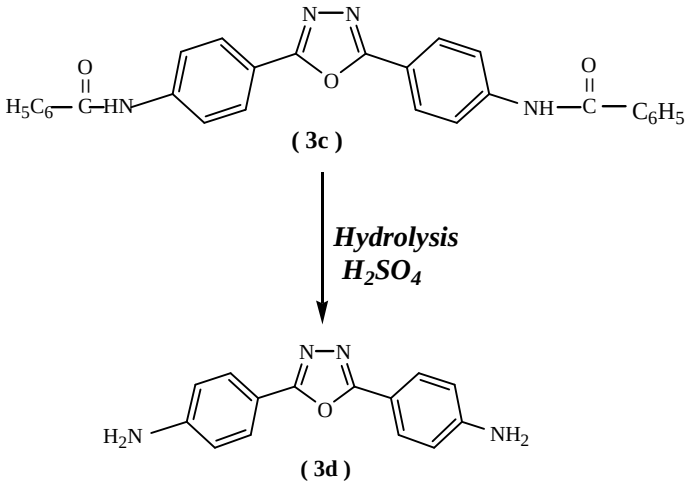

Three stretching bands appeared at 1676, 1605 and 1512 which could be attributed to C = O stretching of ester, amide group (amide I) and N–H bending (amide II) respectively, as shown in Figure 3.16.

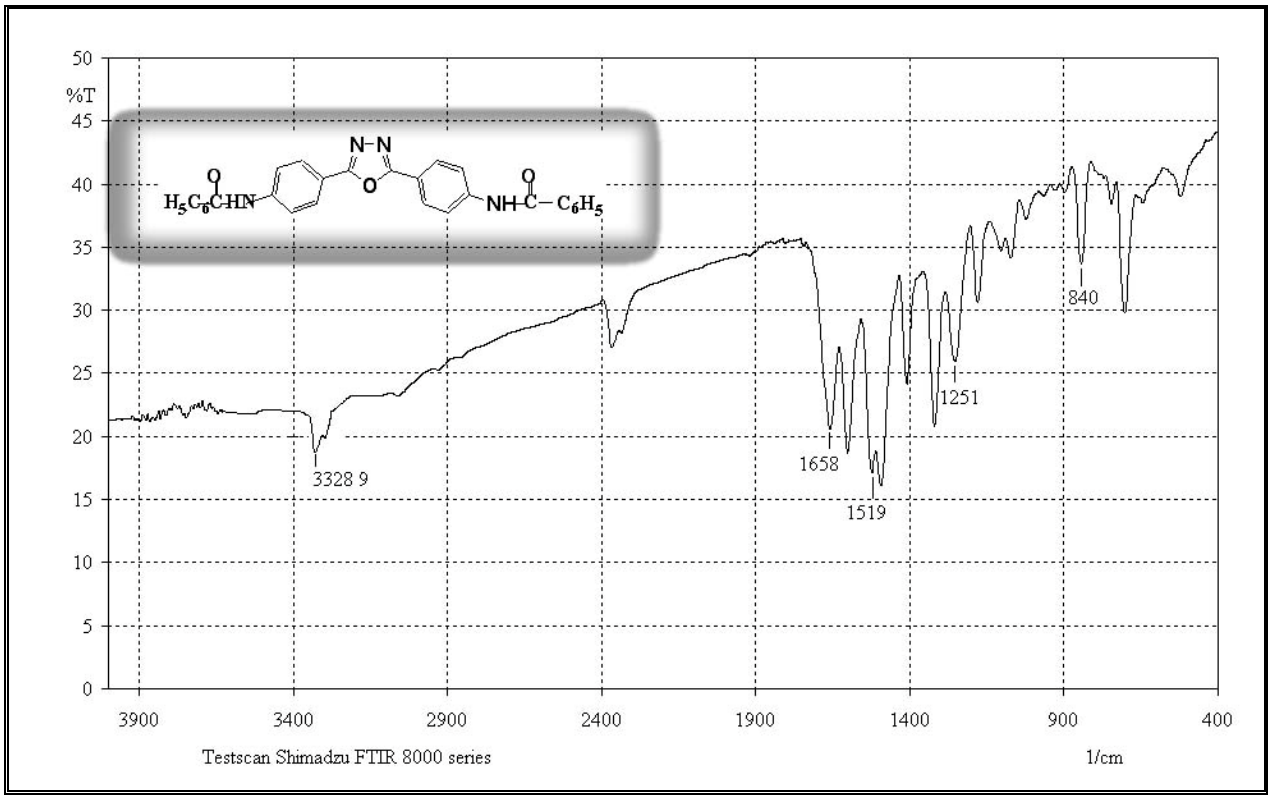

Figure 3.15 FTIR spectrum of compound 2,5-bis-[benzanilide]-1,3,4-oxadiazole 3_c

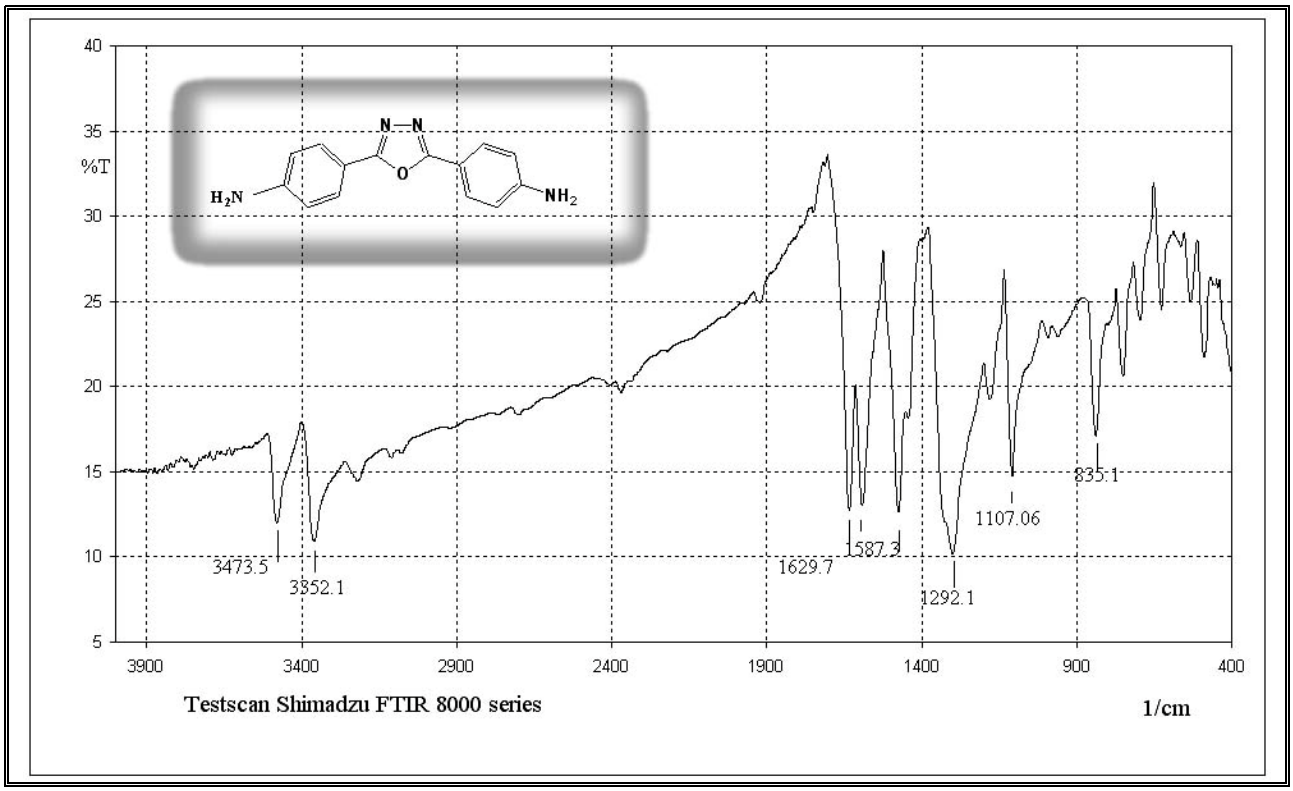

Figure 3.16 FTIR spectrum of compound 2,5-bis-[4-amino phenyl]-1,3,4-oxadiazole (3_d)

3.4 Synthesis and Characterization of Compounds 2,5-bis-[4-(4´-alkoxybenzylideneamino)phenyl]-1,3,4-oxadiazole 3_{e1} -3_{i1}:

The compounds (3_{e1}-3_{i1}) were synthesized by refluxing compound 3_d with two equivalents of the appropriate 4- alkoxy benzaldehyde:

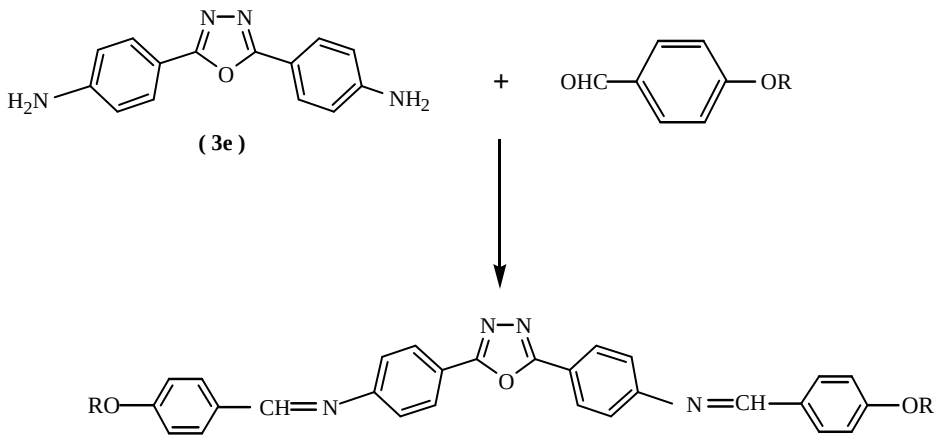

($3_{e1,f1,g1,h1,i1}$)

The synthesized compounds were characterized by FTIR and ^{1}HNMR. The characteristic bands for compound 3_{h1} is shown in Figure 3.17 (KBr disc, cm^{-1}) as a typical example for the compounds. It showed the disappearance of absorption band of NH_2 and the appearance of typical absorption of C=N stretching at 1643. Bands at 2977-2847 assigned to the stretching C–H aliphatic. Table 3.1 summarizes the FTIR spectral data of compounds 3_{e1}–3_{i1}.

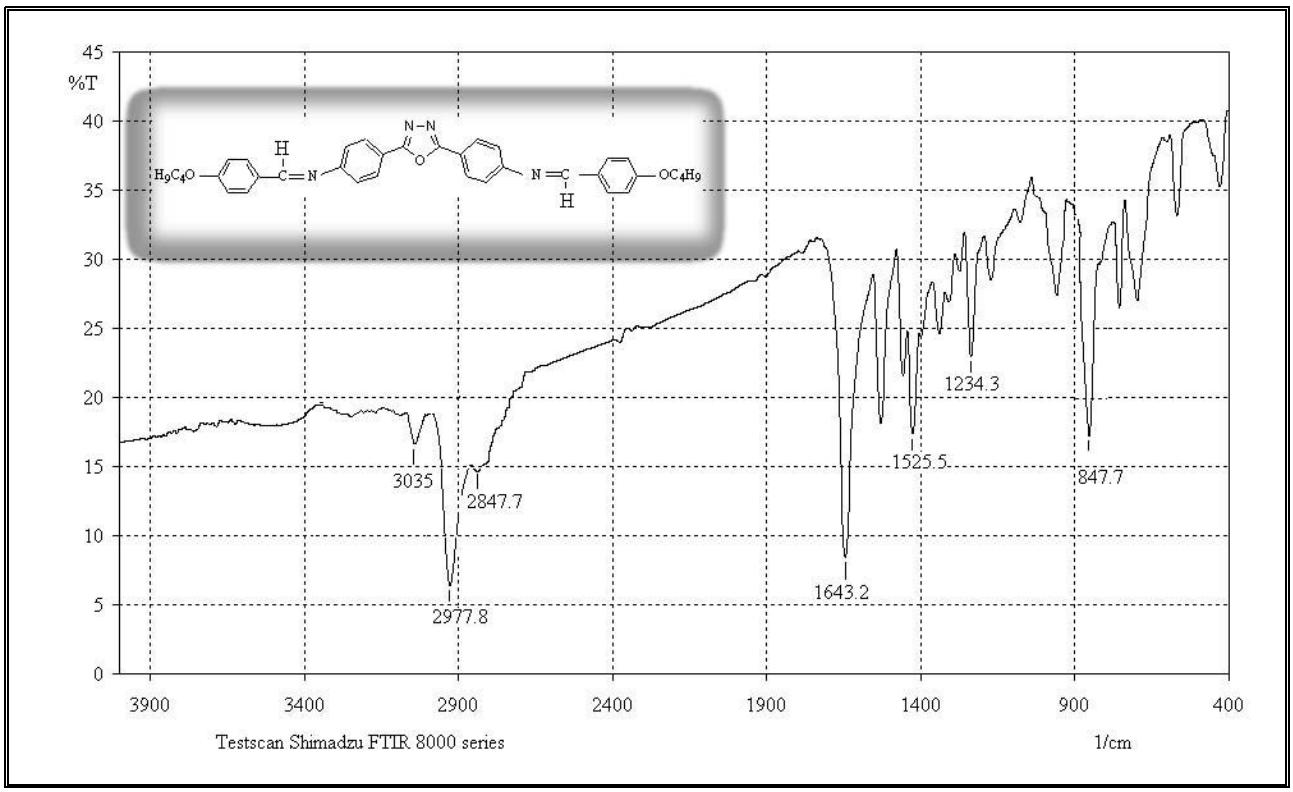

Figure 3.17 FTIR spectrum of compound 2,5-bis-[4-(4´-butoxybenzylideneamino)phenyl]-1,3,4-oxadiazole (3_{h1})

Table 3.1 FTIR spectral data (cm^{-1}) using KBr disc for the synthesized compounds 3_{e1}–3_{i1}.

R group	Comp. No.	υ C–H Asym., sym.	υ C–H Arom.	υ C=N	υ C –O –C	
					Asym.	Sym.
CH_3	3_{e1}	2979,2856	3040	1643	1257.5	1026
C_2H_5	3_{f1}	2922.9, 2856.4	3038	1650	1267.1	1056.9
C_3H_7	3_{g1}	2954.7- 2869.9	3030	1651	1255.6	1074.3
C_4H_9	3_{h1}	2977-2847	3035	1643	1253.4	1022.2
C_5H_{11}	3_{i1}	2925- 2858	3034	1641	1253.6	1034.5

The ^{1}HNMR spectrum of compound 3_{e1} is shown in Figure 3.18. The following characteristic chemical shifts (DMSO, ppm) were appeared: A doublets leaning on each other at δ 7.0-8.3 could be attributed to the eight protons of the alkoxy phenyl ring while the other two doublets at δ 6.57-7.07 suggested the attribution of the eight protons of the benzene nucleus attached to the heterocyclic ring. The ^{1}HNMR also showed a sharp two proton singlet at δ 8.36 which could be assigned to the vinylic proton. Six protons appeared as sharp singlets at δ 3.8 that are attributed to –OCH_3 group.

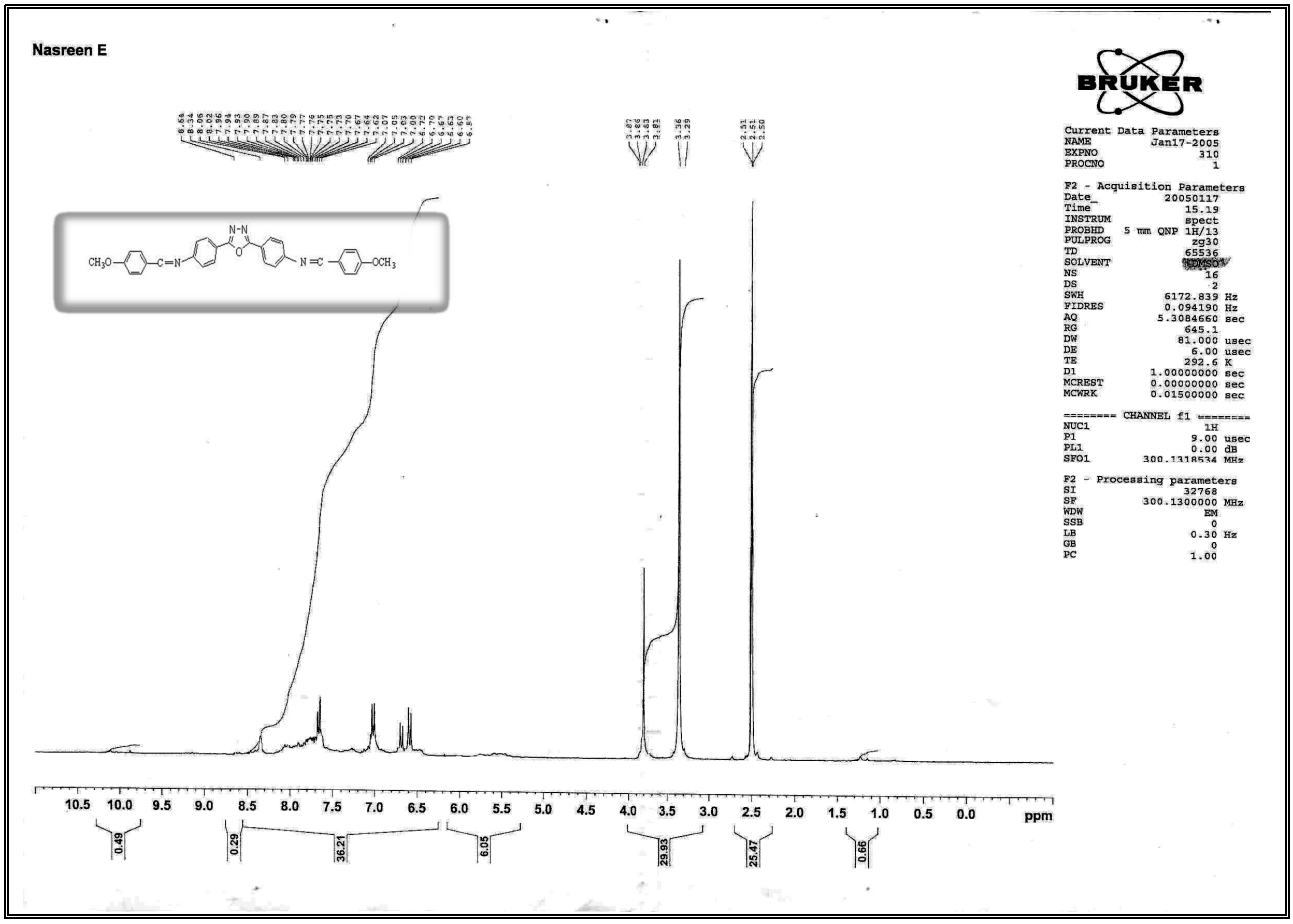

Figure 3.18 ^{1}HNMR spectrum of compound 2,5-bis-[4-(4´-methoxy-benzylideneamino) phenyl]-1,3,4-oxadiazole (3_{e1})

^{1}HNMR spectrum of compound 3_{g1} in Figure 3.19 shows the following features(DMSO, ppm): two pair of doublet of doublet at δ 7.08-7.5 and 7.94-8.2 leaning on each other which could be attributed to the two *p*-substituted benzene rings which have different substituents at position 1 and 4, thus comprising an AB system. The ^{1}HNMR spectrum also showed a triplet at δ 4.05- 4.1 that could be assigned to $O^{1}CH_2$ protons due to the splitting caused by the adjacent $^{2}CH_2$ protons. A four protons multiplet at δ 1.4-1.8 due to $^{2}CH_2$ are also observed in this spectrum. The vinylic protons appeared as a singlet at δ 8.5, while the $^{3}CH_3$ group appeared as a six protons triplet at δ 0.9-1.0.

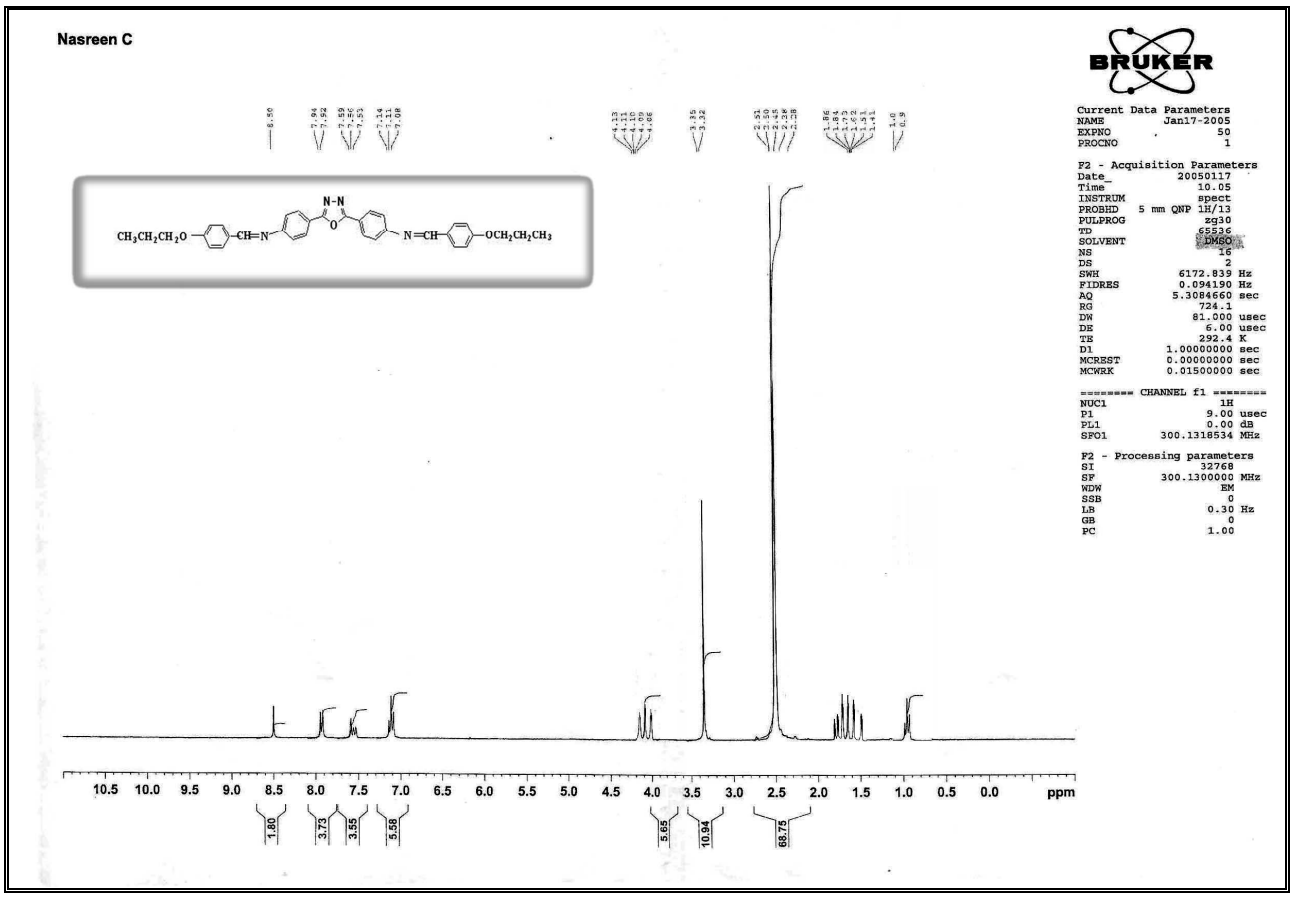

Figure 3.19 ^{1}HNMR spectrum of compound 2,5-bis-[4-(4´-propoxy- benzylideneamino) phenyl]-1,3,4-oxadiazole (3_{g1})

3.5 Synthesis and Characterization of Compounds 2,5-bis-[4-(4´-alkoxybenzanilide)phenyl]-1,3,4-oxadiazole 3_{e2}-3_{i2}:

The compounds (3_{e2}-3_{i2}) were synthesized by refluxing compound 3_d with two equivalents of the appropriate 4- alkoxybenzoyl chloride in dry pyridine:

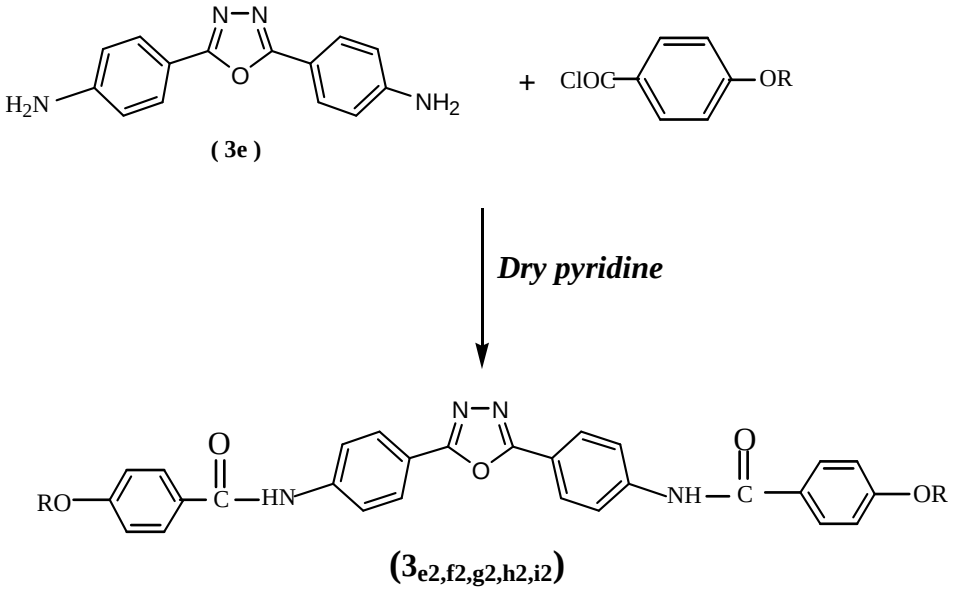

($3_{e2,f2,g2,h2,i2}$)

The synthesized compounds were characterized by FTIR and ^{1}HNMR. A Typical FTIR spectrum for these compounds is shown in Figure 3.20 for compound 3_{g2} using KBr disc, cm^{-1}. It showed the appearance of an absorption band at 3276 which could be assigned to N–H stretching, instead of the two absorption bands for the NH_2 stretching of compound 3_d. A new stretching band appeared at 1726 which could be attributed to C=O stretching of amide group (amide I) and a band at 1527 due to N–H bending (amide II). Table3.2 lists FTIR spectral data of compounds 3_{e2}–3_{i2}.

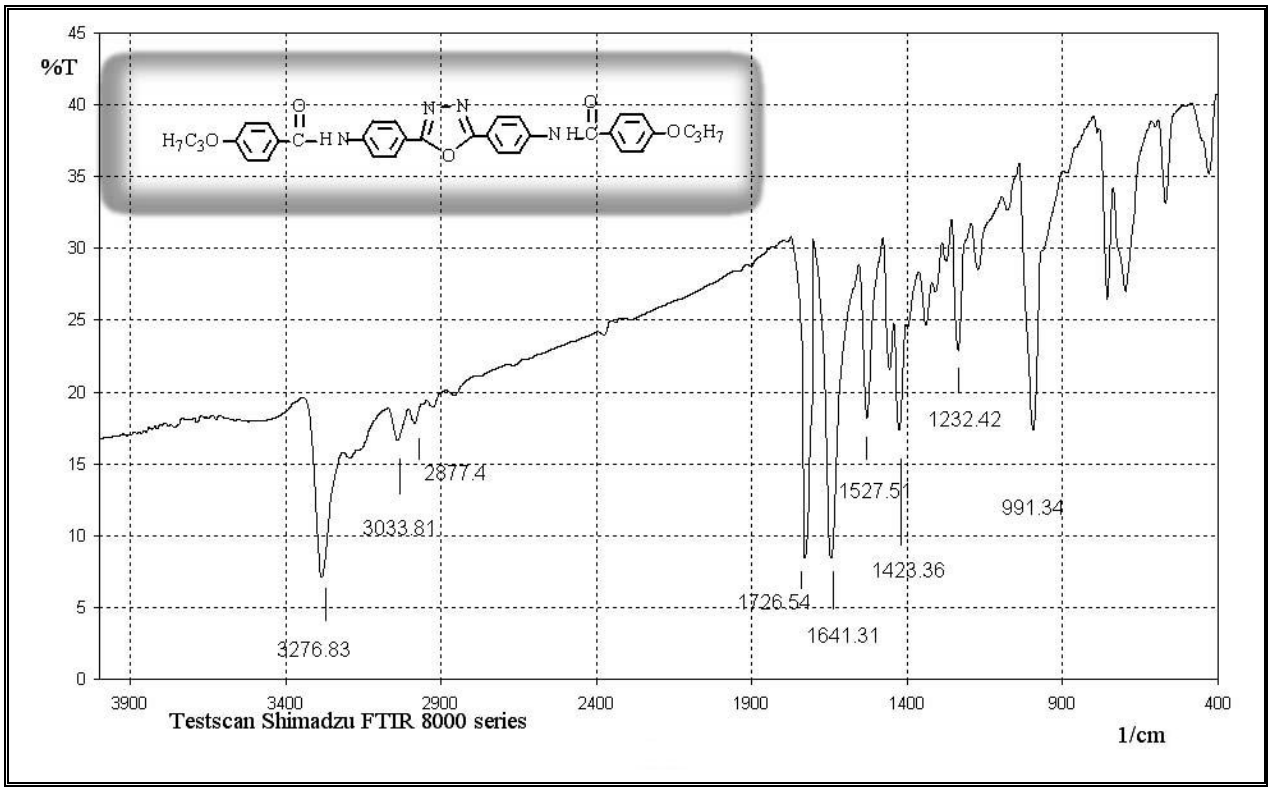

Figure 3.20 FTIR spectrum of compound 2,5-bis-[4-(4´-propoxybenzanilide)phenyl]-1,3,4-oxadiazole 3_{g2}

Table 3.2 FTIR spectral data (cm^{-1}) using KBr disc for the synthesized compounds 3_{e2}–3_{i2}.

R group	Comp. No.	υ N–H	υ C–H (Aromatic)	υ C–H (Aliphatic)	υ C=O
CH_3	3_{e2}	3280	3030	2940-2820	1715
C_2H_5	3_{f2}	3300	3050	2920-2840	1720
C_3H_7	3_{g2}	3276	3033	2960-2877	1726
C_4H_9	3_{h2}	3285	3040	2940-2880	1710
C_5H_{11}	3_{i2}	3275	3040	2940-2860	1700

Compound 2,5-bis-[4-(4´-methoxybenzanilide)phenyl]-1,3,4-oxadiazole 3_{e2} was also studied by ^{1}HNMR spectral data. The spectrum in Figure 3.21 showed the following features (DMSO, ppm): two pair of doublet of doublet at δ 6.4-7.4 and 7.7-8.2 leaning on each other which could be attributed to the two *p*-substituted benzene rings having different substituents at position 1 and 4, thus comprising an AB system. The spectrum also showed a sharp singlet at δ 3.8 that could be

attributed to $-OCH_3$ group, while the amidic proton appeared as sharp singlet at δ 10.5.

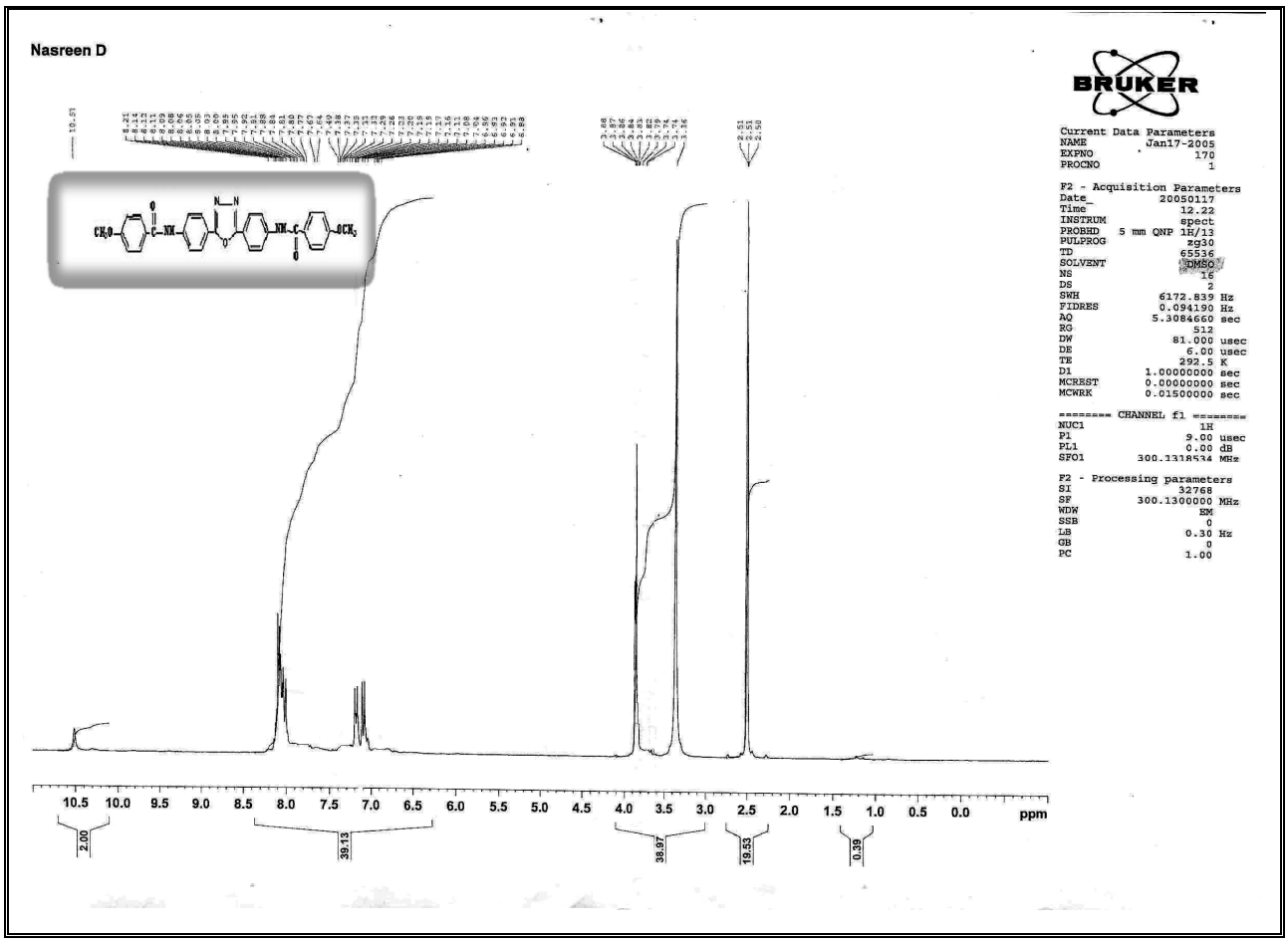

Figure 3.21 ^{1}HNMR spectrum of compound 2,5-bis-[4-(4´-methoxybenzanilide)phenyl]-1,3,4-oxadiazole (3_{e2})

The ^{1}HNMR spectrum for compound 3_{g2} is shown in Figure 3.22. It showed the following features (DMSO, ppm): two pair of doublet of doublet at δ 6.95-7.5 and 7.59-8.3 leaning on each other could be attributed to the two *p*-substituted benzene rings having different substituents at position 1 and 4, thus comprising an AB system. It also showed a triplet at δ 3.78- 3.91 that could be assigned to O^1CH_2 protons due to the splitting caused by the adjacent $^2CH_2$ protons. A four protons multiplet at δ 1.9-1.96 due to $^2CH_2$ were also observed. The amide protons appeared as a singlet at δ 9.8, while the $^3CH_3$ group appears as a six protons triplet

at δ 1.09-1.14. The ^{1}HNMR spectrum of this compound together with the FTIR spectrum give positive evidence for the structure suggested for compound 3_{g2}.

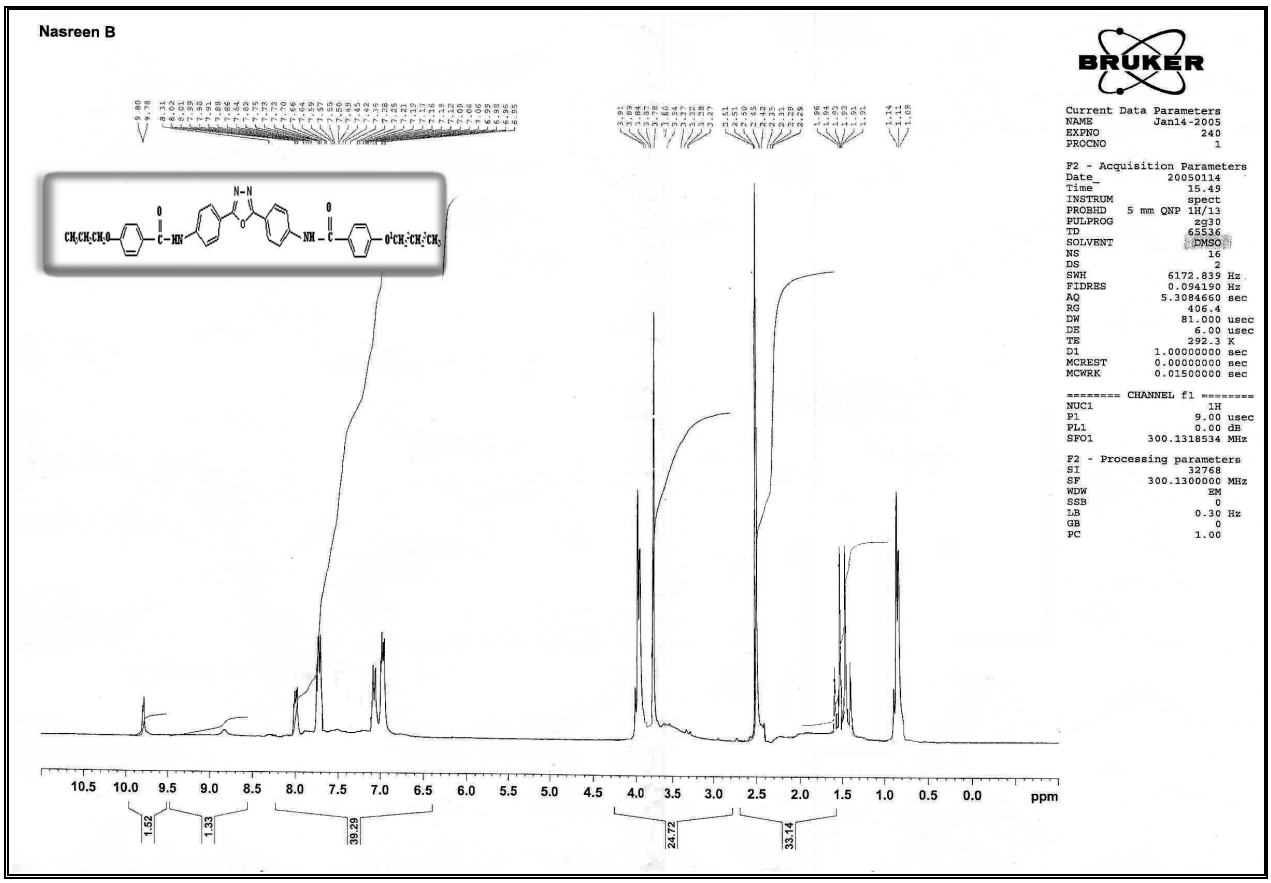

Figure 3.22 ^{1}HNMR spectrum of compound 2,5-bis-[4-(4´-propoxybenzanilide)phenyl]-1,3,4-oxadiazole (3_{g2})

3.6 Liquid Crystalline Properties of the Synthesize Compounds

The introduction of an oxadiazole ring into the principle structure of heteroaromatic systems opened the possibility of generating new mesogenic units. The hetero atoms could cause considerable changes of polarity, polarizability and geometry of the molecules and influenced the type and the phase transition temperature of the mesophases[92].

3.6.1 Mesomorphic Properties of the 2-thiobutanoyl-5-[4-(4´-methoxybenzylideneamino)phenyl]1,3,4-oxadiazole (1_e) and 4-[4´-(4˝-methoxybenzylideneamino)benzoyloxy]propyl benzoate (2_d) :

The tendency of a compound to show one type of mesophase or another is determined by linearity, rigidity, polarizability and by the direction of dipole moment(perpendicular or oblique to the molecular axis). These properties are indispensable for displaying liquid crystallinity[93].

Liquid crystalline properties of compound **1_e** was examined by means of differential scanning calorimeter (DSC) and hot stage polarizing microscope. Compound **1_e** showed a nematic mesophase of a typical thread- like texture as shown in Figure 3.23. The DSC thermogram of compound **1_e** is shown in Figure 3.24, which shows two transitions, the temperature at the maximum of the first transition peaks was chosen as the actual transition temperature, Crystal to Nematic (C → N), at 143ºC, and the second one is the transition from Nematic to Isotropic (N → I).

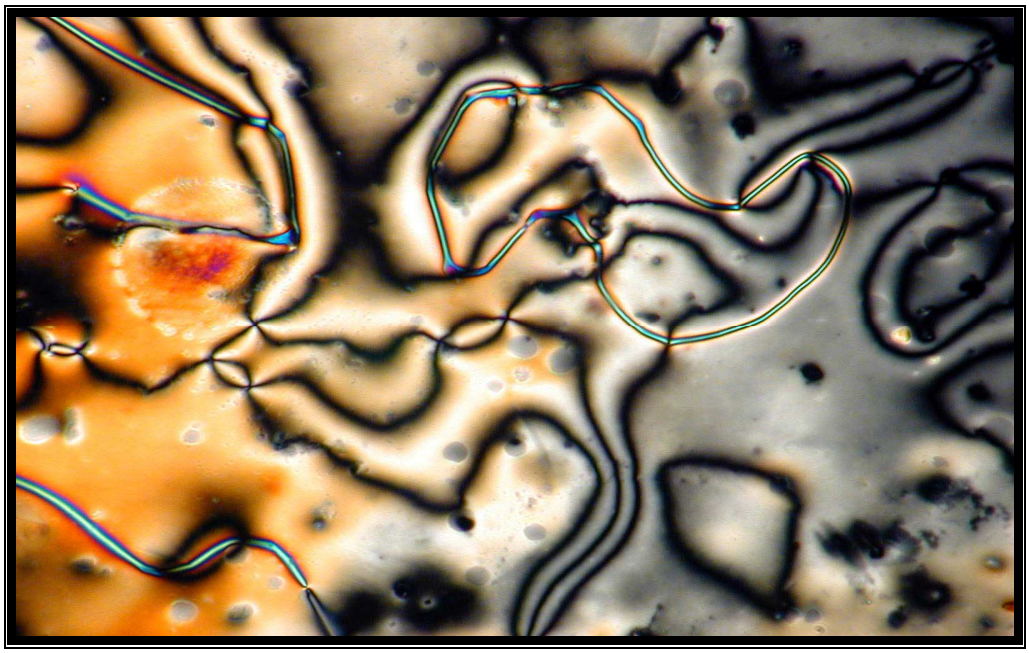

Figure 3.23 Nematic texture of model compound 2-thiobutanoyl-5-[4-(4´-methoxybenzylideneamino)phenyl]1,3,4-oxadiazole (1_e)

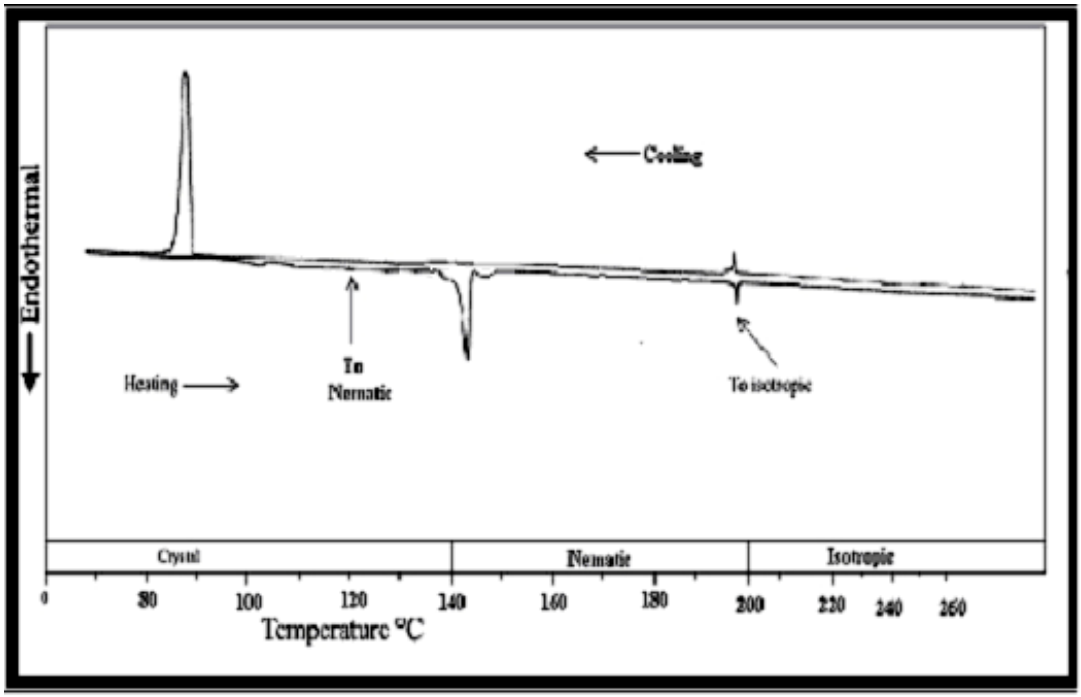

Figure 3.24 DSC Thermogram of compound 2-thiobutanoyl-5-[4-(4´-methoxybenzylideneamino)phenyl]1,3,4-oxadiazole (1_e)

Compound **2_d** showed in Figures 3.25 a and b displayed a nematic mesophase with monotropic smectic mesophase S_A.

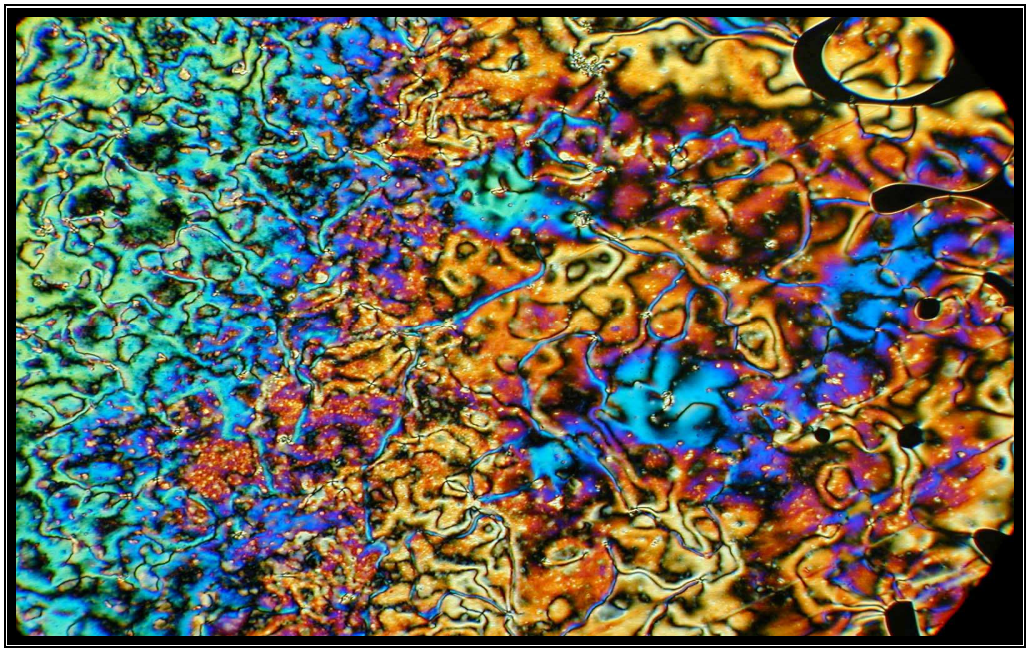

Figure 3.25a Nematic texture of model compound 4-[4´-(4˝-methoxybenzylideneamino)benzoyloxy]propyl benzoate (2_d)

Figure 3.25b Smectic A texture of model compound 4-[4´-(4˝-methoxybenzylide-neamino)benzoyloxy]propyl benzoate (2_d)

Figure 3.26 showed the DSC thermogram of this compound. The endotherms at 152ºC and 255ºC are assigned to the crystal → nematic and nematic → isotropic transitions, while the exotherms at 142ºC and 84ºC are assigned to the isotropic → smectic A and smectic A → crystal transitions.

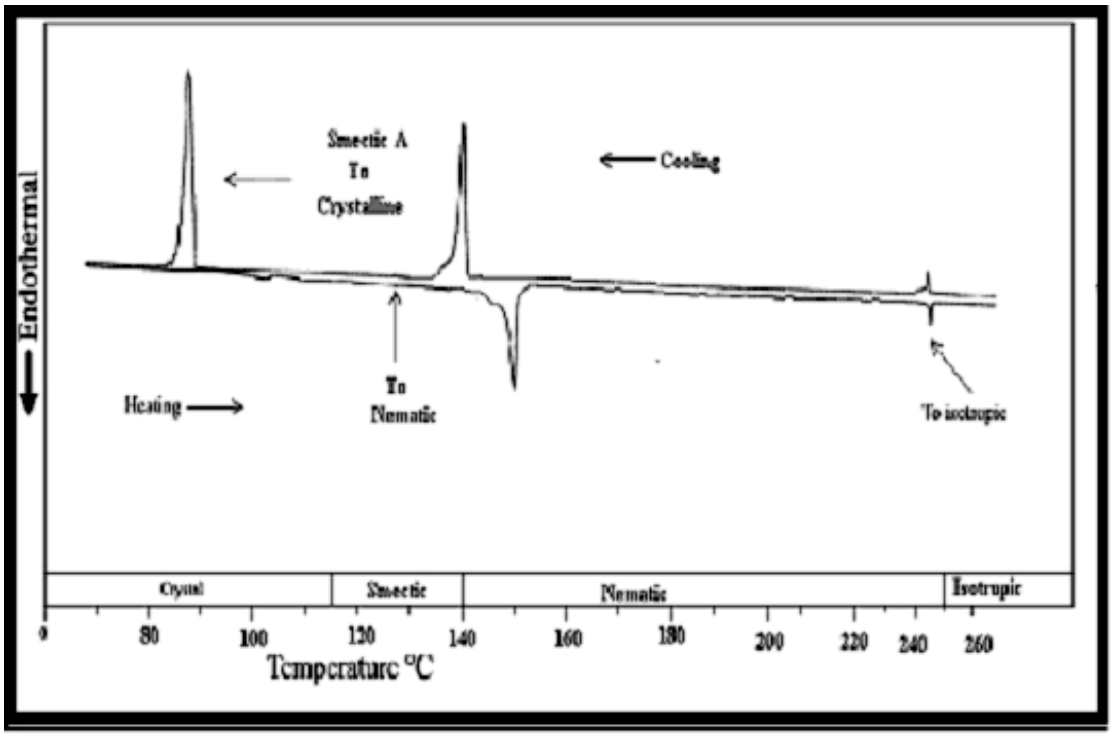

Figure 3.26 DSC Thermogram of compound 4-[4´-(4˝-methoxybenzylidene-amino)benzoyloxy]propyl benzoate (2_d)

It is well known that the type of mesophase (smectic or nematic) is determined mainly by the intermolecular attractions which operate between the sides and planes of the molecules, i.e., the strengths of the lateral and terminal attraction forces[(94)]. It appeared that a relatively small or compact group situated terminally in a molecule would enhance the nematic properties of the compound. For the oxadiazole containing compound, the lateral attractions could arise from the dipolar parts of the molecules {I}, one might predict that compound $\mathbf{1_e}$ would be a smectic

compound. In fact compound **1_e** is considered as purely nematic, the nematic- isotropic transition temperature being 140-200ºC. Our prediction should of course have taken into account the two terminal methoxy and 2-thiobutanoyl groups which lied high in the order of group efficiency for nematic mesophase formation, possibly by their influence on terminal intermolecular attractions.

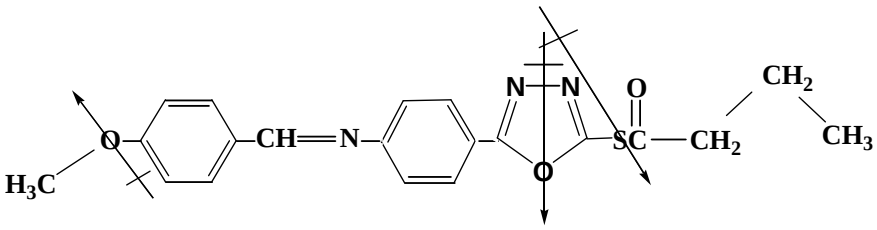

{I}

Monotropic smectic properties for compound **2_d** was observed. This molecule has a relatively short alkoxy group, and although there was no dipole moment acting across the molecule in a central position, there was a strong dipole moment of the methoxy group and the polarizability of the propyl chain of the ester group {II}, both of which would lead to increase lateral attractions.

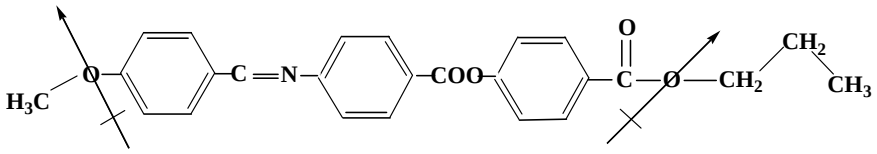

{II}

The two compounds **1_e** and **2_d** were not therefore, different, and the nematic behavior of the oxadiazole compound and the smectic behavior of the ester might be determined, in the first instance by the crystal lattice types adopted by the compounds. The oxadiazole group will cause some deviation from linearity[(95)], this may make it difficult for the molecule to be assumed a layer crystal lattice conducive to smectic behavior, also the

bend in the molecular shape was reduced to a certain degree if the oxadiazole ring was shifted to the terminal position of the rigid aromatic core and the oxadiazole ring might be looked upon as a polar terminal substituents.

Comparing compound $\mathbf{1_e}$ with 2-alkyl-1,3,4-oxadiazole derivatives {III} did not show liquid crystalline properties[96]. We must conclude, therefore, that 1,3,4-oxadiazole derivative might exhibit liquid crystalline properties only if the rigid core contained more than two rings.

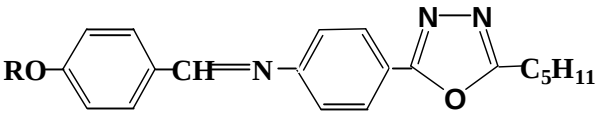

{III}

R= C_nH_{2n+1}

n= 5-9

3.6.2 Mesomorphic Properties of the 2,5-bis-[4-(4´-alkoxybenzylideneamino)phenyl]-1,3,4-oxadiazole:

The Mesomorphic properties of two compounds of this series $\mathbf{3_{e1}}$ and $\mathbf{3_{g1}}$ were studied by means of DSC and hot stage polarizing microscope.

Individual thermal microscopic observation of this series revealed that compound $\mathbf{3_{e1}}$ did not show liquid crystal properties, while compound $\mathbf{3_{g1}}$ displayed a nematic mesophase of typical threadlike texture, on further heating these threads shrinks to form nematic droplets near isotropic transition temperature as shown in Figure 3.27, while Figure 3.28 shows the DSC thermogram of this compound.

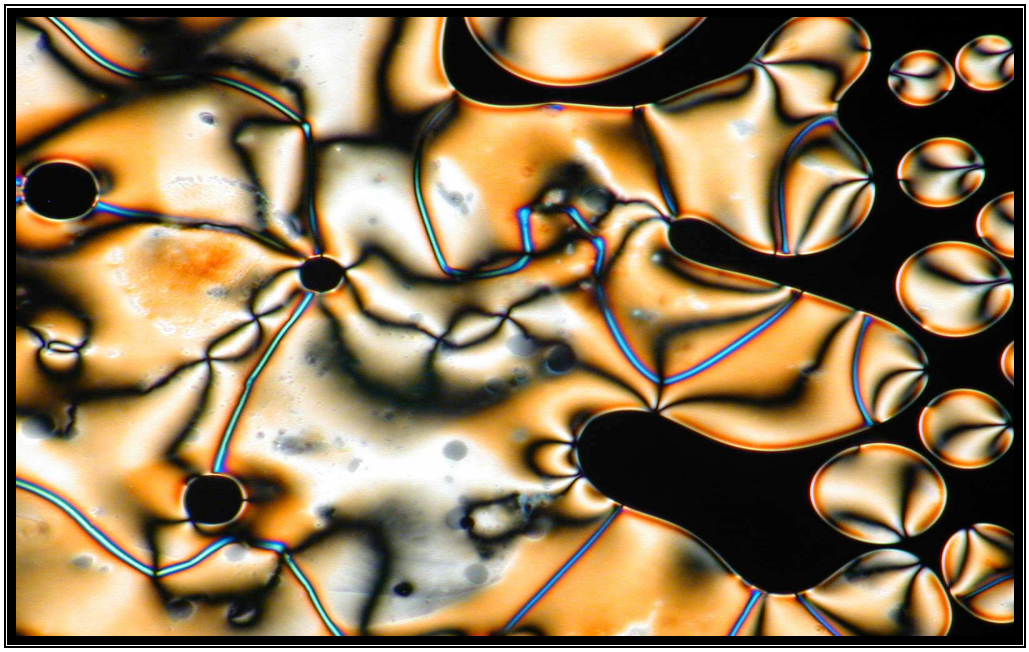

Figure 3.27 Nematic texture of model compound 2,5-bis-[4-(4´-propoxybenzylid-eneamino)phenyl]-1,3,4-oxadiazole (3_{g1})

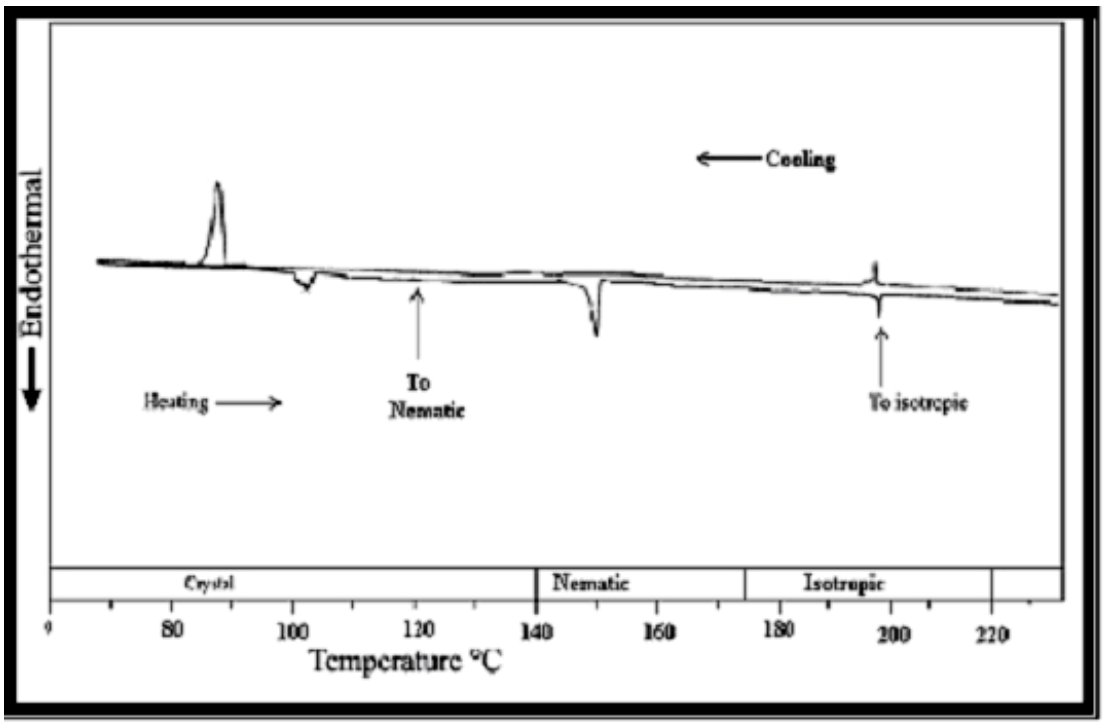

Figure 3.28 DSC Thermogram of compound 2,5-bis-[4-(4´-propoxybenzylideneamino)phenyl]-1,3,4-oxadiazole (3_{g1})

The absence of mesomorphicity of compound $\mathbf{3_{e1}}$ might be due to the length of alkoxy group which is less than half the length of the molecules. Herbert[97] found that mesophase formation ability starts when the alkyl chain is almost half the length of the whole molecule. This could be due to two reasons: Firstly, the number could represent an onset of chain rotation or a change in angle of till within planes of molecules, Secondly, this change would favor the usual parallel fashion of the molecular axis leading to mesophase formation.

3.6.3 Mesomorphic Properties of the 2,5-bis-[4-(4´-alkoxybenzanilid-e)phenyl]-1,3,4-oxadiazole:

Liquid crystalline properties of these two compounds were studied by means of (DSC) and hot stage polarizing microscope.. Microscopic observations of compounds $\mathbf{3_{e2}}$ and $\mathbf{3_{g2}}$, revealed that compound $\mathbf{3_{e2}}$ did not show liquid crystal properties, while compound $\mathbf{3_{g2}}$ showed nematic mesomorphism, Figure 3.29 shows the texture appearance under polarizing microscopy, while Figure 3.30 shows the DSC thermogram of this compound.

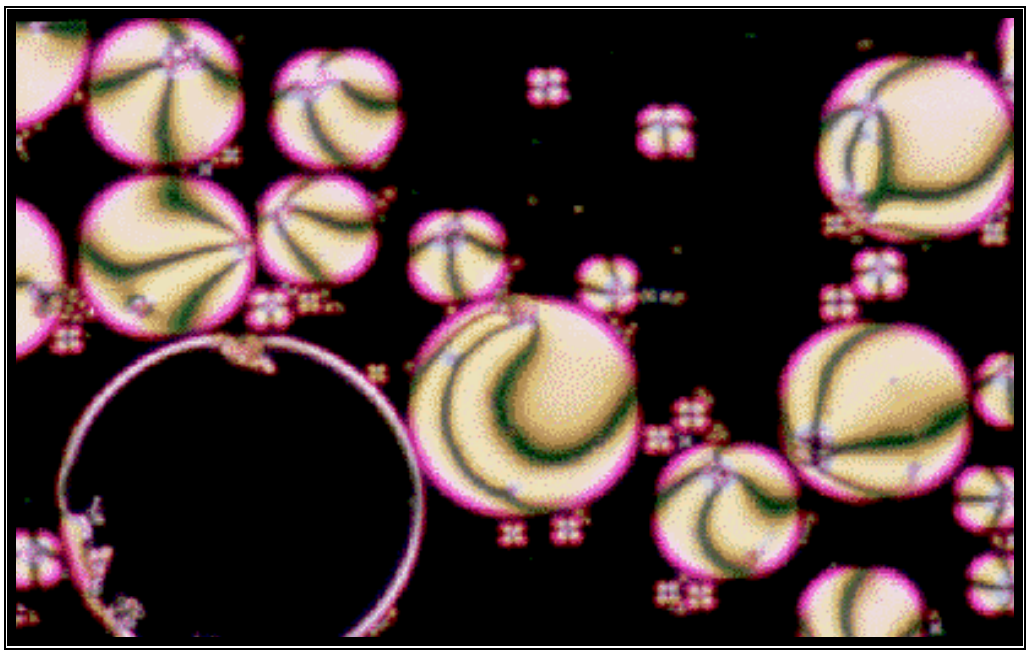

Figure 3.29 Nematic texture of model compound 2,5-bis-[4-(4´-propoxybenzanil-ide)phenyl]-1,3,4-oxadiazole (3_{g2})

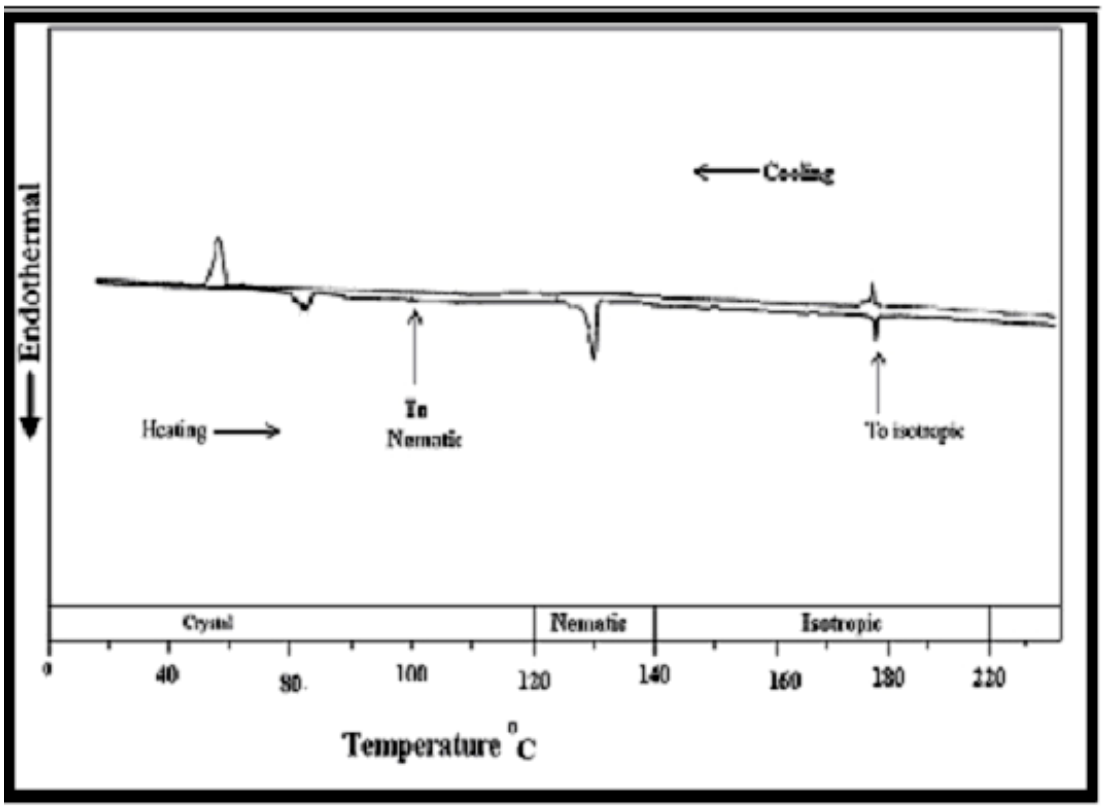

Figure 3.30 DSC Thermogram of compound 2,5-bis-[4-(4´-propoxybenzanilid-e)phenyl]-1,3,4-oxadiazole (3_{g2})

3.7 Column Chromatography

3.7.1 The packing ratio

Gas-liquid chromatography were obtained with an chromatograph Pye-Unicam using nitrogen as carrier gas and a flame ionization detector.

The column packing contained 20 wt.% of liquid crystal stationary phase deposited on the solid support, Chromosorb W(60-80 mesh). The column were conditioned at 15ºC above the nematic-isotropic (N-I) transition temperature of the crystal phase stationary liquid for 24 hr. before use. Table 3.3 list the liquid crystal stationary phases used in this work.

Table 3.3 The liquid crystal stationary phases

Stationary phase	Molecular weight	Chemical name and structural formula	Max. analysis Temp.ºC
1_e	381	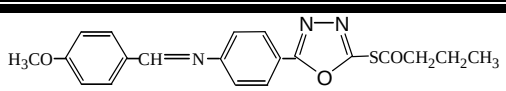	300
2_d	417	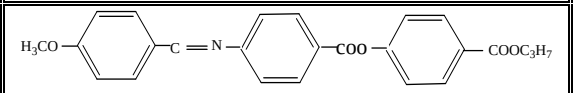	260
PEG	6000	$HO\text{-}CH_2CH_2O)_n\text{-}H$ Polyethylene glycol	255

We choose 20% coating percentage as reported in previous studies to give best chromatographic performance, therefore no attention was made to use other coating percentage[98-100]. The retention time is affected by several factors such as column length, nature and type of stationary phase, how well the column is packed the speed of carrier gas, the

pressure as well as the nature of the analyzed compounds. In order to be more accurate, we calculate $t_{\acute{R}}$ (Adjusted) retention time, by measuring t_m, the time of unretened species (ethanol) in this case and calculating t'_R using this equation:

$$t'_R = t_R - t_m \qquad \ldots\ldots \quad 3.1$$

Table 3.4 shows the times for unretened species for the three columns.

Table 3.4 The time of unretened species t_m (min.) of Ethanol

No.	Packing material	140ºC	160ºC	180ºC	200ºC	220ºC	240ºC	260ºC	280ºC	300ºC
1	1_e	3.500	3.450	3.400	3.350	3.300	3.250	3.200	3.150	3.100
2	2_d	5.520	5.400	5.350	5.200	5.150	5.000	4.950	-	-
3	PEG 20%	2.449	2.403	2.352	2.301	2.251	2.203	2.155	2.102	2.063

3.7.2 Column performance evaluation

The effect of the flow rate on the plate height have been studied, to evaluate the optimum flow rate as shown in Figure 3.31. The van Deemter curve shows the existence of an optimum velocity at which a given column exhibits its highest number of theoretical plates[(101)]. The flow rate was varied from 5 – 40 ml/min, for each value the retention time was measured and the corrected retention time t'_R was calculated

using equation 3.1. The effective plate number $\mathbf{N_{eff}}$ was calculated for each value of $\mathbf{t'_R}$ using:

$$\mathbf{N_{eff} = 16\ (t'_R/w)^2} \qquad \text{.....} \quad \mathbf{3.2}$$

The length element of a chromatographic column occupied by a theoretical plate is the plate height **H**:

$$\mathbf{H = L/N} \qquad \text{.....} \quad \mathbf{3.3}$$

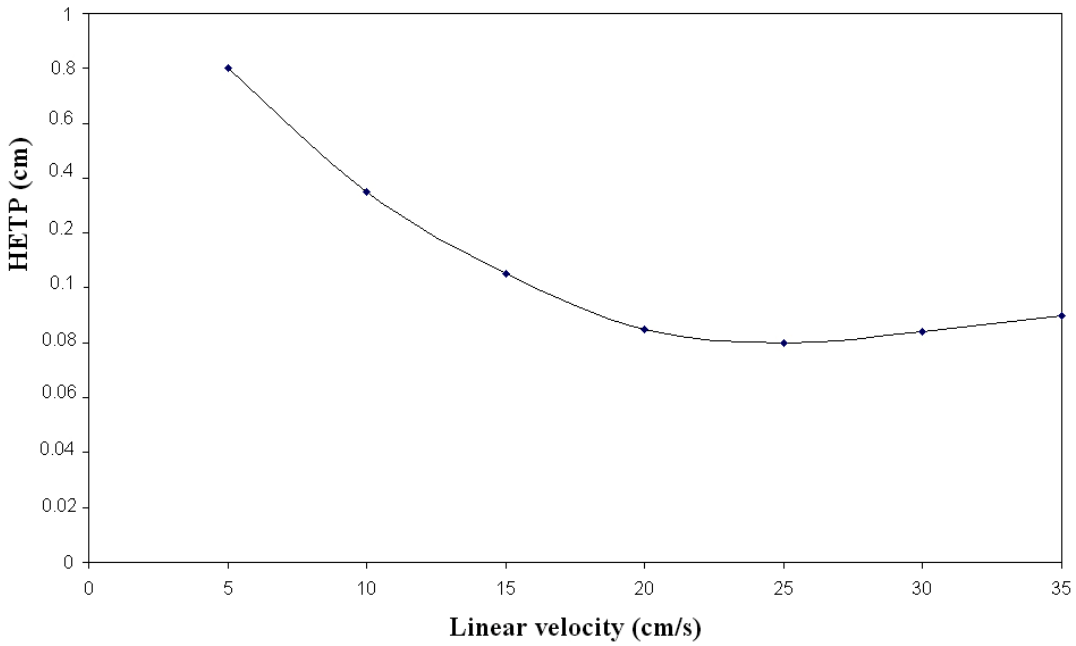

Figure 3.31 Effect of mobile phase flow rate on plate height for positional isomers (cresols). Column dimension: 1.75 m x 3mm i.d. Stationary phase: 2-thiobutanoyl-5-[4-(4´methoxybenzylideneamino)phenyl]1,3,4-oxadiazole coated on Chromosorb [60-80 mesh, 20%]; Carrier gas: nitrogen; Injection volume: 1µl; Injuctor temperature: 275ºC; Detector: FID; Oven temperature 140- 300ºC.

3.7.3 2-thiobutanoyl-5-[4-(4´methoxybenzylideneamino)phenyl]1,3,4-oxadiazole 1_e as a stationary phase:

The analysis of positional isomer o-, m- and *p*-cresol (mixture A) and poly-aromatic hydrocarbons (PAH) naphthalene, fluorene, phenanthrene and anthracene (mixture B) were performed on 20% of the above liquid

crystal column. The retention time of each compound in the mixtures was measured at the mesophase transition range 140 – 300ºC.

The analysis of mixture A is shown in Figure 3.32, while the analysis of mixture B is shown in Figure 3.33. The data of the retention times are listed in Tables 3.5 and 3.6. In order to make comparison with the separation on the traditional column, the separation of mixture B was done on column 20% PEG and at the same conditions, no separation was obtained, this work is assessed the importance of liquid crystal as stationary phase. Figure 3.34 show the separation of mixture B on column 20% PEG.

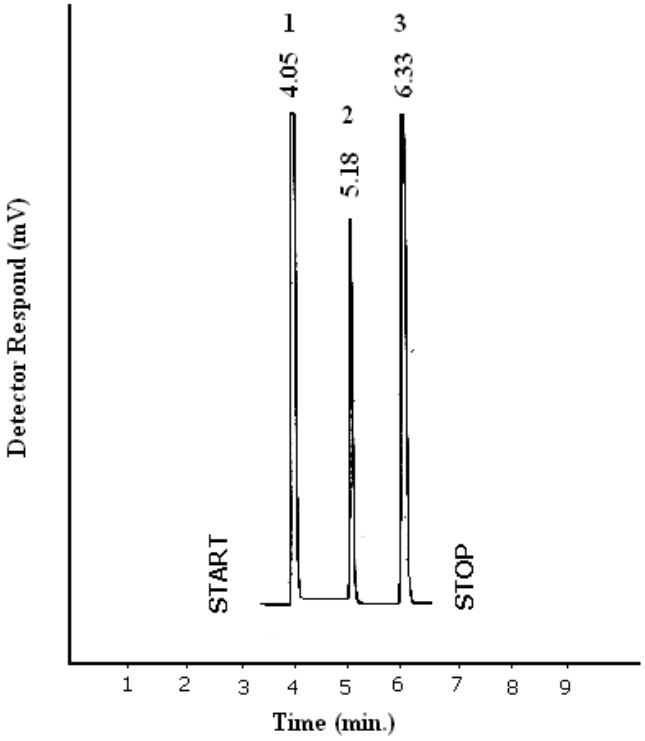

Figure 3.32 Chromatogram of positional isomers (cresols) of 2-thiobutanoyl-5-[4-(4´methoxybenzylideneamino)phenyl]1,3,4-oxadiazole (1_e). Condition oven temperature 160ºC; F_c 25 ml/min and detector temperature 250ºC, peak: o -cresol 1, *p*-cresol 2, m- cresol 3.

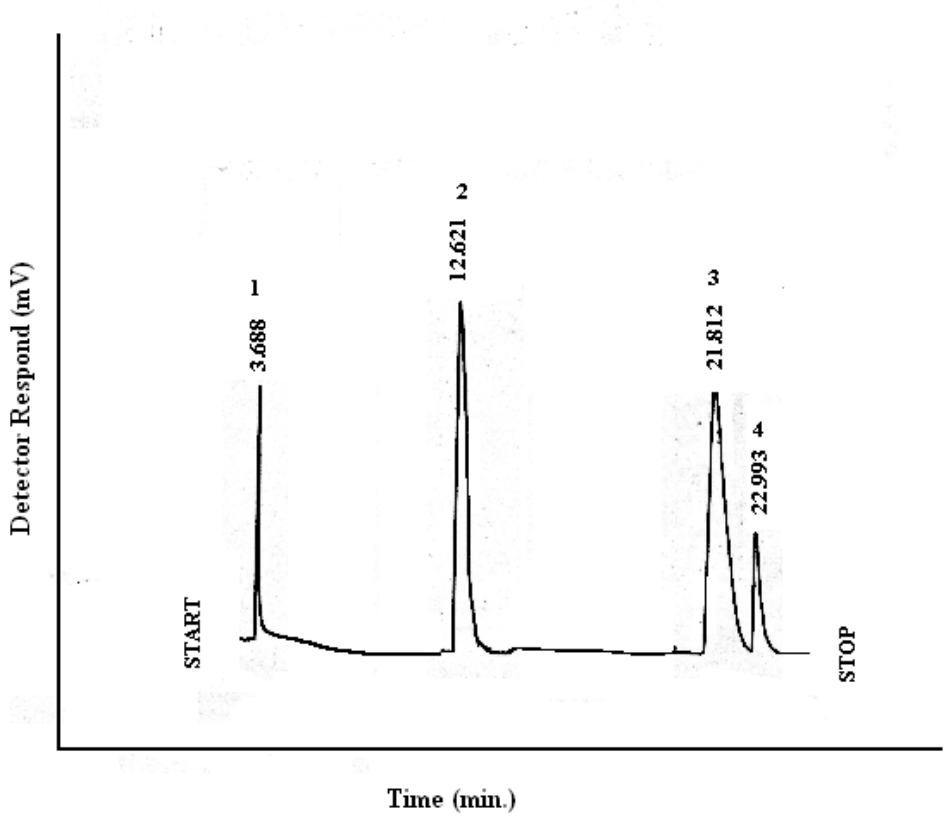

Figure 3.33. Chromatogram of PAHs mixture B of 20% 2-thiobutanoyl-5-[4-(4´methoxybenzylideneamino)phenyl]1,3,4-oxadiazole (1_e). Condition oven temperature 160ºC; F_c 25 ml/min and detector temperature 250ºC, peak, naphthalene 1, fluorine 2, phenanthrene 3, anthracene 4.

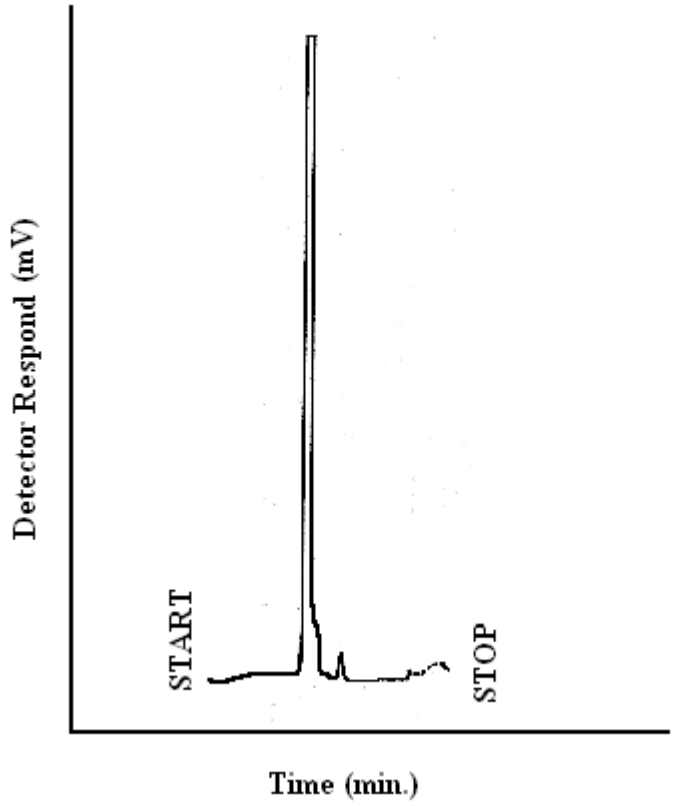

Figure 3.34. Chromatogram of PAHs mixture B on 20% PEG Condition oven temperature 160ºC; F_c 25 ml/min and detector temperature 250ºC, peak, naphthalene1, fluorine 2, phenanthrene 3, anthracene 4.

Table 3.5 Adjusted retention times (t'_R / minute) for mixture A on 20% 2-thiobutanoyl-5-[4-(4´-methoxybenzylideneamino)phenyl]1,3,4-oxadiazole (1_e)

Temp.ºC / Comp.	Retention Time (t'_R /min.)								
	140ºC	160ºC	180ºC	200ºC	220ºC	240ºC	260ºC	280ºC	300ºC
o -cresol	4.060	4.051	3.813	3.447	3.388	3.206	2.922	2.663	2.381
p-cresol	5.191	5.188	4.838	4.389	4.289	3.961	3.641	3.191	2.712
m-cresol	5.721	6.337	5.823	5.165	5.132	4.751	4.331	3.881	3.255

Table 3.6 Adjusted retention times (t'_R / minute) for mixture B on 20% 2-thiobutanoyl-5-[4-(4´-methoxybenzylideneamino)phenyl]1,3,4-oxadiazole (1_e)

Temp.ºC / Comp.	Retention Time ($t_{Ŕ}$ /min.)								
	140ºC	**160ºC**	**180ºC**	**200ºC**	**220ºC**	**240ºC**	**260ºC**	**280ºC**	**300ºC**
Naphthalene	3.421	3.688	2.731	2.128	1.877	1.532	1.401	1.398	1.353
Fluorene	9.812	12.621	8.322	6.455	5.822	4.349	4.022	3.998	3.873
Phenanthrene	16.332	21.812	11.511	8.457	7.531	4.977	4.891	4.023	3.997
Anthracene	16.185	22.993	11.759	8.612	7.553	5.021	4.923	4.123	4.132

Better separation was obtained at the temperature 160ºC, this related to the higher order of the liquid crystal stationary phase which makes it easier for molecules of substances are retained stronger and stay longer in the column. As the temperature increase the retention time decrease this arise as the fact that with increase in temperature the order of a liquid crystal decreases which result in a smaller influence of substances which molecules are of the shape hindering their interaction with the structure of liquid crystals of lower order.

The order of elution's of cresol isomers (mixture A) was *ortho*, *para* and *meta*, this could be explained to the ability of the nitrogen atom of imine group to form inter molecular hydrogen bonding as shown below:

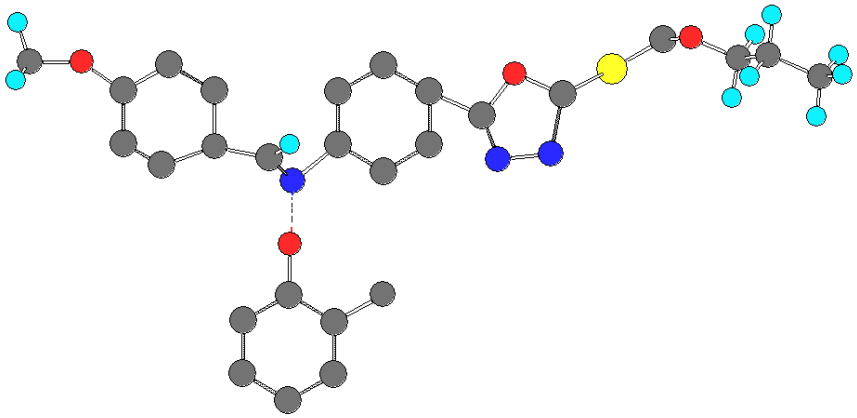

= Carbon , = Hydrogen , = Nitrogen , = Oxygen , = Sulfur

Because of the presence of methyl group ortho to the phenolic hydroxide, it cause a steric effect inhibit the formation of hydrogen bonding, so *ortho*- isomer eluted first. According to this explanation, *para*- isomer should eluted finely, this not happen because the liquid crystal molecule have a banana shape and it is not planar, so it doesn't have affinity to the planar molecule i.e. *para*- isomer.

The elution of PAHs (mixture B) were naphthalene, fluorine, phenanthrene and anthracene. Chang et al. reported that the elution patterns of PAHs were almost consistent with their L/B (length to breadth) ratio[(102)] and their boiling point.

Resolution $\mathbf{R_s}$ is the term used to describe the degree of separation of successive solute peaks. The chromatograms used to obtain the resolution $\mathbf{R_s}$ of mixture A and B on column $\mathbf{1_e}$ using[(103)]:

$$\mathbf{R_s = 2(t'_{RB} - t'_{RA})/(w_A + w_B)} \quad \text{.....} \quad \mathbf{3.4}$$

Where t'_{RA} and t'_{RB} are the retention times of peaks 1 and 2 and W_A and W_B are the widths of the peaks at the baseline. The R'_s values for the two mixtures on column 1_e are listed in Tables 3.7 and 3.8.

Table 3.7 Resolution R_s for mixture A on 1_e .

Temp.°C / Comp.	Resolution R_s								
	140° C	**160° C**	**180°C**	**200°C**	**220°C**	**240°C**	**260°C**	**280°C**	**300°C**
***p*-cresol/ o-cresol**	1.07	1.89	1.28	1.26	1.13	1.14	1.13	1.12	1.09
m-cresol/ *p*-cresol	0.32	1.23	1.16	1.21	1.08	1.07	1.06	1.00	1.00

Table 3.8 Resolution R_s for mixture B on 1_e .

Temp.°C / Comp.	Resolution R_s								
	140°C	**160°C**	**180°C**	**200°C**	**220°C**	**240°C**	**260°C**	**280°C**	**300°C**
Flu./Naph.	15.58	21.78	13.63	10.55	9.62	6.87	6.37	6.34	6.14
Phen./Flu.	16.30	20.42	7.97	3.20	2.84	1.06	1.03	0.98	0.97
Anth./Phen	0.86	1.12	0.62	0.60	0.44	0.42	0.40	0.38	0.33

The separation is also dependent on the relative retention characteristics of the solute characteristics of the solute components **α**, often called the selectivity factor[(104)].

$$\alpha = V'_B/V'_A \qquad \text{…..} \quad 3.5$$

where V'_A, V'_B are the adjusted specific retention volumes of solute components A and B respectively.

The selectivity factor were calculated for each adjacent peaks. Tables 3.9 and 3.10 show the values of the selectivity factor for mixtures A and B respectively.

Table 3.9 Selectivity factor (α) for mixture A on 1_e .

Temp.°C / Comp.	Selectivity factor α								
	140° C	160° C	180°C	200°C	220°C	240°C	260°C	280°C	300°C
***p*-cresol/ o-cresol**	1.27	1.28	1.26	1.22	1.26	1.23	1.24	1.19	1.13
m-cresol/ *p*-cresol	1.10	1.22	1.20	1.17	1.19	1.19	1.18	1.21	1.20

Table 3.10 Selectivity factor (α) for mixture B on 1_e .

Temp.°C / Comp.	Selectivity factor α								
	140°C	160°C	180°C	200°C	220°C	240°C	260°C	280°C	300°C
Flu./Naph.	2.86	3.42	3.04	3.03	3.10	2.83	2.87	2.85	2.86
Phen./Flu.	1.66	1.72	1.38	1.31	1.29	1.14	1.21	1.00	1.17
Anth./Phen	1.03	1.05	1.02	1.01	1.00	1.00	1.00	1.02	1.03

The best selectivity factors were obtained at the temperature of 15ºC above the formation of the nematic mesophase, i.e. at 160ºC. This has been attributed to the nematic lattice layer are ordered in its optimum structural configuration system. This mesophase represent the actual nematic phase planes compared to that at higher temperature, in which its properties are closer to the isotropic liquids phase than to the solid state. This phenomenon has also been noticed previously[(105)].

In order to assess the performance and separation efficiency of column it is necessary to determine the effective plate number N_{eff} of column, which is defined by equation 3.2 [106]. The plate number shows a maximum at temperature 160ºC, we therefore consider this temperature to be the optimum.

The N_{eff} value of 1_e column for mixtures A and B are listed in Tables 3.11 and 3.12, respectively.

Table 3.11 The effective plate number (N_{eff}) for mixture A on 1_e

Temp.ºC / Comp.	N_{eff}								
	140ºC	**160ºC**	**180ºC**	**200ºC**	**220ºC**	**240ºC**	**260ºC**	**280ºC**	**300ºC**
o-cresol	1826	2143	1529	1489	1452	1388	1115	926	740
***p*-cresol**	879	2691	2593	1926	1839	1568	1325	1018	735
m-cresol	1239	1909	1723	1268	1252	1073	892	716	503

Table 3.12 The effective plate number (N_{eff}) for mixture B on 1_e

Temp.ºC / Comp.	N_{eff}								
	140ºC	**160ºC**	**180ºC**	**200ºC**	**220ºC**	**240ºC**	**260ºC**	**280ºC**	**300ºC**
Naphthalene	967	1507	616	374	291	193	162	161	151
Fluorene	10667	17649	7673	4616	3755	2095	1792	1771	1662
Phenanthrene	22044	39319	10950	5910	4689	2055	1977	1337	1319
Anthracene	27027	50320	13161	7059	5429	2399	2306	1618	1625

3.7.4 4-[4´-(4˝methoxybenzylideneamino)benzoyloxy]propyl benzoate(2_d):

This liquid crystal has a nematic transition temperature range (155-260ºC). The analysis of mixtures A and B were performed on 20% of the above liquid crystal column. The retention time of each compound in the mixtures was measured at the mesophase transition temperature range 140 – 260ºC.

The analysis of mixture A is shown in Figure 3.35, while the analysis of mixture B is shown in Figure 3.36. The data of the retention times are listed in Tables 3.13 and 3.14 for Mixture A and B, respectively.

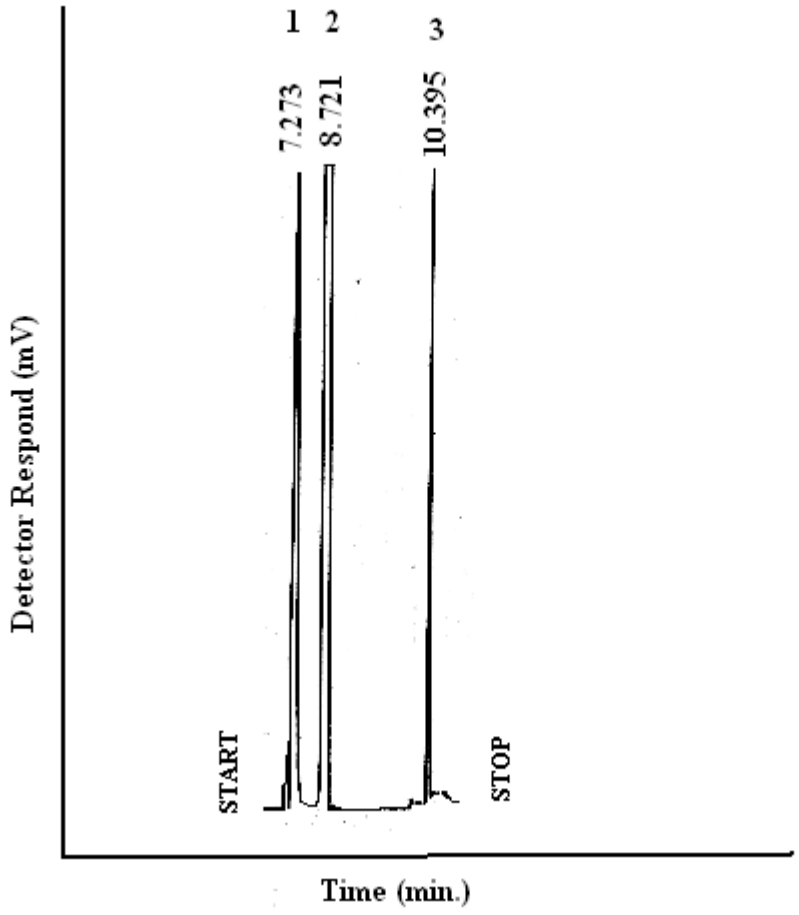

Figure 3.35. Chromatogram of positional isomers (cresols) mixture A of 20% 4-[4´-(4˝methoxybenzylideneamino)benzoyloxy]propylbenzoate(2_d):Condition oven temperature 180ºC; F_c 25 ml/min and detector temperature 250ºC, peak, m-cresol 1, o-cresol 2, *p*-cresol 3.

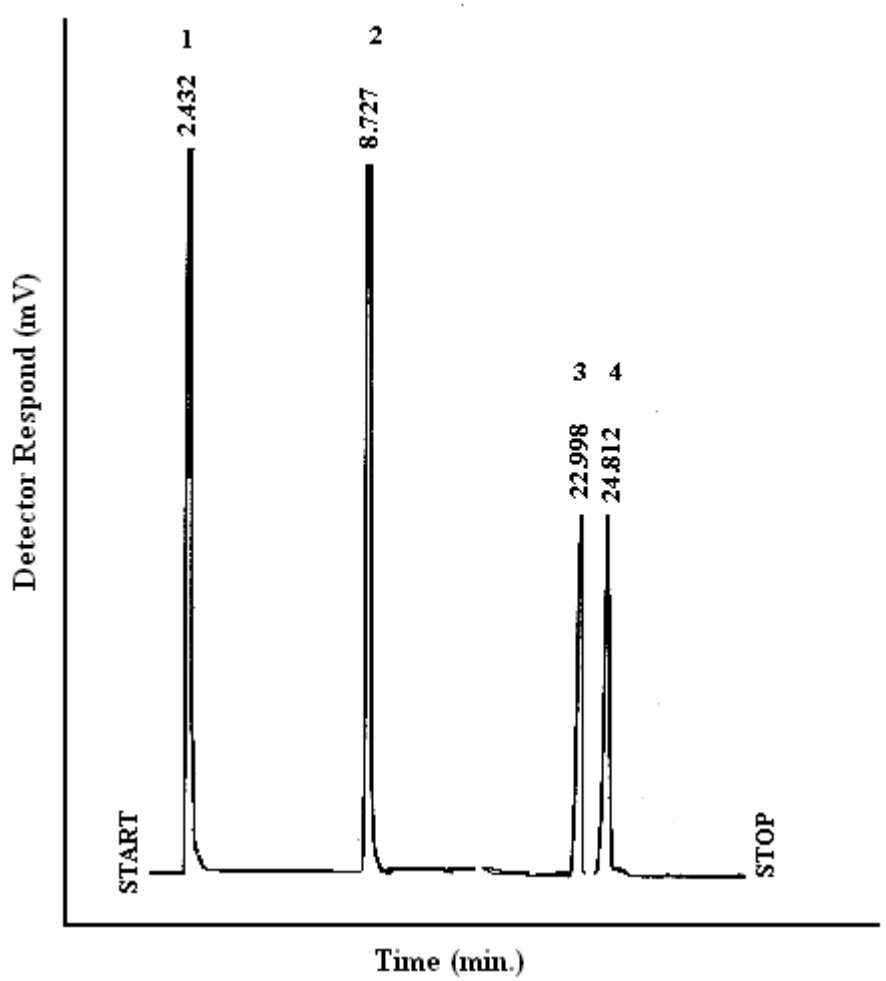

Figure 3.36 Chromatogram of PAHs mixture B of 20% 4-[4´-(4˝methoxybenzylideneamino)benzoyloxy]propylbenzoate(2_d). Condition oven temperature 180ºC; F_c 25 ml/min and detector temperature 250ºC, peak, naphthalene 1, fluorine 2, phenanthrene 3, anthracene 4.

Table 3.13 Adjusted retention times (t'_R / minute) for mixture A on 20% 4-[4´-(4˝methoxybenzylideneamino)benzoyloxy]propyl benzoate (2_d)

Temp.ºC / Comp.	Retention Time (t'_R /min.)						
	140ºC	**160ºC**	**180ºC**	**200ºC**	**220ºC**	**240ºC**	**260ºC**
m-cresol	7.933	7.328	7.273	6.712	6.523	5.825	5.187
o-cresol	8.128	7.570	8.721	7.133	6.827	5.917	5.544
***p*-cresol**	9.323	8.732	10.395	8.082	7.734	6.791	6.188

Table 3.14 Adjusted retention times (t'_R / minute) for mixture B on 20% 4-[4´-(4˝methoxybenzylideneamino)benzoyloxy]propyl benzoate (2_d)

Temp.°C / Comp.	Retention Time ($t_{Ŕ}$ /min.)						
	140°C	160°C	180°C	200°C	220°C	240°C	260°C
Naphthalene	2.230	2.331	2.432	1.427	1.387	0.820	1.199
Fluorine	7.745	6.827	8.727	4.496	3.998	3.571	3.435
Phenanthrene	19.918	18.183	22.998	8.752	6.352	5.693	5.578
Anthracene	19.928	18.291	24.812	8.835	6.531	5.921	5.891

The order of elution of (mixture A) on column 2_d was *meta, ortho* and *para*. The larger retention of *para*- cresol isomer, could be account to the larger diffusion coefficient of *para*-cresol compared to *meta* and *ortho*-cresol. Because the planarity of compound 2_d, isomers whose molecules are more planar, or whose length to breadth ratio is larger, are eluted from a column later than molecules less planar or of the smaller length to breadth ratio even if their molecular weights and boiling points favor the reverse order of elution[107].

The selectivity factors were calculated for each adjacent peaks at all the separation temperatures . Tables 3.15 and 3.16 list the values of the selectivity factor for mixtures A and B respectively.

Table 3.15 Selectivity factor α for mixture A on 2_d .

Temp.°C / Comp.	Selectivity factor α						
	140°C	160°C	180°C	200°C	220°C	240°C	260°C
o-cresol/ m-cresol	1.02	1.03	1.20	1.06	1.04	1.01	1.06
***p*-cresol/ *o*-cresol**	1.14	1.15	1.19	1.13	1.13	1.14	1.11

Table 3.16 Selectivity factor α for mixture B on 2_d .

Temp.°C / Comp.	Selectivity factor α						
	140°C	160°C	180°C	200°C	220°C	240°C	260°C
Flu./Naph.	3.47	2.92	3.59	3.15	2.88	2.92	2.86
Phen./Flu.	2.57	2.66	2.63	1.94	1.58	1.59	1.62
Anth./Phen	1.00	1.00	1.07	1.00	1.02	1.04	1.05

Tables 3.17 and 3.18 list the values of the resolution for mixtures A and B respectively.

Table 3.17 Resolution R_s for mixture A on 2_d .

Temp.°C / Comp.	Resolution R_s						
	140°C	160°C	180°C	200°C	220°C	240°C	260°C
o-cresol/ m-cresol	0.27	0.33	2.01	0.58	0.43	0.15	0.51
***p* –cresol/o-cresol**	1.65	1.61	2.32	1.31	1.00	0.97	0.85

Table 3.18 Resolution R_s for mixture B on 2_d .

Temp.°C / Comp.No.	Resolution R_s						
	140°C	160°C	180°C	200°C	220°C	240°C	260°C
Flu./Naph.	9.14	11.52	16.14	7.86	6.69	6.42	5. 73
Phen./Flu.	20.30	26.40	33.18	9.89	5.47	4.93	4.91
Anth./Phen	0.02	0.25	3.64	0.16	0.35	0.32	0.22

The N_{eff} values of 2_d column for mixtures A and B are listed in Tables 3.19 and 3.20,respectively.

Table 3.19 The effective plate number (N_{eff}) for mixture A on 2_d

Temp.°C / Comp.	N_{eff}						
	140°C	**160°C**	**180°C**	**200°C**	**220°C**	**240°C**	**260°C**
m-cresol	2054	1753	1727	1471	1389	1107	878
o-cresol	1737	1507	2000	1338	1225	920	808
***p*-cresol**	3291	2887	4092	2473	2265	1746	1450

Table 3.20 The effective plate number (N_{eff}) for mixture B on 2_d

Temp.°C / Comp.	N_{eff}						
	140°C	**160°C**	**180°C**	**200°C**	**220°C**	**240°C**	**260°C**
Naphthalene	451	492	536	184	174	61	130
Fluorine	7010	5447	8901	2362	1868	1490	1379
Phenanthrene	26437	22032	35245	5104	2688	2159	2073
Anthracene	24429	20580	37895	4801	2623	2155	2134

3.7.5 The Thermodynamic Properties of G C.

Gas chromatography can used to provide successful information on the solute – solvent interaction at low solute concentrations. The special texture of the liquid crystal compounds leads to the specific solvent behavior with respect to the another stationary phases. This behavior

depends upon the specific molecular interaction (time or volume) on these liquid crystal compounds[108].

Specific retention volumes, V_R, were calculated from the corrected peak retention times and column operating condition, using the well known equation derived by Littlewood et al.[109].

$$V_R\ (ml.g^{-1}) = (F_c.t'_R/w).J \quad \text{.....} \quad 3.6$$

Where V_R is the specific retention volume, t'_R is the corrected retention time, w is the weight of the solvent (liquid crystal), F_c is the corrected flow rate which is equal to[110]

$$F_c = F_o\ (T_c/T_a).(P-P_w/P) \quad \text{.....} \quad 3.7$$

Where F_o is the outlet flow rate, T_a, T_c are the ambient and column temperature, respectively, P, P_w is the atmospheric pressure and water vapor pressure at ambient temperature T_a. J is the mobile phase compressibility correction factor, which is estimated from James and Martin equation[111].

$$J = (3/2)[(P_i/Po)^2-1/(P_i/P_o)^3-1\ ] \quad \text{.....} \quad 3.8$$

P_i, P_o are the inlet and the outlet column pressure (mm.Hg), respectively.

The adjusted specific retention time t'_R is given in equation 3.1, and the adjusted specific volume V'_R for a solute is [112]:

$$V'_R = V_R - V_m \quad \text{.....} \quad 3.9$$

where t_m, V_m are the hold – up time and volume, respectively. The data of V'_R are listed in Tables 3.21 – 3.24.

Table 3.21 Adjusted specific retention volume (V'_R) for mixture A on 20% 2-thiobutanoyl-5-[4-(4´-methoxybenzylideneamino)phenyl]1,3,4-oxadiazole (1_e)

Temp.°C / Comp.	Retention volume ($V_{Ŕ}$ /ml.g^{-1})								
	140°C	160°C	180°C	200°C	220°C	240°C	260°C	280°C	300°C
o-cresol	31.830	32.144	31.453	29.140	29.336	28.443	26.692	24.917	22.907
***p*-cresol**	40.697	41.165	39.908	37.104	37.138	35.142	33.260	29.850	29.092
m-cresol	44.852	50.284	48.033	43.664	44.437	42.177	39.563	36.314	31.316

Table 3.22 Adjusted specific retention volume (V'_R) for mixture B on 20% 2-thiobutanoyl-5-[4-(4´-methoxybenzylideneamino)phenyl]1,3,4-oxadiazole (1_e)

Temp.°C / Comp.	Retention volume ($V_{Ŕ}$ /ml.g^{-1})								
	140°C	160°C	180°C	200°C	220°C	240°C	260°C	280°C	300°C
Naphthalene	26.820	29.264	22.528	17.990	16.252	13.591	12.798	13.081	13.017
Fluorine	76.926	100.147	68.648	54.570	50.412	38.584	36.740	37.409	37.262
Phenanthrene	128.042	173.078	94.954	71.495	65.210	44.244	44.079	37.643	38.455
Anthracene	132.111	182.449	96.999	72.855	65.401	46.223	44.971	38.578	39.753

Table 3.23 Adjusted specific retention volume (V'_R) for mixture A on 20% 4-[4´-(4˝methoxybenzylideneamino)benzoyloxy]propyl benzoate (2_d)

Temp.°C / Comp.	Retention volume ($V_{Ŕ}$ /ml.g^{-1})						
	140°C	160°C	180°C	200°C	220°C	240°C	260°C
m-cresol	90.912	82.579	84.934	79.303	77.890	73.494	66.554
o-cresol	93.140	87.372	101.184	84.278	83.501	74.654	71.135
***p*-cresol**	106.841	100.784	121.392	95.491	94.594	85.682	79.398

Table 3.24 Adjusted specific retention volume (V'_R) for mixture B on 20% 4-[4´-(4˝methoxybenzylideneamino)benzoyloxy]propyl benzoate (2_d)

Temp.°C / Comp.	Retention volume (V'_R /ml.g^{-1})						
	140°C	160°C	180°C	200°C	220°C	240°C	260°C
Naphthalene	25.555	26.904	28.400	16.860	16.964	10.345	10.251
fluorene	88.757	78.850	101.913	53.120	48.899	45.055	44.074
Phenanthrene	228.26	209.868	268.570	103.404	77.691	71.828	71.571
Anthracene	228.374	211.114	289.850	104.385	79.880	74.705	74.003

Plots of the logV'_R against the reciprocal absolute temperatures (Kelvin) for the 20% coating columns shown in Figures 3.37- 3.40.

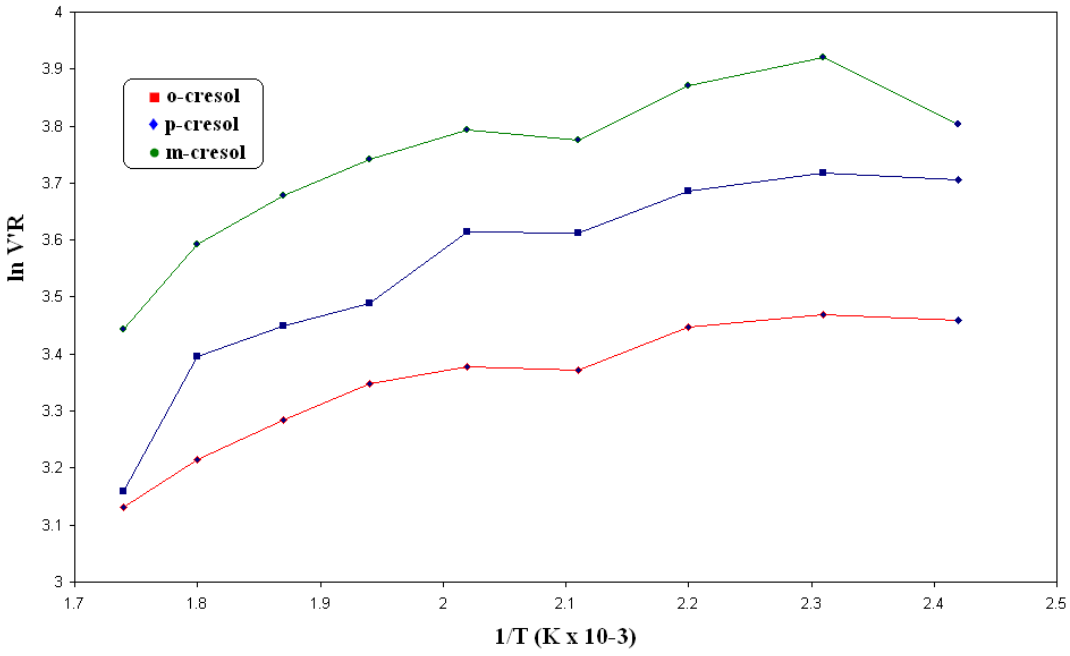

Figure 3.37 Natural logarithm retention volume (ln V'_R) versus reciprocal absolute temperature for mixture A on 20% 2-thiobutanoyl-5-[4-(4´methoxybenzylideneamino)phenyl]1,3,4-oxadiazole (1_e).

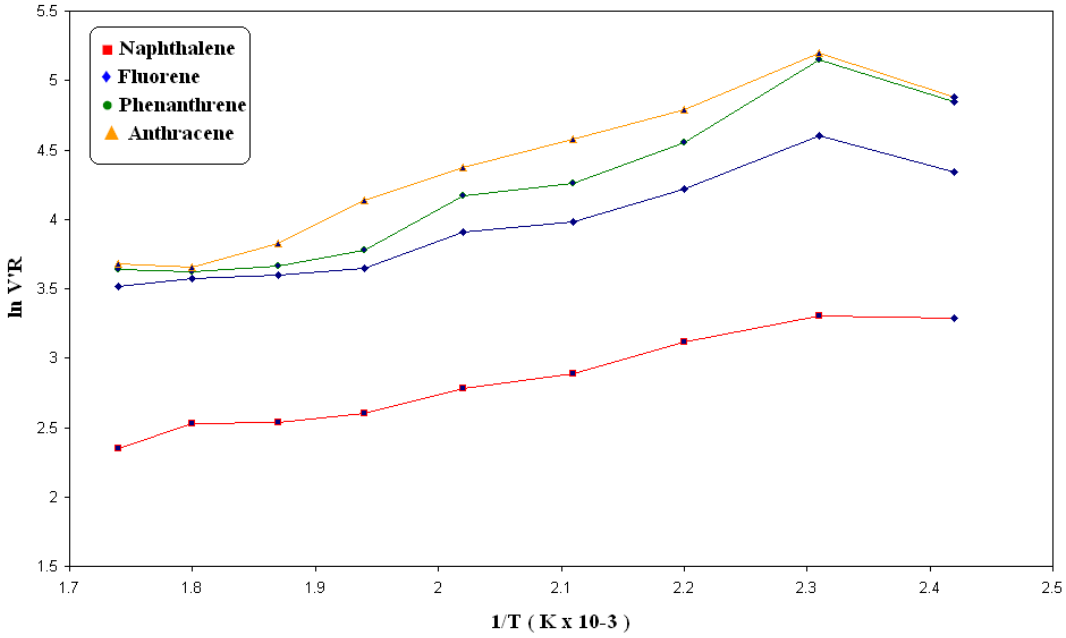

Figure 3.38. Natural logarithm retention volume (ln V'_R) versus reciprocal absolute temperature for mixture B on 20% 2-thiobutanoyl-5-[4-(4´methoxybenzylideneamino)phenyl]1,3,4-oxadiazole (1_e).

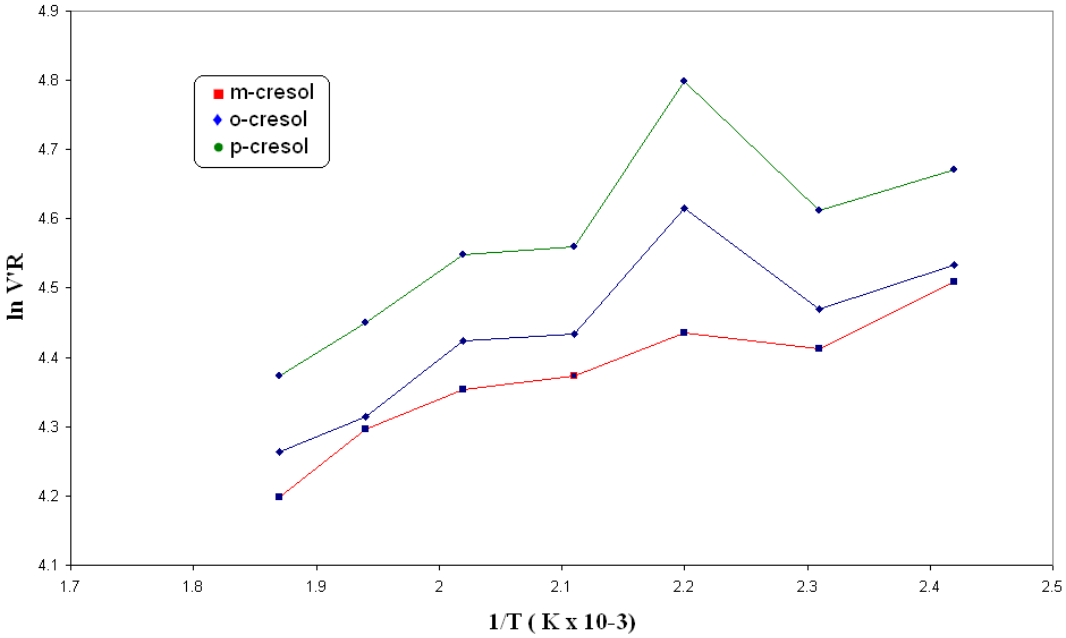

Figure 3.39 Natural logarithm retention volume (ln V'_R) versus reciprocal absolute temperature for mixture A on 20% coating 4-[4´-(4˝methoxybenzylideneamino)benzoyloxy]propyl benzoate(2_d).

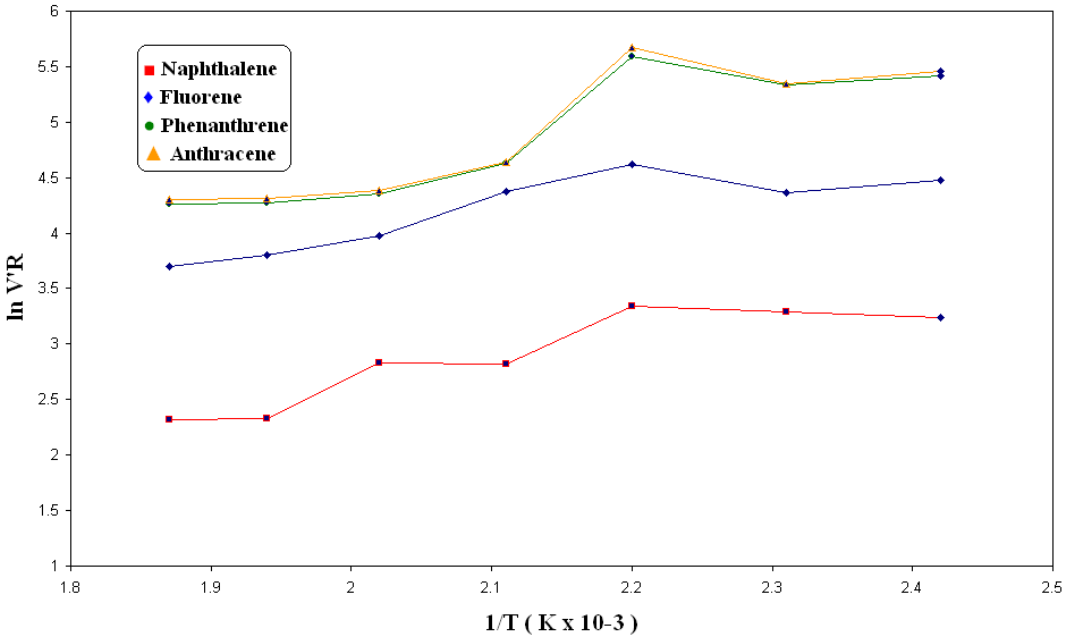

Figure 3.40. Natural logarithm retention volume (ln V'_R) versus reciprocal absolute temperature for mixture B on 20% coating 4-[4´-(4˝methoxybenzylideneamino)benzoyloxy]propyl benzoate(2_d).

The retention volumes of each compounds was found to decreased with increasing temperature accept at the nematic temperature 180°C or 160°C the retention volumes increase. This may be attributed to the increase in the solutes interaction with the stationary phase. Below these nematic temperature (the temperature at which good separation was achieves) the solute – stationary phase interaction is adsorption on the solid crystalline phase. As the temperature increases the adsorptivity of these phase decreases. Above the nematic temperature an abrupt increase in specific retention volumes was recorded, and the plot between ln V_R against 1/T was no longer linear.

Many studies[113-114] using differential thermal analysis (DTA) and x-ray technique showed that changes occur at temperature in the vicinity of the nematic temperature. These changes include some structural rearrangement of the stationary phases at this temperature and molecular

chains are packed together in the crystal as parallel rods. At higher temperature such molecular chains become more flexible and the helical chains are also to more locally, maintaining a certain degree of order. However, the percentage increase in specific retention volumes differs from one solute to another on the same stationary phase to another towards the same solute.

The negative values of the slope represent the molar heat of the enthalpy of the solution[109] according to:

$$\text{Log } V_R = \{-\Delta H / 2.303.R.T\} + \text{constant} \quad \text{.....} \quad 3.10$$

The constant values were estimated using computer least-square analysis method program.

Solute activity coefficients at infinite dilution (γ) has been determined using the equation[115]

$$\gamma = 1.704 \times 10^7 / P^o_2 MV \quad \text{.....} \quad 3.11$$

where M is the solvent (liquid crystal) molecular weight and P^o_2 is the pure saturated vapor pressure (mm.Hg). the γ values are shown in Tables 3.25 – 3.28.

Table 3.25 The solute activity coefficient (γ) for mixture A on 20% 2-thiobutanoyl-5-[4-(4´-methoxybenzylideneamino)phenyl]1,3,4-oxadiazole (1_e)

Temp.°C / Comp.	Solute activity coefficient (γ)								
	140°C	**160°C**	**180°C**	**200°C**	**220°C**	**240°C**	**260°C**	**280°C**	**300°C**
o-cresol	0.308	0.270	0.240	0.232	0.194	0.172	0.142	0.120	0.092
***p*-cresol**	0.315	0.277	0.272	0.268	0.223	0.193	0.158	0.135	0.096
m-cresol	0.743	0.574	0.473	0.420	0.352	0.342	0.294	0.257	0.204

Table 3.26 The solute activity coefficient (γ) for mixture B on 20% 2-thiobutanoyl-5-[4-(4´-methoxybenzylideneamino)phenyl]1,3,4-oxadiazole (1_e)

Temp.°C / Comp.	Solute activity coefficient (γ)								
	140°C	160°C	180°C	200°C	220°C	240°C	260°C	280°C	300°C
Naphthalene	0.122	0.096	0.108	0.118	0.113	0.119	0.109	0.094	0.084
Fluorine	0.245	0.152	0.209	0.231	0.220	0.254	0.236	0.206	0.184
Phenanthrene	0.404	0.277	0.410	0.476	0.457	0.591	0.587	0.540	0.469
Anthracene	0.467	0.308	0.477	0.553	0.538	0.667	0.602	0.551	0.483

Table 3.27 The solute activity coefficient (γ) for mixture A on 20% 4-[4´-(4˝methoxybenzylideneamino)benzoyloxy]propyl benzoate (2_d)

Temp.°C / Comp.	Solute activity coefficient (γ)						
	140°C	160°C	180°C	200°C	220°C	240°C	260°C
m-cresol	0.108	0.099	0.055	0.075	0.070	0.062	0.060
o-cresol	0.125	0.120	0.061	0.085	0.077	0.071	0.064
***p*-cresol**	0.285	0.257	0.103	0.199	0.173	0.165	0.155

Table 3.28 The solute activity coefficient (γ) for mixture B on 20% 4-[4´-(4˝methoxybenzylideneamino)benzoyloxy]propyl benzoate (2_d)

Temp.°C / Comp.	Solute activity coefficient (γ)						
	140°C	160°C	180°C	200°C	220°C	240°C	260°C
Naphthalene	0.117	0.105	0.067	0.134	0.140	0.142	0.125
fluorene	0.193	0.170	0.113	0.217	0.207	0.199	0.180
Phenanthrene	0.207	0.199	0.161	0.300	0.3505	0.332	0.294
anthracene	0.447	0.231	0.181	0.352	0.363	0.347	0.301

For solute in columns 1_e and 2_d, $\gamma < 1$; which represent negative deviation from ideality and weak solute-solvent interactions, as well as the γ values of each compound was found to decrease with increasing temperatures, i.e. in the nematic phase than the corresponding isotropic liquid state.

On careful inspection of the plots of log γ verses 1/T (K^{-1}) Figures 3.41-3.44 illustrates that at the transition temperature both discontinuity and a change in slope occur, indicating that hydrocarbon molecules experience a marked change in environment as they enter a new phase. i.e. interaction of solutes with the solvent in the liquid crystalline region differs from the interaction in the isotropic liquid. This has been attributed to that the nematic lattice layers are ordered in its optimum structural configuration system. This mesophase represents the actual nematic phase planes compared to that at higher temperature[116].

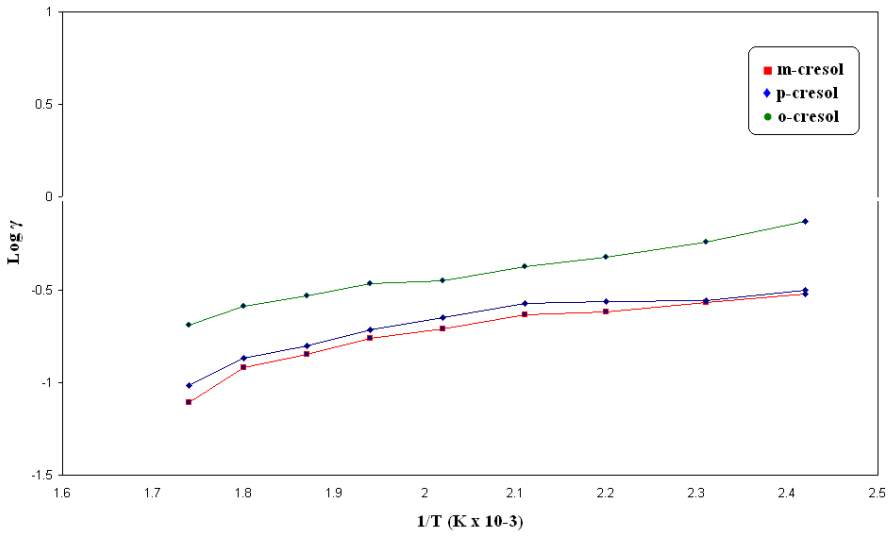

Figure 3.41. The logarithm of solute activity factor (log γ) versus reciprocal absolute temperature for mixture A on 20% 2-thiobutanoyl-5-[4-(4´methoxybenzylideneamino)phenyl]1,3,4-oxadiazole 1_e.

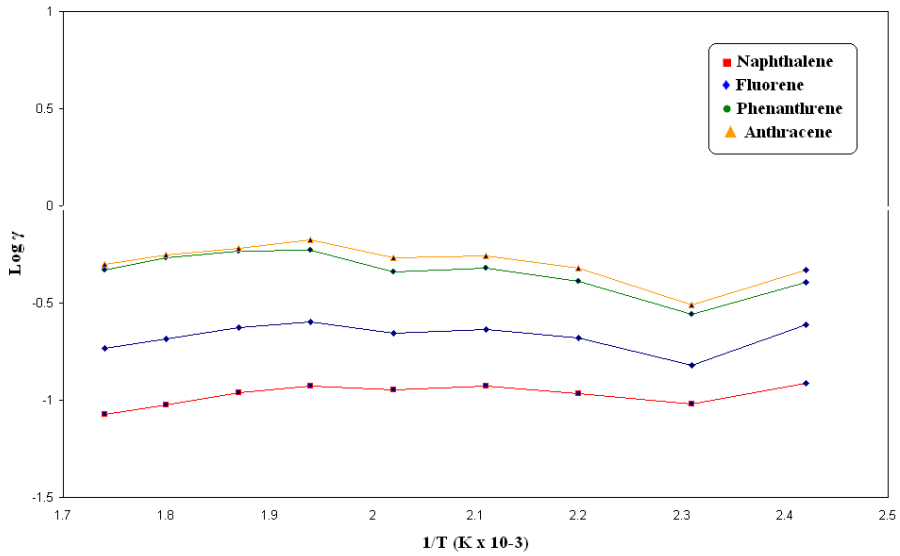

Figure 3.42. The logarithm of solute activity factor (log γ) versus reciprocal absolute temperature for mixture B on 20% 2-thiobutanoyl-5-[4-(4´methoxybenzylideneamino)phenyl]1,3,4-oxadiazole 1_e.

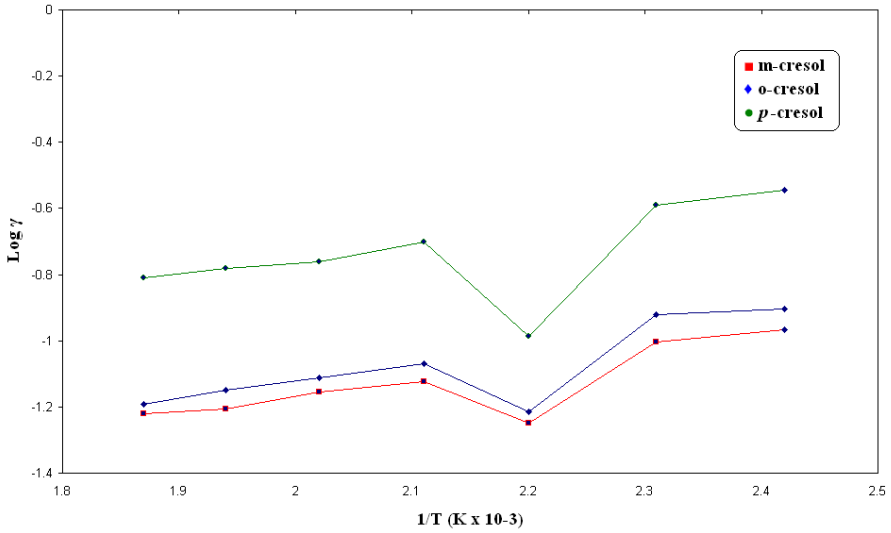

Figure 3.43 The logarithm of solute activity factor (log γ) versus reciprocal absolute temperature for mixture A on 20% 4-[4´-(4˝methoxybenzylideneamino)benzoyloxy]propyl benzoate(2_d).

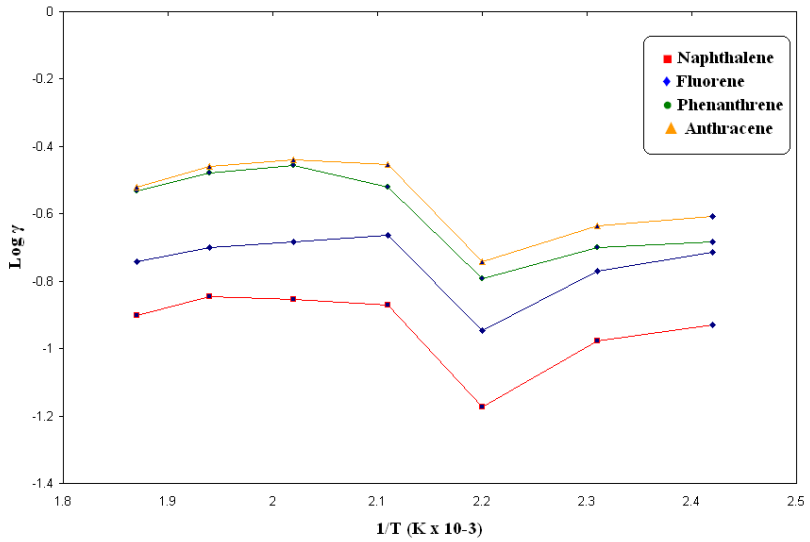

Figure 3.44. The logarithm of solute activity factor (log γ) versus reciprocal absolute temperature for mixture B on 20% 4-[4´-(4˝methoxybenzylideneamino)benzoyloxy]propyl benzoate(2_d).

The free energy were calculated from the relation[117]

$$\Delta G = RT \ln\gamma \qquad \text{------} \quad 3.12$$

All calculated free energies for the two coated liquid crystal compounds have negative values. These results demonstrated that the dissolvation process with these liquid crystal compounds were spontaneous[118]. In addition, these values are increased negatively as temperature increasing which indicated the decrease in the order of solute molecules with nematic lattices with increased temperature.

The entropy is also calculated using:

$$\Delta G = \Delta H - T\Delta S \qquad \text{------} \quad 3.13$$

For the two studied column, the calculated enthalpies, entropies and free energies presented in Tables 3.29 – 3.32.

The results in Tables 3.29 – 3.32 show that the enthalpy change (ΔH) are in both phases negative which indicate a strong exothermic mixing effect. It is also clear from these tables that ΔH in the mesophase regions

are greater than that in the isotropic liquid phases which means that the dissolution process in liquid crystalline state sacrificing some translational and rotational energy because of the difficulty of dissolving molecules in a highly ordered structure. The negative entropy (ΔS) for almost all process are normally accompanied by negative enthalpy changes.

Table 3.29 The Gibbs free energy (ΔG kj/mol^{-1}), Enthalpy (ΔH kj/mol^{-1}) and entropy (ΔS kj/mol^{-1}. k^{-1}) of mixture A on 20% 2-thiobutanoyl-5-[4-(4´-methoxybenzylideneamino)phenyl]1,3,4-oxadiazole (1_e)

Compound	140ºC			160ºC			180ºC			200ºC		
	ΔG	ΔH	ΔS	ΔG	ΔH	ΔS	ΔG	ΔH	ΔS	ΔG	ΔH	ΔS
o-cresol	-4.043	-11.327	-17.638	-4.713	-12.349	-17.636	-5.374	-13.359	-17.628	-5.745	-14.075	-17.613
***p*-cresol**	-4.158	-10.316	-14.912	-4.621	-11.068	-14.891	-4.903	-11.640	-14.873	-5.178	-12.208	-14.863
m-cresol	-1.020	-5.722	-11.387	-1.998	-6.917	-11.362	-2.819	-7.956	-11.341	-3.411	-8.788	-11.369

continue:

Compound	220ºC			240ºC			260ºC			280ºC		
	ΔG	ΔH	ΔS	ΔG	ΔH	ΔS	ΔG	ΔH	ΔS	ΔG	ΔH	ΔS
o-cresol	-6.721	-15.398	-17.601	-7.507	-16.529	-17.588	-8.649	-18.022	-17.586	-9.748	-19.471	-17.583
***p*-cresol**	-6.150	-13.474	-14.856	-7.016	-14.629	-14.842	-8.176	-16.095	-14.859	-9.206	-17.421	-14.857
m-cresol	-4.279	-9.875	-11.352	-4.576	-10.397	-11.347	-5.424	-11.470	-11.345	-6.246	-12.517	-11.341

Table 3.30 The Gibbs free energy (ΔG kj/mol^{-1}), Enthalpy (ΔH kj/mol^{-1}) and entropy (ΔS j/mol^{-1}.k^{-1}) of mixture B on 20% 2-thiobutanoyl-5-[4-(4´-methoxybenzylideneamino)phenyl]1,3,4-oxadiazole (1_e)

Compound	140ºC			160ºC			180ºC			200ºC		
	ΔG	ΔH	ΔS	ΔG	ΔH	ΔS	ΔG	ΔH	ΔS	ΔG	ΔH	ΔS
Naphthalene	-7.223	-8.189	-2.340	-8.436	-9.445	-2.332	-8.354	-9.404	-2.319	-8.394	-9.489	-2.316
Fluorine	-4.829	-5.561	-1.773	-6.781	-7.535	-1.742	-4.662	-5.449	-1.738	-5.762	-6.581	-1.732
Phenanthrene	-3.112	-2.752	0.871	-4.713	-4.339	0.862	-3.357	-2.970	0.853	-2.919	-2.517	0.849
Anthracene	-2.614	-2.087	1.274	-4.239	-3.688	1.271	-2.787	-2.212	1.268	-2.329	-1.730	1.265

Continue:

Compound	220ºC			240ºC			260ºC			280ºC		
	ΔG	ΔH	ΔS	ΔG	ΔH	ΔS	ΔG	ΔH	ΔS	ΔG	ΔH	ΔS
Naphthalene	-8.936	-10.073	-2.307	-9.085	-10.263	-2.298	-9.789	-11.013	-2.297	10.870	-12.139	-2.296
Fluorine	-6.206	-7.058	-1.729	-5.844	-6.729	-1.726	-6.398	-7.316	-1.724	-7.263	-8.214	-1.721
Phenanthrene	-3.209	-2.791	0.847	-2.243	-1.810	0.844	-2.360	-1.911	0.841	-2.833	-2.369	0.839
Anthracene	-2.540	-1.917	1.262	-1.727	-1.081	1.259	-2.248	-1.578	1.257	-2.740	-2.045	1.255

Table 3.31 The Gibbs free energy (ΔG kj/mol^{-1}), Enthalpy (ΔH kj/mol^{-1}) and entropy (ΔS kj/mol^{-1}.k^{-1}) of mixture A on 20% 4-[4´-(4˝methoxybenzylideneamino)benzoyloxy]propyl benzoate (2_d)

Compound	140ºC			160ºC			180ºC			200ºC		
	ΔG	ΔH	ΔS	ΔG	ΔH	ΔS	ΔG	ΔH	ΔS	ΔG	ΔH	ΔS
m-cresol	-7.642	-11.656	-9.721	-8.325	-12.525	-9.700	-10.923	-15.302	-9.698	-10.186	-14.771	-9.695
o-cresol	-7.140	-10.622	-8.433	-7.632	-11.281	-8.428	-10.533	-14.349	-8.426	-9.694	-13.675	-8.418
***p*-cresol**	-4.310	-6.092	-4.315	-4.891	-6.758	-4.312	-8.560	-10.548	-4.309	-6.348	-8.400	-4.304

Continue:

Compound	220ºC			240ºC			260ºC		
	ΔG	ΔH	ΔS	ΔG	ΔH	ΔS	ΔG	ΔH	ΔS
m-cresol	-10.899	-15.675	-9.689	-11.859	-16.823	-9.678	-12.467	-17.624	-9.676
o-cresol	-10.509	-14.657	-8.415	-11.281	-15.596	-8.413	-12.181	-16.662	-8.409
***p*-cresol**	-7.191	-9.310	-4.299	-7.684	-9.882	-4.286	-8.257	-10.539	-4.283

Table 3.32 The Gibbs free energy (ΔG kj/mol^{-1}), Enthalpy (ΔH kj/mol^{-1}) and entropy (ΔS kj/mol^{-1}.k^{-1}) of mixture B on 20% 4-[4´-(4˝methoxybenzylideneamino)benzoyloxy]propyl benzoate (2_d)

Compound	140ºC			160ºC			180ºC			200ºC		
	ΔG	ΔH	ΔS	ΔG	ΔH	ΔS	ΔG	ΔH	ΔS	ΔG	ΔH	ΔS
Naphthalene	-7.367	-8.253	-2.147	-8.113	-9.041	-2.145	-10.180	-11.272	-2.141	-7.904	-8.915	-2.138
Fluorene	-5.648	-6.297	-1.573	-6.378	-7.058	-1.571	-8.198	-8.908	-1.568	-6.008	-6.748	-1.566
Phenanthrene	-5.408	-4.853	1.343	-5.811	-5.229	1.344	-6.878	-6.270	1.342	-4.734	-4.099	1.341
Anthracene	-4.801	-4.217	1.412	-5.275	-4.663	1.413	-6.437	-5.797	1.411	-4.106	-3.439	1.410

Continue:

Compound	220ºC			240ºC			260ºC		
	ΔG	ΔH	ΔS	ΔG	ΔH	ΔS	ΔG	ΔH	ΔS
Naphthalene	-8.058	-9.111	-2.136	-8.325	-9.419	-2.134	-9.214	-10.350	-2.132
fluorene	-6.455	-7.226	-1.564	-6.879	-7.680	-1.562	-7.589	-8.420	-1.560
Phenanthrene	-4.297	-3.636	1.339	-4.702	-4.015	1.338	-5.424	-4.709	1.340
anthracene	-4.153	-3.457	1.411	-4.514	-3.789	1.413	-5.320	-4.567	1.412

3.8 Suggestion for Future Work:

1- Characterize other liquid crystal compounds such as 3_{g1} and 3_{g2} as stationary phases.

2- Synthesis of bis-[4-(4'-propoxybenzilidene)biphenyl] **(A)** and bis-[4-(4'-propoxybenzamide)biphenyl] **(B)** and compare their chromatographic performance with above liquid crystal compounds.

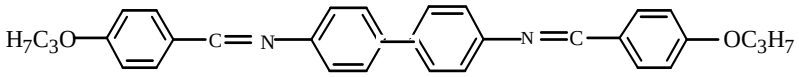

(A)

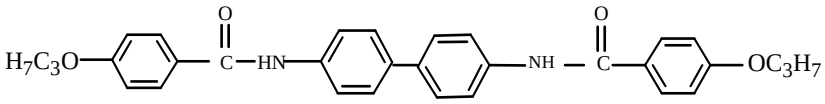

(B)

3- Use mixed liquid crystal compounds as stationary phases to increase the selectivity of separation and to change the operation column temperature.

4- Study the ability of the prepared liquid crystal compounds for the separation of different hydrocarbons such as normal alcohols, fatty acid, cis and trans isomers such as cis/ trans decalin and cis/ trans stilbene.